EDITE - ED 130

Doctorat ParisTech

T H È S E

pour obtenir le grade de docteur délivré par

TELECOM ParisTech

Spécialité « Communication et Electronique »

présentée et soutenue publiquement par

Miltiades FILIPPOU

le 11 juillet 2014

Performance et Coordination dans les Réseaux Radios Cognitifs Multi-Antennes

Directeur de thèse : **David GESBERT**

Jury
M. Luc DENEIRE, Professeur, Laboratoire I3S   Président du jury
M. Mérouane DEBBAH, Professeur, SUPELEC   Rapporteur
M. Constantinos PAPADIAS, Professeur, AIT   Rapporteur
M. Dirk SLOCK, Professeur, EURECOM   Examinateur
M. Tommy SVENSSON, Professeur, Chalmers University of Technology   Examinateur

TELECOM ParisTech
école de l'Institut Télécom - membre de ParisTech

T
H
È
S
E

DISSERTATION

In Partial Fulfillment of the Requirements
for the Degree of Doctor of Philosophy
from Telecom ParisTech

Specialization

Communication and Electronics

Ècole doctorale Informatique, Télécommunications et Èlectronique (Paris)

Presented by

Miltiades C. FILIPPOU

Performance and Coordination in Multi-Antenna Cognitive Radio Networks

Defense scheduled on July 11th 2014

before a committee composed of:

Prof. Luc DENEIRE	President of the Jury
Prof. Mérouane DEBBAH	Reporter
Prof. Constantinos PAPADIAS	Reporter
Prof. Dirk SLOCK	Examiner
Prof. Tommy SVENSSON	Examiner
Prof. David GESBERT	Thesis Supervisor

THÈSE

présentée pour obtenir le grade de
Docteur de
Telecom ParisTech

Spécialité

Communication et Electronique

École doctorale Informatique, Télécommunications et Électronique (Paris)

Présentée par

Miltiades C. FILIPPOU

Performance et Coordination dans les Réseaux Radios Cognitifs Multi-Antennes

Soutenance de thèse prévue le 11 juillet 2014

devant le jury composé de:

Prof. Luc DENEIRE	Président du jury
Prof. Mérouane DEBBAH	Rapporteur
Prof. Constantinos PAPADIAS	Rapporteur
Prof. Dirk SLOCK	Examinateur
Prof. Tommy SVENSSON	Examinateur
Prof. David GESBERT	Directeur de thèse

Abstract

Spectrum sharing is principally examined in the context of opportunistic spectrum usage and cognitive radio networks (CRNs). Signal processing algorithms have been developed with the aim of coordinating the spectrum sharing between primary and cognitive (secondary) systems. In such a way, the users would have the ability to dynamically select the available channel where they need to operate, assuring Quality of Service (QoS) is a key design factor of such systems.

This factor consists of meeting the specified QoS of the multiple primary users (PUs), i.e., preserving the operation of a licensed user from harmful interference emitted from newcoming secondary transmissions, while, at the same time achieving high system throughput at the secondary side. In other words, the additional opportunistic usage of radio spectrum should not violate the operation of the already established radio service [1]. As service providers seek solutions in order to enhance performance, especially in ill-favored areas served by their own base stations (BSs), numerous approaches targeting to inter-operator interference mitigation have appeared in the last few years [1], [2]. Among these approaches, the solutions which consist in exploiting the additional degrees of freedom made available by the use of multiple antennas seem the most promising, specifically so at the transmitter side, where such arrays are both easily feasible and affordable [3].

Interference can be efficiently controlled or even eliminated as recent works have shown [4]. However, a number of challenges arise, when concentrating on CRNs. One of them is a fair, throughput-based comparison of the different CRN approaches proposed so far. Another important challenge is the fact that much better performance can be often reached by a joint design of beamforming (BF) solutions both applied at the primary network as well as at the secondary network, while, in practice such a joint design is hard to implement. The reason for the mentioned difficulty is that a joint design of a transmission scheme requires complete exchange of channel state information (CSI) between the primary and the secondary system. The latter difficulty can be avoided at the cost of some performance leading to the so-called *coordinated* BF solutions. Nevertheless, coordinated BF solutions still rely on the sharing of CSI between primary and secondary systems. Consequently, an interesting challenge arises as to whether the overhead represented by CSI exchange is worth the gain obtained under coordinated precoding schemes. An additional challenge considers the problem of channel estimation within the context of cognitive radio (CR) technologies. Since the performance of the BF solutions applied greatly depends on the quality of channel estimation, pilot assignment algorithms should be designed towards improving channel estimation quality.

In this thesis, we aim to respond to the above described challenges under different, albeit related prisms: design of distributed precoding strategies, channel estimation, as well as from a performance analytical viewpoint. More concretely, in Chapter 2, an analytical performance study is carried out for multiple-input-single-output (MISO) CRNs, with the intent of compar-

ing the performance of the two most popular CRN approaches, namely, the *interweaved* and *underlay* CRN setups. This comparison is conducted on an equal footing, by measuring the ergodic rate of a newcoming secondary user (SU), given an outage probability constraint for primary communication. Closed form expressions of the outage probability of primary (licensed) communication are given for all examined cases, as well as expressions describing the achievable ergodic rate of the SU. Interestingly, it can be observed that one CRN approach outperforms the other, for specific regimes of system parameters, such as the number of transmit antennas, the activity profile of primary communication, the targeted outage probability at the PU, as well as the quality of spectrum sensing applied in terms of the interweaved approach.

In Chapter 3, the problem of the coexistence of two multiple-antenna wireless links is formulated. More specifically, the uplink of a non-hierarchical single-input-multiple-output (SIMO) system is studied and the optimal, in the ergodic rate sense, BF problem is examined. Also, a realistic *mixed* feedback scenario is considered, whereby a transmitter is allowed to estimate instantaneous CSI from the users it serves, but not from interfering users. In other words, only statistical (covariance) information can be obtained regarding interference. For this scenario, novel ergodic rate expressions are derived, which, are utilized in order to derive closed-form expressions of the optimal BF vectors. In addition, a new user selection scheme is proposed, exploiting the derived, rate-optimal BF vectors.

In Chapter 4, we take on the problem of optimizing multiple antenna combining at the transmitters in the downlink of an underlay CRN, however substantial revisions are proposed in constrast with the classical underlay model, so far adopted in much of the literature. First, we consider a more realistic *rate target constraint* at the primary receiver instead of the less meaningful maximum interference temperature. Second, we propose a *limited* CSI structure, similar to the one mentioned above, whereby transmitters only have access to partly instantaneous feedback (i.e., about direct links) and partly statistical feedback (i.e., about interfering channels). Third, a *distributed* decision making scenario is formulated, according to which a transmitter must make a precoding decision, solely based on *local* CSI. As a result of this formulation, a distributed precoding algorithm is derived by exploiting the problem's connection with *team decision theory*.

With the aim of reducing the complexity of the algorithm described in Chapter 4, a novel coordination scheme is developed in Chapter 5, where the two transmitters coordinate *without any exchange of information or any iteration* to ensure that the average rate constraint imposed at the PU, is fulfilled while maximizing the average rate of the SU. The coordination is done on the basis of statistical information, such that the algorithm can be run off-line. The proposed scheme outperforms conventional schemes from the literature and is characterized by low complexity. It can, thus, be used in settings with low signal processing capabilities and a weak backhaul infrastructure.

Finally, in Chapter 6, we address the problem of channel estimation in an underlay, interference-prone CR setup. A primary and a secondary transmitter are considered, both with multiple antenna capability, serving multiple users. Although in the previous chapters we propose the use of BF techniques to handle secondary-caused interference, this is not practically feasible, unless the involved channels are accurately estimated in the first place. As channel estimation itself is corrupted by interference (introducing the problem of *pilot contamination* in large antenna regimes), we propose a channel covariance-based pilot assignment algorithm to address channel estimation at the primary system, while removing contamination caused by secondary transmissions.

Acknowledgements

First and foremost I would like to express my gratitude to my supervisor, Prof. David Gesbert. Had it not been for David's brilliant and wise guidance as well as his continuous support, this thesis would not have been a reality. David always encouraged me to be creative and an out-of-the-box thinker and I am much grateful to him for that. Also, his quality as a person helped best towards creating and maintaining an enjoyable and spontaneous atmosphere within the group.

Academic research is a hard task, which becomes a reality in the presence of talented collaborators and colleagues. Thus, I would like to express my appreciation to Dr. George Ropokis, Dr. Paul de Kerret, Haifan Yin, and Prof. Yingzhuang Liu, for the fruitful cooperation we had in terms of producing technical works, which consist the basis of this dissertation.

Also importantly, I would like to express my thankfulness to all my Greek and international friends. When deadlines loom, tension can build. But all my friends and colleagues helped me towards relaxing the atmosphere and -also importantly- keeping me on task. Hence, special thanks go to: Panos, Efthymios, Nick, Iraklis, Rajeev, Akis, Petros, Pavlos, Robin, Lorenzo, Xingping, George, Valia, Thanasis as well as to Thanos, Apostolos, Christos, Efthymis, Arun, Froso, Stelios, Giannis, Delia, Socratis, Konstantinos, Dimitris, Ntora, Salvatore, Luca and many others.

Last but not least, I would like to dedicate this thesis to my family and Yulia, who supported me with all their hearts during this challenging adventure. Their constant support, love and boundless encouragement, greatly helped me towards completing this work.

Contents

List of Figures

List of Tables

Acronyms

Here are the main acronyms used in this document. The meaning of an acronym is usually indicated once, when it first appears in the text.

4G   Fourth Generation.

AWGN Additive White Gaussian Noise.

BF   Beamforming.

BS   Base Station.

CA   Coverage Area.

CR   Cognitive Radio.

CRN   Cognitive Radio Network.

CSCG Circularly-Symmetric Complex Gaussian.

CSI   Channel State Information.

CSIT   Channel State Information at the Transmitter.

DGE   Dominant Generalized Eigenvector.

FCC   Federal Communications Commission.

i.i.d.   independent and identically distributed.

IC   Interference Channel.

LS   Least Squares.

MAC   Medium Access Control.

MC   Monte Carlo.

MIMO Multiple Input Multiple Output.

MISO   Multiple Input Single Output.

MMSE Minimum Mean Squared Error.

MRC   Maximal Ratio Combining.

MSE   Mean Squared Error.

PDF   Probability Density Function.

PU   Primary User.

QCQP   Quadratically Constrained Quadratic Problem.

QoS   Quality of Service.

RF   Radio Frequency.

SDP   Semidefinite Program.

SDR   Semidefinite Relaxation.

SIMO   Single Input Multiple Output.

SINR   Signal-to-Interference-plus-Noise Ratio.

SISO   Single Input Single Output.

SNR   Signal-to-Noise Ratio.

SP   Service Provider.

SU   Secondary User.

SZF   Statistical Zero Forcing.

TX   Transmitter.

UE   User Equipment.

ULA   Uniform Linear Array.

ZF   Zero Forcing.

Notations

j	The complex number verifying $j^2 = -1$.
$\mathbb{R}, \mathbb{C}, \mathbb{N}$	The set of all real, complex and natural numbers, respectively.
$\mathbb{C}^{m \times n}$	The set of $m \times n$ matrices with complex-valued entries.
$\mathbf{I}_n$	Identity matrix of size $n \times n$.
$\lvert a \rvert$	Absolute value of complex number a.
$\lVert \mathbf{a} \rVert$	Euclidean norm of vector $\mathbf{a}$.
$\mathrm{tr}(\mathbf{A})$	Trace of square matrix $\mathbf{A}$.
$\mathbf{A}^H$	Complex conjugate transpose (Hermitian) of matrix $\mathbf{A}$.
$\mathbf{A}^{-1}$	Inverse of matrix $\mathbf{A}$.
$rank(\mathbf{A})$	Rank of matrix $\mathbf{A}$.
$\mathbf{A} \succeq 0$	$\mathbf{A}$ is a positive semidefinite matrix.
$\mathbf{u_A}(1)$	Eigenvector corresponding to the largest eigenvalue of matrix $\mathbf{A}$.
$\otimes$	Kronecker matrix product.
max, min	Maximum and minimum.
$\mathcal{CN}(\mathbf{m}, \mathbf{C})$	CSCG distribution of mean $\mathbf{m}$ and covariance matrix $\mathbf{C}$.
$\bar{i}$	$\bar{i}$ denotes the complementary index of i, when the cardinality of the considered set is equal to two, i.e., $\bar{i} = i \bmod 2 + 1$.
$\mathbb{E}\{X\}$	Expected value of random variable X.
$\mathbb{E}_Y\{g(X, Y)\}$	Expected value of function $g(X, Y)$, conditioned on the knowledge of Y.
$\mathcal{P}(A)$	Probability of event A.
$\mathcal{Q}(\cdot)$	Complementary Gaussian distribution function, defined as in [5, 4.1].
$E_1(\cdot)$	Exponential integral function, defined as in [6, 5.1.1].
$\Gamma(n), n \in \mathbb{N}$	Gamma function, defined as in [6, 6.1.6].
$\gamma(n, x)$	Lower incomplete Gamma function, defined as in [6, 6.5.2].
$\Gamma(n, x)$	Upper incomplete Gamma function, defined as in [6, 6.5.3].
$\psi(\cdot)$	Digamma (psi) function, defined as in [6, 6.3.1].

Part I

Introduction

Chapter 1

Motivation and Models

1.1 Background of CR Technology

The electromagnetic *radio spectrum* is a natural resource required for wireless communications. Spectrum utilization is internationally regulated by governments with the aim of providing essential services as well as protecting these services from harmful interference. However, the massive spread of current wireless services and wireless communication evolution have given rise to a great need for bandwidth, with the aim of offering various applications and services with high data rates. This conclusion can be made by a glance at the National Telecommunications and Information Administration's frequency allocation chart[1]. According to this chart, it is reported that almost the entity of all frequency bands has been allocated, leading to a shortage in bandwidth for emerging wireless services [7].

Nevertheless, according to a report published by the Federal Communications Commission (FCC), in 2002, it is stated that the accessible radio spectrum is becoming vastly underutilized [8]. More concretely, the second finding on page 3 of this report, exactly reveals the phenomenon of *spectrum underutilization*:

"In many bands, spectrum access is a more significant problem than physical scarcity of spectrum, in large part due to legacy command-and-control regulation that limits the ability of potential spectrum users to obtain such access."

Consequently, the above described radio spectrum underutilization has given rise to the notion of *spectrum holes* (also frequently referred as *white spaces* in the literature), a definition of which is provided below [9]:

"A spectrum hole is a band of frequencies assigned to a primary user (PU), but, at a particular time and specific geographic location, the band is not being utilized by that user."

The existence of spectrum shortage due to a static, long-term exclusivity of regulated spectrum use in large geographic areas [10], along with the described spectrum underutilization, have given rise to the idea of CR [11]. A definition of such a system is given in [12]:

---

[1]www.ntia.doc.gov/osmhome/allochrt.pdf.

"CR is an intelligent wireless communication system that is aware of its surrounding environment (i.e., outside world), and uses the methodology of understanding-by-building to learn from the environment and adapt its internal states to statistical variations in the incoming radio frequency (RF) stimuli by making corresponding changes in certain operating parameters (e.g., transmit-power, carrier-frequency, and modulation strategy) in real-time, with two primary objectives in mind:

- *highly reliable communications whenever and wherever needed;*

- *efficient utilization of the radio spectrum."*

1.2 State-of-the-art for CR Systems

1.2.1 CR Systems: an emerging and challenging technology

The concept of CR constitutes both an emerging and promising technology. One of the most crucial components of this concept is the ability to measure, sense and learn a channel. Moreover, it is the ability to have knowledge of the parameters related to radio channel characteristics, the availability of spectrum and power, user requirements, applications as well as other operating restrictions [13].

Due to their coexistence with incumbent systems, as well as because of diverse QoS requirements, opportunistic access nodes bring up a number of interesting challenges. One of those challenges consists in the *avoidance* of interference as opportunistic users should avoid interfering with incumbent ones. Also, CR systems should support QoS-aware communication, considering the spectrum environment, which is both heterogeneous and dynamic. Furthermore, opportunistic systems should provide seamless communication, regardless of the existence of transmissions by incumbent systems [14].

1.2.2 CR System Paradigms

CR systems can be categorized into two main paradigms with respect to the existence or absence of user hierarchy. These two main paradigms are *prioritized* and *unprioritized* CR systems. The first group consists in the existence of access hierarchy across users, and will take most of the effort of this thesis, while the second one is based on the notion of *spectrum sharing* (absence of prioritization).

1.2.2.1 Prioritized CR systems

According to this scenario, newcoming users aiming at using the spectrum in an opportunistic manner, are usually referred to as *secondary users* (SUs). On the other hand, incumbent users unconstrainedly occupying spectral resources are referred to as *primary users* (PUs). An illustrative example of such a hierarchy, consists in the operation of SUs in television (TV) bands. A SU could conduct spectrum sensing and utilize frequencies belonging to a TV band if the spectrum is unused [10].

In the following, we will elaborate on the operation of the main design approaches of prioritized CR systems. More specifically, we will focus on systems comprising of a multiple antenna primary transmitter (TX), $TX\ p$ along with its (single antenna) assigned user equipment (UE),

$UE\ p$ as well as a multiple antenna secondary transmitter, $TX\ s$ with its assigned user equipment, $UE\ s$. The channel vectors between $TX\ i$ and $UE\ j$ are denoted as $\mathbf{h}_{ij}$.

Up to the present, three major prioritized CR design approaches have emerged:

1.2.2.1.1 Interweaved CRN approach   The *interweaved* CRN approach (Fig. 1.1) is based on the idea of opportunistic spectrum sharing. Since studies, such as [8] revealed the underutilization of radio spectrum, or, in other words the existence of spectrum holes in space, time or frequency, it was sensible to develop and investigate *spectrum sensing* algorithms and techniques, the goal of which would be to reveal these temporary space-time-frequency voids.

As a result, after localizing such voids, secondary systems can operate in orthogonal dimensions of space, time or frequency, relative to primary communication signals. Hence, this way, spectrum utilization is improved by opportunistic reuse over spectrum holes [10].
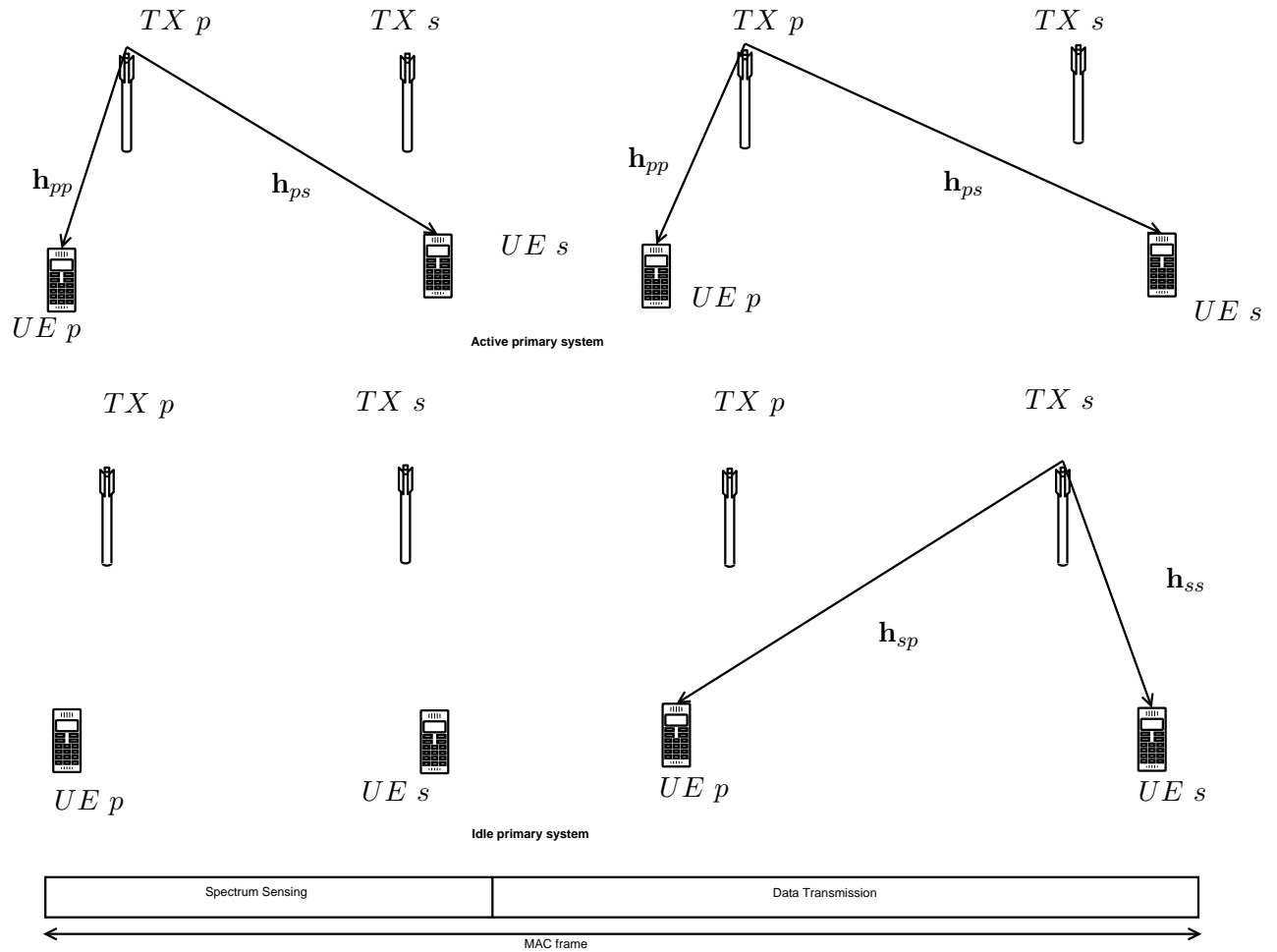
Figure 1.1: Operation of an interweaved CRN during a medium access control (MAC) frame. When the secondary system senses the existence of primary communication (upper part), it remains silent during the data transmission subframe. Conversely, when the primary system is found idle (lower part), the secondary one decides to transmit.

However, phenomena such as channel fading, shadowing, noise as well as the existence of

outdated spectrum sensing, can give rise to sensing imperfections, referred to as *miss-detection* events, which can potentially violate the QoS requirements of PUs. On the contrary, an over-whelming expenditure of available resources towards sensing would definitely improve spectrum sensing quality, however at the cost of a degradation in the throughput of the secondary system. Hence, one observes that an interesting as well as challenging trade-off between spectrum sensing quality and throughput maximization of a secondary network, exists.

1.2.2.1.2   Underlay CRN approach   According to the *underlay* CRN approach (Fig. 1.2), a primary system allows the concurrent reuse of its spectral resources by an unlicensed secondary system, *provided* that the interference generated by secondary transmitters at primary receivers is below a predefined threshold. In 2003, the FCC released a memorandum seeking comment on the above described *interference temperature* model, with the aim of controlling spectrum use [8], [15]. Deciding upon the maximum tolerated interference caused by a secondary transmission towards a primary receiver, is a challenging task in underlay CR scenarios. The interference at a given primary receiver can be determined by a SU by eavesdropping a transmission of the primary system, if the link between them is reciprocal.
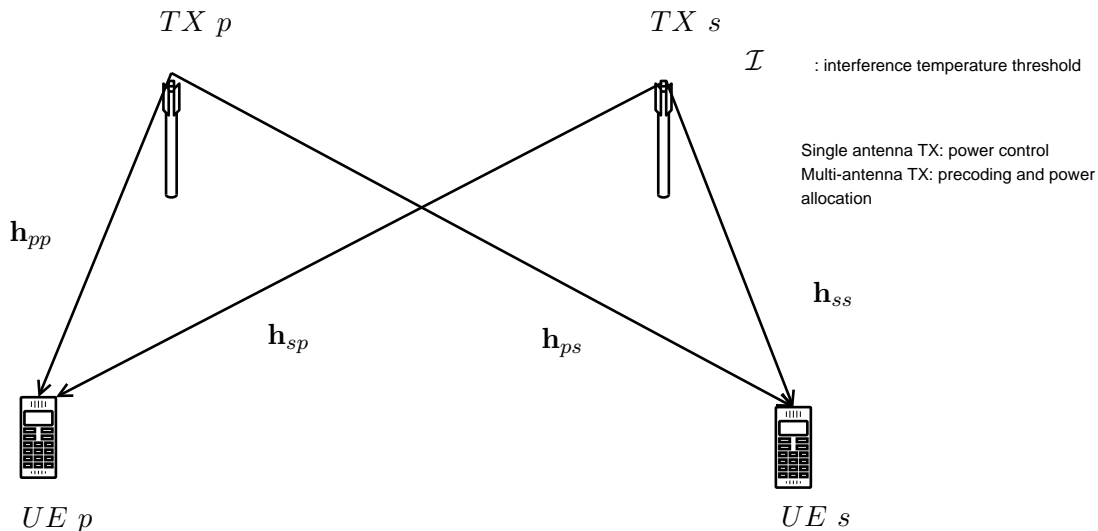
Figure 1.2: Operation of an underlay CRN. The secondary system coexists with the primary, on condition that the interference power towards the PU will be inferior to a predefined level, $\mathcal{I}$.

The operating principle of underlay CRNs, i.e., the limitation of secondary transmitter's power, imposed by a constraint on the interference caused to PUs, demands careful design, since the secondary transmitter can be overly conservative in its output power, in order to comply with the interference temperature-based restrictions [10].

Interestingly, apart from the extensively investigated maximum interference temperature tolerated at the PU, other metrics of maximum tolerable disturbance can be introduced, which will be studied in Chapters 2-5 of this dissertation. One of these metrics is the outage probability of primary communication (which will be investigated in Chapter 2), in other words, the probability with which the rate of primary communication falls below a predefined threshold.

Another disturbance metric in the direction of protecting primary communication is a minimum data (average) rate, that needs to be achieved at the PU side. Such a metric has the

advantage of being more realistic and practical, in comparison with the one based on interference temperature. The reason for this is the fact that this way, also the quality of the direct primary link is taken into consideration, in other words, if the primary link is strong, a higher level of interference can be tolerated at the PU, leading to a resource management which enhances the throughput of secondary communication.

The underlay CRN approach is commonly followed in the licensed spectrum, whereas it can be also applied in the context of unlicensed bands, with the aim of providing different service classes to different users [10].

1.2.2.1.3   Overlay CRN approach   The premise for *overlay* CRNs is that the secondary transmitter has knowledge of the PU's transmitted data sequence (or *message*) as well as of how this sequence is encoded (also called its *codebook*) [10]. As a result, such knowledge can be exploited by the secondary transmitter in various ways with the aim of improving the performance of both systems.

This approach will not be studied in this dissertation. The reason for this is that according to the overlay approach, a great amount of network side information has to be available at secondary nodes. This side information consists in the knowledge of channel gains, encoding techniques, and possibly the transmitted data sequences of PUs. As a result, such a demand leads to complexity levels of encoding and decoding, which are higher than the ones of the other CRN approaches [10].

1.2.2.2   Unprioritized CR systems

In current wireless communications systems, the RF spectrum is typically divided into exclusively allocated (licensed) frequency bands. Unlike this approach, in *unprioritized* CR systems (Fig. 1.3), equal-priority resource sharing is conducted, in other words, unprioritized networks share the available spectrum simultaneously, without any priority restrictions imposed by one (or more of) the operators.
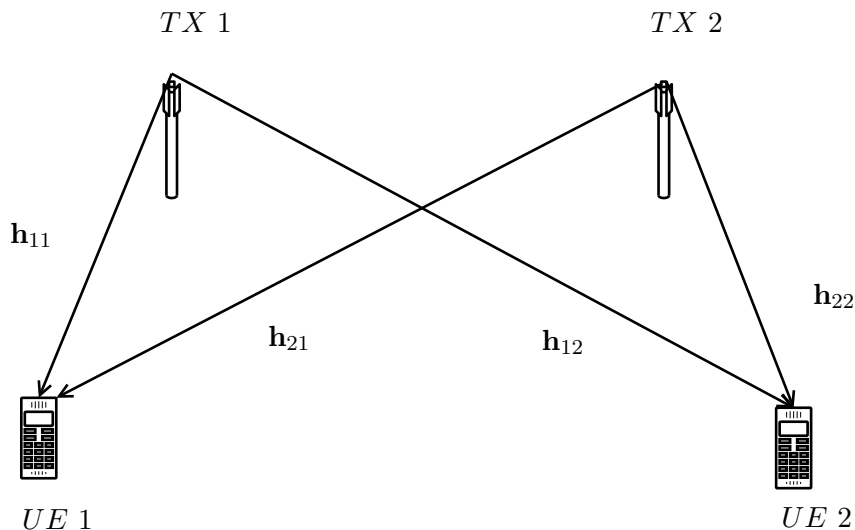
Figure 1.3: Operation of an unprioritized CRN (downlink communication). Both systems transmit simultaneously, and no restriction rules are posed by any of the two systems.

In this context, a number of advantages potentially arise. Some of these advantages consist in: improvement in spectral efficiency, coverage enhancement, an increase in user satisfaction, as well as increased revenues for service operators and decreased operating expenditures [See [16] and references therein].

However, interference caused by neighboring transmissions needs to be effectively managed. Assuming the existence of multiple antennas at the transmitters, operators have to choose between cooperating with other operators and competing with them [17]. This choice is quantified by a designed transmission (precoding) policy.

Consequently, interesting problems arise, with respect to the followed precoding policy. A popular objective in such systems is the maximization of the (average) achievable sum rate of the system. In Chapter 3, such a system is examined, focusing on uplink communication, in the existence of imperfect channel information.

1.2.3 Utilizing Multiple Antennas in CR Systems

A great deal of prior research has focused on investigating the problem of satisfying a QoS-based constraint, for the sake of a primary system, while simultaneously maximizing the throughput of secondary communication. Towards this direction, research on radio resource allocation for CRNs has mainly focused on the frequency or time domain, assuming the existence of single antennas at CRN transmitters. Transmissions exploiting multiple antennas have captured considerable attention in the last few years. Multiple antennas can be used with the aim of achieving efficient co-channel interference suppression for multiuser transmissions along with an improvement in reliability via space-time processing [See [3] and references therein].

Nevertheless, the potential of using multiple antennas within the context of opportunistic spectrum sharing has not yet been adequately understood and explored. Multiple antennas can be used in order to spatially allocate transmit directions. Such an allocation results to providing CRN secondary transmitters with more degrees of freedom in space in addition to time and frequency. In such a way, secondary systems can interestingly balance between maximizing their own throughput and satisfying a QoS constraint regarding primary communication.

1.3 Contributions and Outline of the Dissertation

The main focus of this disseration is the performance analysis of some of the basic CRN architectures, namely the interweaved and the underlay one, as well as the design and evaluation of signal processing algorithms for underlay CRNs, in the presence of limited CSI exchange between primary and secondary transmitters. The mentioned algorithms aim at maximizing the throughput of newcoming SUs, while avoiding the violation of QoS guarantees at an established primary network. Moreover, also signal processing and user selection schemes are proposed for the case of unprioritized CRNs.

The throughput comparison study, along with the designed signal processing schemes seek to provide answers to a number of questions, such as:

- Does a prioritized CRN approach (either the interweaved or the underlay one), outperform the other for different system scenarios, under a common QoS constraint on primary communication? Different system scenarios correspond to different circumstances related

to: the activity profile of primary communication, the existence of multiple antennas, the quality of spectrum sensing and others.

- What is the form of a rate-optimal receive BF vector, with respect to a SIMO unprioritized CRN?

- Focusing on downlink communication of a MISO underlay CRN, is it possible to design a transmission policy, according to which, the average throughput of secondary communication is maximized, subject to an average rate constraint at the PU? How can one formulate this problem, when imperfect as well as local CSIT exists?

- Is it possible to design a low complexity transmission policy for the previously presented problem?

- Since direct channel links need to be estimated, within the prioritized CRN context, is it possible to design a pilot assignment scheme, which will improve channel estimation quality? What would the performance of such a scheme be in the presence of a large number of antennas at the transmitters?

An outline of the dissertation is provided below and the contributions achieved in each chapter are summarized.

Chapter 2 - A Performance Comparison Study of Interweaved and Underlay Multiple-Antenna CRNs

In this chapter, two of the most popular CRN design approaches, namely, the interweaved and the underlay approach, are evaluated, given a multiple antenna setting, and compared in terms of the secondary system's throughput, subject to a common QoS constraint for the primary system. In order to conduct such a comparison, we derive closed form expressions for the outage probability at the PU, along with expressions describing the achievable average rate of the SU. Then, the key design parameters of each approach are optimized in terms of maximizing the secondary ergodic capacity for a given outage probability at the PU and a throughput-based comparison takes place with reference to various system parameters such as the targeted PU outage probability constraint, the number of transmit antennas, as well as the activity profile of the primary network and the quality of the spectrum sensing process for the interweaved approach. This way, the advantages and drawbacks of each of the two examined CRN approaches are revealed.

The work in this chapter has resulted to the following publications:

- *M.C. Filippou, D. Gesbert, and G.A. Ropokis, "Underlay versus Interweaved Cognitive Radio Networks: a Performance Comparison Study", in proc. of the 9th International Conference on Cognitive Radio Oriented Wireless Networks (CROWNCOM 2014), Oulu, Finland, 2014*

- *M.C. Filippou, D. Gesbert, and G.A. Ropokis, "A Comparative Performance Analysis of Interweaved and Underlay Multi-Antenna Cognitive Radio Networks", submitted to IEEE Transactions on Wireless Communications, Apr. 2014*

Chapter 3 - Rate Optimal BF and User Selection for Unprioritized SIMO CRNs

In this chapter, the uplink of a SIMO CRN with equal priority for the two systems is considered and a rate-optimal receive BF problem is formulated and then solved. We particularly consider a *mixed* CSI scenario, whereby the multiple antenna receivers (BSs) are allowed to estimate the channels of their assigned users, whereas they are merely able to acquire statistical (covariance) information of interfering users. Having considered such a CSI scenario, we derive a novel, simple approximation for the users' ergodic rates (conditioned on the knowledge of their direct link), by focusing on an interference-limited system. Then, for the regime mentioned, we derive the rate-optimal receive BF vector and, finally, we propose novel, low complexity, user selection schemes, aiming at maximizing the average sum rate of the system.

The work in this chapter has been published in:

- *M.C. Filippou, D. Gesbert, and G.A. Ropokis, "Optimal Combining of Instantaneous and Statistical CSI in the SIMO Interference Channel", in proc. of Vehicular Technology Conference (VTC-Spring), Dresden, Germany, 2013*

Chapter 4 - Team Decisional BF for Underlay MISO CRNs

The problem of the coexistence of two multiple-antenna wireless links within an underlay CR scenario, focusing on downlink communication, is examined in this chapter. The novelty brought by our setup is three-fold. First, a more realistic target constraint at the primary receiver, is considered, in contrast with the less meaningful maximum tolerable interference temperature. Second, a mixed CSI structure is considered, similar to the one described in Chapter 3. Third, a *distributed* decision making scenario is formulated, by which instantaneous channel information is not shared among primary and secondary transmitters. Instead, a transmitter must form its precoding strategy based only on local CSI. This way, the problem is recast as a team decision theoretic problem and the optimal precoders are obtained by solving semidefinite programs (SDPs). As a result, a distributed precoding algorithm is derived, which is then compared with classical BF solutions. It is numerically shown that significant gains in favour of the designed algorithm, are illustrated over a range of scenarios.

The work in this chapter has been published in:

- *M.C. Filippou, G.A. Ropokis, and D. Gesbert, "A Team Decisional Beamforming Approach for Underlay Cognitive Radio Networks", in proc. of the 24th Annual IEEE International Symposium on Personal, Indoor and Mobile Radio Communications (PIMRC 2013), London, United Kingdom, 2013*

Chapter 5 - Underlay MISO CRN Precoding with Statistical Coordination

In this chapter, an underlay MISO CR scenario, is studied. According to this scenario, a primary transmitter, equipped with multiple antennas, communicates with a single-antenna PU and a newcoming, secondary multiple antenna transmitter serves a single-antenna SU. The goal of the two transmitters is to effectively coordinate in order to maximize the ergodic rate of the SU, subject to a constraint imposed on the achievable ergodic rate of the PU. Importantly, a mixed CSI scenario, as described in the previous two chapters, is considered, hence, the primary transmitter has to exploit its statistical knowledge of the multi-user channel so as to coordinate with the secondary transmitter. Such a setting, gives rise to a team decisional

problem, reminiscent of the one formulated in Chapter 4. A novel *statistical coordination* scheme is developed, where the two transmitters coordinate in the lack of instantaneous CSI exchange, to ensure that the primary QoS constraint is satisfied, while the average rate of the SU is maximized. It is shown that the proposed scheme outperforms conventional schemes taken from the literature and has low complexity.

The work in this chapter has resulted to the following publication:

- *P. de Kerret, M.C. Filippou, and D. Gesbert, "Statistically Coordinated Precoding for the MISO Cognitive Radio Channel", in proc. of the Asilomar Conference on Signals, Systems, and Computers (Asilomar 2014), Pacific Grove, U.S.A., 2014*

Chapter 6 - Channel Estimation for Large Antenna CRNs: a Pilot Decontamination Approach

By exploiting the results presented in [18], in this chapter, we address the problem of channel estimation in an underlay CRN setup, consisting of a primary and a secondary operator. The main difference between cellular systems and underlay CRNs is the notion of priority for the cognitive scenario. In order to handle this design requirement, we propose a novel pilot assignment scheme which is implemented with respect to the secondary operator. This scheme aims at maximizing the channel estimation quality for SUs, while minimizing the impact created by the latter onto primary channel estimation performance. It is shown analytically and by simulation that as the number of antennas grows large, one can achieve interference-free channel estimation at the primary operator while letting the SUs communicate. More specifically, we conclude to the fact that the mean squared error (MSE) performance of the covariance aided channel estimation, in case this regards a PU, strongly depends on the degree with which the signal subspaces of the covariance matrices of the direct and of the interfering channel overlap with each other. With the aim of quantifying this result, we design a suitable coordination protocol for assigning pilot sequences to SUs of the above described two-operator CRN.

The works related to this chapter have been published in:

- *M.C. Filippou, D. Gesbert, and H. Yin, "Decontaminating Pilots in Cognitive Massive MIMO Networks", in proc. of the 9th International Symposium on Wireless Communication Systems (ISWCS 2012), Paris, France, 2012 (invited paper)*

- *H. Yin, D. Gesbert, and M.C. Filippou, "Decontaminating Pilots in Massive MIMO Systems", in proc. of the IEEE International Conference on Communications, (ICC 2013), Budapest, Hungary, 2013*

- *H. Yin, D. Gesbert, M.C. Filippou, and Y. Liu, "A Coordinated Approach to Channel Estimation in Large-Scale Multiple-Antenna Systems", in IEEE Journal on Selected Areas in Communications, vol.31, no.2, pp.264-273, Feb. 2013*

Part II

Performance Comparison of CRN Approaches

Chapter 2

A Performance Comparison Study of Interweaved and Underlay Multiple-Antenna CRNs

2.1 Introduction

Quite surprisingly and to the best of our knowledge, little effort has been made to compare the throughput performance of the interweaved and the underlay CRN approach, based on a meaningful, fair, and even less so in an analytical manner. Indeed, the philosophies behind each CRN approach seem incompatible at first glance. The underlay approach seems to be typically reserved for applications with only loose QoS guarantees at the legacy (primary) network. On the other hand, the interweaved design is expected to offer a near-zero disturbance at the PU, hence seems to offer hard QoS guarantees.

Upon closer inspection, it is clear that the QoS achieved at the PU under the interweaved approach, strongly depends on the sensing capability at the secondary side. Sensing imperfections due to a number of factors such as channel fading, shadowing, noise or delays, give rise to miss-detection events, which, in turn, lead to outage events at the PU due to unintentional, harmful interference towards it [7]. Arguably, a strictly conservative spectrum sensing design would ensure that near zero interference is generated at the PU. However, this strategy would inevitably lead to a wasteful spending of secondary communication resources, as it is practically difficult to sense and communicate at the same time for the secondary system. Therefore, a low outage probability at the PU, induced by a high accuracy sensing goes at the cost of data rate for the SU. An interesting question lies in whether a similar trade-off can be explored for the underlay scenario and ultimately compared with that obtained in the interweaved case. Our answer is positive.

In the underlay case, a low outage probability at the PU is maintained through a suitable power control policy at the secondary transmitter, augmented with a possible BF solution, when the latter is equipped with several antennas. More generally, a specific precoding and power allocation policy will lead to a specific point in the so-called outage (at PU) versus average rate (at SU) region.

The above observations motivate us to compare the throughput performance of the interweaved and underlay CRN approaches on an equal footing. More concretely, our aim is to

compare these two CRN approaches with respect to the achievable SU ergodic rate, subject to
a common outage probability at the PU. Marking the difference with prior CRN work, where
the main quality indicator at the PU is in terms of the interference power not exceeding an
arbitrary threshold, we use a definition of outage with a greater relevance to the actual PU
quality-of-experience. Here, an outage event is declared when the *rate* at the PU falls below a
given threshold, *whether due to interference or a fading event in its own channel*. The intuition
is that a PU with a higher quality channel is likely to tolerate more interference, which ought
to benefit the data rate of the secondary system.

In this context, some interesting prior work is noteworthy. In [19], the throughput potential
of different prioritized CR techniques has been investigated from an information theoretical
point of view. Nevertheless, no expressions describing the achievable ergodic rate of the SU or
the outage probability of the primary system are given considering a fading environment. Also,
in [20], although expressions for the instantaneous rate of the SU are given, the assumption
of perfect spectrum sensing is adopted, which is rather unrealistic within the prioritized CRN
context. Furthermore, in [21], [22] and [23] novel spectrum sharing models are proposed, either
mixed ones or variants of the interweaved model, though no explicit performance comparison
of the two mentioned CRN approaches is presented. Additionally, works such as [24–30] focus
on the derivation of either approximations or closed form expressions for the ergodic rate of SU
as well as for the outage probability of the primary system. Yet, no performance comparison
between interweaved and underlay CRN approaches is illustrated in these works.

In this chapter, both the interweaved and underlay CRN approaches are investigated with
respect to a MISO (prioritized) CRN and compared with reference to the ergodic rate of the SU
for a target outage probability of the PU, as well as for various primary communication activity
profiles and transmit antenna numbers. More concretely, our contributions are the following:

- Closed form expressions for the outage probability of primary communication, regarding
  both MISO interweaved and underlay CRN approaches, are derived.

- Expressions for the ergodic rate of the SU are derived with respect to both MISO CRN
  approaches.

- Rate-optimal values of the generic design parameters of each CRN approach are found,
  corresponding to a common outage probability at the PU.

- The optimal SU ergodic throughput levels of the two investigated CRN approaches are fi-
  nally compared, under a target outage level of the PU, for various primary communication
  activity profiles and transmit antenna numbers. It is shown that the performance compar-
  ison results are driven by a set of key system parameters, such as the number of transmit
  antennas, the activity profile of the primary system, the precoding scheme applied at the
  secondary transmitter, as well as the spectrum sensing protocol design parameters.

2.2 System and Channel Model

The system under investigation, which is illustrated in Fig. 2.1 consists of a MISO primary
system, comprising of a base station (BS), *BS p*, equipped with M antennas, as well as its
assigned PU, *UE p*. Focusing on downlink communication, the primary system is willing to share
its resources with a MISO secondary system consisting of a BS, *BS s*, also equipped with M

antennas, along with its assigned SU, $UE\ s$. It is assumed that $1 \times M$ channels $\mathbf{h}_{ij}, \quad i,j \in \{p,s\}$ between $BS\ i$ and user $UE\ j$ as well as channel $\mathbf{h}_{00}$ between $BS\ p$ and one of the antennas at $BS\ s$ (which will be later devoted to spectrum sensing within the interweaved CRN context), are Rayleigh fading ones, i.e., $\mathbf{h}_{ij} \sim \mathcal{CN}(\mathbf{0}, \sigma_{ij}^2 \mathbf{I}_M)\ \ i,j \in \{p,s\}$ and $\mathbf{h}_{00} \sim \mathcal{CN}(\mathbf{0}, \sigma_{00}^2 \mathbf{I}_M)$.
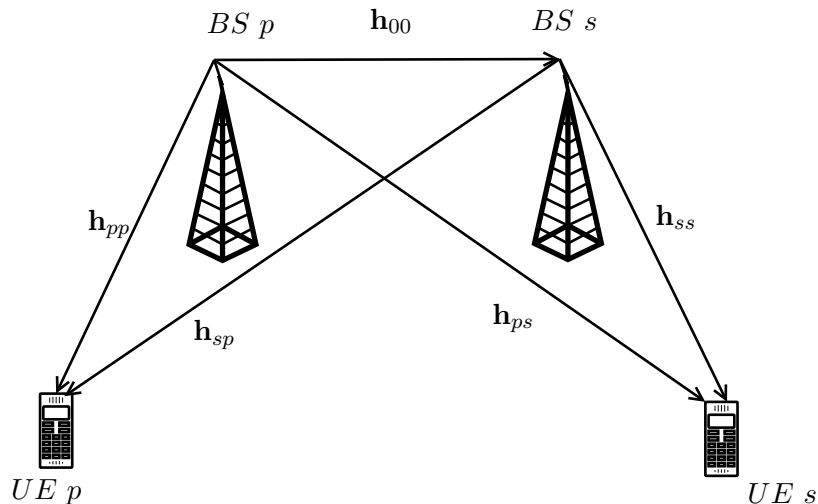
Figure 2.1: MISO CRN - System topology.

In the following two sections, closed form expressions for the outage probability of primary communication as well as expressions for the ergodic rate of the SU, will be derived for both the interweaved and underlay CRN approach. It is assumed that $BS\ p$ can perfectly estimate channel $\mathbf{h}_{pp}$ and $BS\ s$ has a perfect estimate of channel vector $\mathbf{h}_{ss}$, while it has statistical knowledge of channels $\mathbf{h}_{pp}$ and $\mathbf{h}_{sp}$.

2.3 Performance Analysis of the Interweaved Approach

2.3.1 General model

We consider first the interweaved approach, as it is shown in Fig. 2.2, where each MAC frame is assumed to have a duration of T time units, including a subframe dedicated to *spectrum sensing*, which lasts for $\tau < T$ time units. The rest of the frame is dedicated to data transmission. Moreover, during each sensing phase, $BS\ s$ receives $N = \tau f_s$ samples, where f_s is the sampling frequency of the received signal. It is also assumed that during sensing, $BS\ s$ is kept silent and all instantaneous channels remain constant within a MAC frame. Note that we assume here that the spectrum sensing process takes place at the secondary transmitter as opposed to e.g., at the receiving terminal side, thereby bypassing the need for a dedicated sensing feedback channel.
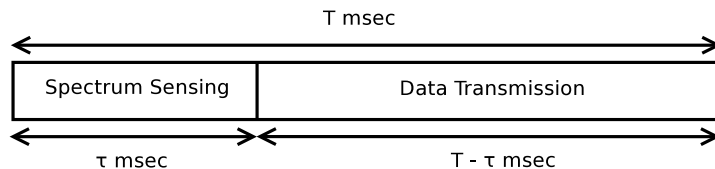
Figure 2.2: MAC frame structure.

Energy detection is applied as it is a popular and easily applicable spectrum sensing scheme [31]. At the n-th, $n = 1, 2, \ldots, N$ time instant, the binary hypothesis test for spectrum sensing is expressed as

$$y_s[n] = \begin{cases} z[n], & \text{if } \mathcal{H}_0 \\ \mathbf{h}_{00}\mathbf{w}_p s_p[n] + z[n], & \text{if } \mathcal{H}_1, \end{cases} \tag{2.1}$$

where additive noise $z[n]$ is a circularly symmetric complex Gaussian (CSCG), independent, identically distributed (i.i.d.) process with $z[n] \sim \mathcal{CN}(0, N_0)$, P_p is a fixed power level at BS p and the information symbol $s_p[n]$ is selected from a CSCG codebook, i.e., $s_p[n] \sim \mathcal{CN}(0, 1)$ and is independent of $z[n]$. Vector $\mathbf{w}_p \in \mathbb{C}^{M \times 1}$ is the applied BF vector at BS p. We assume that when the primary system is in transmission mode, Maximal Ratio Combining (MRC) BF with full power is applied at BS p, since the goal of the primary transmitter is to maximize the rate of the PU. Similarly, when the secondary system decides to transmit, also full power MRC BF is applied at BS s. Hence, we obtain the following expressions for the unit-norm beamformers (BFs):

$$\mathbf{w}_p = \sqrt{P_p} \frac{\mathbf{h}_{pp}^H}{\|\mathbf{h}_{pp}\|} = \sqrt{P_p} \tilde{\mathbf{h}}_{pp}^H \tag{2.2}$$

and

$$\mathbf{w}_s^{int} = \sqrt{P_s} \frac{\mathbf{h}_{ss}^H}{\|\mathbf{h}_{ss}\|} = \sqrt{P_s} \tilde{\mathbf{h}}_{ss}^H, \tag{2.3}$$

respectively.

As it can be easily derived, signal $s[n] = \mathbf{h}_{00}\mathbf{w}_p s_p[n]$, for a fixed channel $\mathbf{h}_{00}$, will have a variance of $\sigma_s^2 = \mathbb{E}\{|s[n]|^2\} = P_p |\mathbf{h}_{00}\tilde{\mathbf{h}}_{pp}^H|^2$.

For a fixed sensing time, τ, along with a fixed energy detection threshold, ϵ, by applying the central limit theorem, the probability of false alarm, $\mathcal{P}_{fa}$, as well as the corresponding probability of detection, $\mathcal{P}_d$, can be derived, with reference to a specific MAC frame, by applying [32, Proposition 1, Proposition 2]. The above probabilities can then be written as

$$\mathcal{P}_{fa} = \mathcal{Q}\left(\sqrt{N}\left(\frac{\epsilon}{N_0} - 1\right)\right), \quad \mathcal{P}_d = \mathcal{Q}\left(\frac{\epsilon - \mu_1}{\sigma_1}\right), \tag{2.4}$$

where $\mu_1 = \sigma_s^2 + N_0 = P_p |\mathbf{h}_{00}\tilde{\mathbf{h}}_{pp}^H|^2 + N_0$ and $\sigma_1^2 = \frac{N_0^2}{N}\left(\frac{P_p |\mathbf{h}_{00}\tilde{\mathbf{h}}_{pp}^H|^2}{N_0} + 1\right)^2$.

The average detection probability with reference to random variable $\beta_{00} = |\mathbf{h}_{00}\tilde{\mathbf{h}}_{pp}^H|^2$, is given by

$$\mathcal{P}_d^{avg} = \int_0^\infty \mathcal{P}_d(\beta_{00}) f_{\beta_{00}}(\beta_{00}) d\beta_{00}. \tag{2.5}$$

Although we need an expression for $\mathcal{P}_d^{avg}$ as a function of τ and ϵ so as to maximize the rate of the SU over these two parameters, doing this proves to be difficult due to the lack of a closed form expression of (2.5). Instead, we now resort to a bounding argument to solve this problem approximately. Note that the accuracy of this bounding strategy is justified by our simulations in section 2.6.

To obtain a bound on (2.5), we use the fact that the detection probability in (2.4), although neither strictly concave nor convex as a function of β_{00}, is concave in the region of interest for β_{00} (the region corresponding to high detection probability). Therefore, the applied bound is the following

$$\mathcal{P}_{d,B} = \mathcal{Q}\left(\sqrt{N}\left(\frac{\epsilon}{P_p\sigma_{00}^2 + N_0} - 1\right)\right). \tag{2.6}$$

Regarding the average false alarm probability, it remains the same under any fading channel, for given τ and ϵ, since $\mathcal{P}_{fa}$ is considered for the case where only noise is present, thus

$$\mathcal{P}_{fa}^{avg} = \mathcal{P}_{fa}. \tag{2.7}$$

2.3.2 Outage probability of primary communication

Although the interference power at the PU is used as a quality indicator in much of the CRN literature, we point out that when it comes to primary data rate, it is the signal-to-interference-plus-noise ratio (SINR) at the PU which rather governs performance. To reflect this, we assume an outage at the PU when, given that the primary network is active, the SINR of the PU is below a predefined threshold, γ_0. This can occur in two cases:

1. when BS s fails to sense primary activity (missed detection), potentially resulting to a PU SINR that is less than γ_0 or

2. when the secondary system has correctly detected the presence of a primary signal and remains silent for the rest of the MAC frame. Yet, the desired signal received at the PU suffers from deep fades, so that the SINR falls below threshold γ_0.

In the proposition that follows, a closed form expression of the outage probability at the PU is given.

Proposition 1. The outage probability of primary communication for a MISO interweaved CRN is given by the following expression

$$\mathcal{P}_{out}^{int} = (1 - \mathcal{P}_d)\mathcal{P}_1 + \mathcal{P}_d\mathcal{P}_2, \tag{2.8}$$

where

$$\mathcal{P}_1 = 1 - \frac{e^{-\gamma_0 N_0 B\left(\frac{1}{\lambda_{X_1}} - \tilde{\mu}\right)}}{\lambda_{X_2}\lambda_{X_1}^M} \sum_{k=0}^{M-1} \frac{\lambda_{X_1}^{M-k}}{k!\tilde{\mu}^{k+1}}\Gamma(k+1, \gamma_0 N_0 B\tilde{\mu}), \tag{2.9a}$$

$$\mathcal{P}_2 = \frac{\gamma\left(M, \frac{\gamma_0 N_0 B}{\lambda_{X_1}}\right)}{\Gamma(M)}, \tag{2.9b}$$

with $\lambda_{X_1} = P_p\sigma_{pp}^2$, $\lambda_{X_2} = \gamma_0 P_s\sigma_{sp}^2$, $\tilde{\mu} = \frac{1}{\lambda_{X_1}} + \frac{1}{\lambda_{X_2}}$ and P_s stands for the maximum instantaneous available power at the secondary transmitter.

Proof. See Appendix .1. □

2.3.3 Ergodic rate of secondary communication

By applying the upper bound for the average detection probability, $\mathcal{P}_{d,B}$, the ergodic rate of the SU will have a lower bound, that is given as

$$
\mathbb{E}\{R_s^{int}\} \geq \frac{(T-\tau)}{T}\Bigg(\mathcal{P}(\mathcal{H}_0)(1-\mathcal{P}_{fa})B\mathbb{E}\Big\{ \underbrace{\log_2\Big(1+\frac{P_s\|\mathbf{h}_{ss}\|^2}{N_0 B}\Big)}_{\mathcal{A}_1} \Big\}
$$

$$
+ \mathcal{P}(\mathcal{H}_1)(1-\mathcal{P}_{d,B})B\mathbb{E}\Big\{ \underbrace{\log_2\Big(1+\frac{P_s\|\mathbf{h}_{ss}\|^2}{N_0 B + P_p|\mathbf{h}_{ps}\tilde{\mathbf{h}}_{pp}^H|^2}\Big)}_{\mathcal{A}_2} \Big\}\Bigg).
\tag{2.10}
$$

We first focus on computing expectation $\mathbb{E}\{\mathcal{A}_1\}$. Random variable $Y_1 = P_s\|\mathbf{h}_{ss}\|^2$ is gamma distributed with PDF $f_{Y_1}(y_1) = \frac{y_1^{M-1}e^{-\frac{y_1}{\lambda_{Y_1}}}}{\Gamma(M)\lambda_{Y_1}^M}$, where $\lambda_{Y_1} = P_s\sigma_{ss}^2$. Hence, using [33, 4.337.5], we have

$$
\mathbb{E}\{\mathcal{A}_1\} = \frac{1}{\ln(2)}\sum_{j=0}^{M-1}\frac{1}{(M-j-1)!}\Bigg(\frac{(-1)^{M-j-3}}{\big(\frac{\lambda_{Y_1}}{N_0 B}\big)^{M-j-1}}e^{\frac{N_0 B}{\lambda_{Y_1}}}E_1\Big(\frac{N_0 B}{\lambda_{Y_1}}\Big) + \sum_{k=1}^{M-j-1}(k-1)!\Big(\frac{-N_0 B}{\lambda_{Y_1}}\Big)^{M-j-k-1}\Bigg).
\tag{2.11}
$$

For the expectation appearing in the second term of (2.10), one obtains

$$
\mathbb{E}\{\mathcal{A}_2\} = \frac{1}{\ln(2)}\mathbb{E}\Big\{\ln\Big(1+\frac{Y_1}{N_0 B + Y_2}\Big)\Big\} = \frac{1}{\ln(2)}\Bigg(\underbrace{\int_0^\infty f_{Y_1}(y_1)\int_0^\infty \ln(N_0 B + y_1 + y_2)f_{Y_2}(y_2)dy_2 dy_1}_{\mathcal{J}_1}
$$

$$
- \underbrace{\int_0^\infty f_{Y_1}(y_1)\int_0^\infty \ln(N_0 B + y_2)f_{Y_2}(y_2)dy_2 dy_1}_{\mathcal{J}_2}\Bigg).
\tag{2.12}
$$

Random variable $Y_2 = P_p|\mathbf{h}_{ps}\tilde{\mathbf{h}}_{pp}^H|^2$ is independent of Y_1 and exponentially distributed with PDF $f_{Y_2}(y_2) = \frac{1}{\lambda_{Y_2}}e^{\frac{-y_2}{\lambda_{Y_2}}}$, where $\lambda_{Y_2} = P_p\sigma_{ps}^2$. The derivation of double integral $\mathcal{J}_1$ gives

$$
\mathcal{J}_1 = \mathcal{J}_{1,1} + \mathcal{J}_{1,2},
\tag{2.13}
$$

where by exploiting [33, 4.337.5]

$$
\mathcal{J}_{1,1} = \ln(N_0 B) + \sum_{j=0}^{M-1}\frac{1}{(M-j-1)!}\Bigg(\frac{(-1)^{M-j-3}}{\big(\frac{\lambda_{Y_1}}{N_0 B}\big)^{M-j-1}}e^{\frac{N_0 B}{\lambda_{Y_1}}}E_1\Big(\frac{N_0 B}{\lambda_{Y_1}}\Big) + \sum_{k=1}^{M-j-1}(k-1)!\Big(\frac{-N_0 B}{\lambda_{Y_1}}\Big)^{M-j-k-1}\Bigg),
\tag{2.14}
$$

and

$$
\mathcal{J}_{1,2} = \frac{1}{\Gamma(M)}\int_0^\infty e^{-u}u^{M-1}e^{\frac{N_0 B + \lambda_{Y_1}u}{\lambda_{Y_2}}}E_1\Big(\frac{N_0 B + \lambda_{Y_1}u}{\lambda_{Y_2}}\Big)du.
\tag{2.15}
$$

Since a closed form expression of the last integral cannot be derived, numerical integration can be applied by employing the well-known Laguerre quadrature rules [6, 25.4.45].

Double integral $\mathcal{J}_2$ can be found in closed form by applying [33, 3.351.3], therefore, the following expression is obtained

$$\mathcal{J}_2 = \ln(N_0 B) + e^{\frac{N_0 B}{\lambda_{Y_2}}} E_1 \left(\frac{N_0 B}{\lambda_{Y_2}} \right). \tag{2.16}$$

In the following section, a closed form expression for the outage probability of the PU, as well as an expression for the ergodic rate of the SU will be derived considering an underlay CRN. Both cases of MRC as well as zero-forcing (ZF) BF at the secondary transmitter, will be examined.

2.4 Performance Analysis of the Underlay Approach

2.4.1 Power and BF policies

In the underlay approach, the secondary transmitter is in principle always active. It maintains the prescribed PU outage probability level by suitably adjusting its transmit power and beam vector. To do so, note that the secondary transmitter requires *some* knowledge about interference channel $\mathbf{h}_{sp}$, which is otherwise not needed in the interweaved scenario. This information is assumed to be obtained via feedback in Frequency Division Duplex (FDD), or reciprocity in Time Division Duplex (TDD) scenarios.

Our channel state information at the transmitter (CSIT) model, nevertheless, leaves the direct primary channel, $\mathbf{h}_{pp}$, unknown at the secondary transmitter, hence the power policy is designed to depend only on the interference channel gain and on the *statistics* of channel $\mathbf{h}_{pp}$. In such conditions, the secondary transmit power is adapted to meet an *average* outage constraint at the PU.

When it comes to transmit BF at the secondary transmitter, we will focus on the MRC strategy, identical to the interweaved case. At the end of this section, we also compare with a ZF strategy, for reference. However, this would require full interference channel knowledge.

2.4.2 Power policy at the secondary link under MRC

In order to meet an average outage level at the PU, the secondary transmitter adapts its power, $P_{s,MRC}^{und}$ in order to meet a certain interference level, $\mathcal{I}$. The optimal interference level is not known a priori but it can be optimized on the basis of the instantaneous interference gain and the statistics of channel $\mathbf{h}_{pp}$. Let $\mathbf{w}_{s,MRC}^{und} = \sqrt{P_{s,MRC}^{und}} \tilde{\mathbf{h}}_{ss}^H$ be the transmission BF policy applied by $BS\ s$. Power $P_{s,MRC}^{und}$ can vary from zero to a maximum instantaneous value, P_s. The maximum instantaneous power level is taken to be equal to the one considered in the interweaved approach in order to conduct a fair comparison from a power consumption perspective. Therefore, an MRC BF policy with truncated power will be applied in this case at $BS\ s$. The truncated power policy is the following

$$P_{s,MRC}^{und} = \begin{cases} \frac{\mathcal{I}}{|\mathbf{h}_{sp}\tilde{\mathbf{h}}_{ss}^H|^2}, & \text{if } \frac{\mathcal{I}}{|\mathbf{h}_{sp}\tilde{\mathbf{h}}_{ss}^H|^2} < P_s \\ \\ P_s, & \text{if } \frac{\mathcal{I}}{|\mathbf{h}_{sp}\tilde{\mathbf{h}}_{ss}^H|^2} \geq P_s. \end{cases} \tag{2.17}$$

In what follows, a closed form expression for the outage probability of primary communication, as well as an approximation of the achievable ergodic rate of the SU, will be derived, focusing on the underlay CRN approach, when MRC BF is used at the secondary transmitter.

2.4.2.1 Outage probability of primary communication

The primary system is in outage when the instantaneous SINR of the PU is below threshold γ_0. In the following proposition, a closed form expression of the outage probability of the PU, for a given interference threshold, $\mathcal{I}$, is given.

Proposition 2. The outage probability of primary communication for a MISO underlay CRN, where MRC-based BF, as well as a truncated power allocation policy, are applied at BS s, is given by

$$
\mathcal{P}_{out,MRC}^{und} = \frac{\gamma\left(M, \frac{\gamma_0 N_0 B}{P_p \sigma_{pp}^2}\right)}{\Gamma(M)} + \frac{e^{\frac{N_0 B}{P_s \sigma_{sp}^2}}}{\Gamma(M)} \left(\frac{P_p \sigma_{pp}^2}{\gamma_0 P_s \sigma_{sp}^2} + 1\right)^{-M} \times
$$
$$
\left(\Gamma\left(M, \frac{N_0 B}{P_s \sigma_{sp}^2} + \frac{\gamma_0 N_0 B}{P_p \sigma_{pp}^2}\right) - \Gamma\left(M, \frac{N_0 B + \mathcal{I}}{P_s \sigma_{sp}^2} + \frac{\gamma_0 (N_0 B + \mathcal{I})}{P_p \sigma_{pp}^2}\right)\right).
$$

(2.18)

Proof. See Appendix .2. □

2.4.2.2 Ergodic rate of secondary communication

Following the BF as well as the truncated power transmission policy described in (2.17), the expression describing the ergodic rate of the SU will be the one that follows

$$
\mathbb{E}\{R_{s,MRC}^{und}\} = \mathcal{P}(\mathcal{H}_0) B \mathbb{E}\left\{\underbrace{\log_2\left(1 + \frac{P_{s,MRC}^{und}\|\mathbf{h}_{ss}\|^2}{N_0 B}\right)}_{\mathcal{B}_1}\right\} + \mathcal{P}(\mathcal{H}_1) B \mathbb{E}\left\{\underbrace{\log_2\left(1 + \frac{P_{s,MRC}^{und}\|\mathbf{h}_{ss}\|^2}{N_0 B + P_p|\mathbf{h}_{ps}\tilde{\mathbf{h}}_{pp}^H|^2}\right)}_{\mathcal{B}_2}\right\}.
$$

(2.19)

2.4.2.2.1 Deriving expectation $\mathbb{E}\{\mathcal{B}_1\}$
Expectation $\mathbb{E}\{\mathcal{B}_1\}$, appearing in the first term of (2.19), is given by the following expression

$$
\mathbb{E}\{\mathcal{B}_1\} = \frac{1}{\ln(2)}\left(\mathbb{E}\left\{\underbrace{\ln\left(1 + \frac{\mathcal{I}\|\mathbf{h}_{ss}\|^2}{N_0 B|\mathbf{h}_{sp}\tilde{\mathbf{h}}_{ss}^H|^2}\right)}_{\mathcal{C}_1}\right\} + \mathcal{P}\left\{\frac{\mathcal{I}}{|\mathbf{h}_{sp}\tilde{\mathbf{h}}_{ss}^H|^2} \geq P_s\right\}\mathbb{E}\left\{\underbrace{\ln\left(1 + \frac{P_s\|\mathbf{h}_{ss}\|^2}{N_0 B}\right)}_{\mathcal{C}_2}\right\}\right), \quad (2.20)
$$

where $\mathcal{P}\left\{\frac{\mathcal{I}}{|\mathbf{h}_{sp}\tilde{\mathbf{h}}_{ss}^H|^2} \geq P_s\right\} = 1 - e^{-\frac{\mathcal{I}}{P_s \sigma_{sp}^2}}$.

Gamma distributed random variable $Z_1 = \|\mathbf{h}_{ss}\|^2$ and exponentially distributed random variable $Z_2 = |\mathbf{h}_{sp}\tilde{\mathbf{h}}_{ss}^H|^2$ are independent, since channel vectors $\mathbf{h}_{ss}$ and $\mathbf{h}_{sp}$ are considered independent and norm $\|\mathbf{h}_{ss}\|$ is independent of direction $\tilde{\mathbf{h}}_{ss}$ [34, A.1.3]. As a consequence, we obtain the following expression for expectation $\mathbb{E}\{\mathcal{C}_1\}$

$$\mathbb{E}\{\mathcal{C}_1\} = \int_0^\infty \int_{\frac{\mathcal{I}}{P_s}}^\infty \ln\left(1 + \frac{\mathcal{I}z_1}{N_0 B z_2}\right) f_{Z_1, Z_2}(z_1, z_2) dz_2 dz_1$$

$$= \underbrace{\int_0^\infty f_{Z_1}(z_1) \int_{\frac{\mathcal{I}}{P_s}}^\infty \ln(\mathcal{I}z_1 + N_0 B z_2) f_{Z_2}(z_2) dz_2 dz_1}_{\mathcal{K}_1} - \underbrace{\int_0^\infty f_{Z_1}(z_1) \int_{\frac{\mathcal{I}}{P_s}}^\infty \ln(N_0 B z_2) f_{Z_2}(z_2) dz_2 dz_1}_{\mathcal{K}_2}.$$

(2.21)

For double integral $\mathcal{K}_1$, by applying [33, 3.352.2] we obtain

$$\mathcal{K}_1 = \mathcal{K}_{1,1} + \mathcal{K}_{1,2},$$

(2.22)

where, by using expressions [33, 3.351.3] and [33, 4.337.5] we have

$$\mathcal{K}_{1,1} = e^{\frac{-\mathcal{I}}{P_s \sigma_{sp}^2}} \left(\ln\left(\frac{N_0 B \mathcal{I}}{P_s}\right) + \sum_{j=0}^{M-1} \frac{1}{(M-j-1)!} \left(\frac{(-1)^{M-j-3}}{\left(\frac{P_s \sigma_{ss}^2}{N_0 B}\right)^{M-j-1}} e^{\frac{N_0 B}{P_s \sigma_{ss}^2}} E_1\left(\frac{N_0 B}{P_s \sigma_{ss}^2}\right) \right. \right.$$
$$\left. \left. + \sum_{k=1}^{M-j-1} (k-1)! \left(\frac{-N_0 B}{P_s \sigma_{ss}^2}\right)^{M-j-k-1} \right) \right).$$

(2.23)

Term $\mathcal{K}_{1,2}$ is given by the following expression

$$\mathcal{K}_{1,2} = \frac{1}{\Gamma(M)} \int_0^\infty e^{-u} u^{M-1} e^{u \frac{\mathcal{I}\sigma_{ss}^2}{\sigma_{sp}^2 N_0 B}} E_1\left(\frac{\mathcal{I}}{P_s \sigma_{sp}^2} + u \frac{\mathcal{I}\sigma_{ss}^2}{\sigma_{sp}^2 N_0 B}\right) du,$$

(2.24)

which can be also computed by employing Laguerre quadrature rules. Double integral $\mathcal{K}_2$ is derived by using integration by parts and applying [33, 3.352.2], thus, giving

$$\mathcal{K}_2 = \ln\left(\frac{N_0 B \mathcal{I}}{P_s}\right) e^{\frac{-\mathcal{I}}{P_s \sigma_{sp}^2}} + E_1\left(\frac{\mathcal{I}}{P_s \sigma_{sp}^2}\right).$$

(2.25)

Finally, by using [33, 4.337.5], expectation $\mathbb{E}\{\mathcal{C}_2\}$ is given by the following expression

$$\mathbb{E}\{\mathcal{C}_2\} = \sum_{j=0}^{M-1} \frac{1}{(M-j-1)!} \left(\frac{(-1)^{M-j-3}}{\left(\frac{P_s \sigma_{ss}^2}{N_0 B}\right)^{M-j-1}} e^{\frac{N_0 B}{P_s \sigma_{ss}^2}} E_1\left(\frac{N_0 B}{P_s \sigma_{ss}^2}\right) + \sum_{k=1}^{M-j-1} (k-1)! \left(\frac{-N_0 B}{P_s \sigma_{ss}^2}\right)^{M-j-k-1} \right).$$

(2.26)

2.4.2.2.2 Deriving expectation $\mathbb{E}\{\mathcal{B}_2\}$ In a similar way, expectation $\mathbb{E}\{\mathcal{B}_2\}$, appearing in the second term of (2.19), is given by the following expression

$$\mathbb{E}\{\mathcal{B}_2\} = \frac{1}{\ln(2)} \left(\mathbb{E}\left\{ \underbrace{\ln\left(1 + \frac{\mathcal{I}\|\mathbf{h}_{ss}\|^2}{|\mathbf{h}_{sp}\tilde{\mathbf{h}}_{ss}^H|^2 (N_0 B + P_p |\mathbf{h}_{ps}\tilde{\mathbf{h}}_{pp}^H|^2)}\right)}_{\mathcal{D}_1} \right\} + \mathcal{P}\left\{ \frac{\mathcal{I}}{|\mathbf{h}_{sp}\tilde{\mathbf{h}}_{ss}^H|^2} \geq P_s \right\} \times$$
$$\mathbb{E}\left\{ \underbrace{\ln\left(1 + \frac{P_s \|\mathbf{h}_{ss}\|^2}{N_0 B + P_p |\mathbf{h}_{ps}\tilde{\mathbf{h}}_{pp}^H|^2}\right)}_{\mathcal{D}_2} \right\} \right).$$

(2.27)

Random variables Z_1, Z_2 as well as exponentially distributed random variable $Z_3 = |\mathbf{h}_{ps}\tilde{\mathbf{h}}_{pp}^H|^2$ are independent, thus, one obtains for expectation $\mathbb{E}\{\mathcal{D}_1\}$ the following expression

$$
\begin{aligned}
\mathbb{E}\{\mathcal{D}_1\} &= \int_0^\infty \int_0^\infty \int_{\frac{\mathcal{I}}{P_s}}^\infty \ln\left(1 + \frac{\mathcal{I}z_1}{z_2(N_0B + P_pz_3)}\right) f_{Z_1,Z_2,Z_3}(z_1,z_2,z_3) dz_2 dz_3 dz_1 \\
&= \underbrace{\int_0^\infty f_{Z_1}(z_1) \int_0^\infty f_{Z_3}(z_3) \int_{\frac{\mathcal{I}}{P_s}}^\infty \ln(\mathcal{I}z_1 + z_2(N_0B + P_pz_3)) f_{Z_2}(z_2) dz_2 dz_3 dz_1}_{\mathcal{L}_1} \\
&\quad - \underbrace{\int_0^\infty f_{Z_1}(z_1) \int_0^\infty f_{Z_3}(z_3) \int_{\frac{\mathcal{I}}{P_s}}^\infty \ln(z_2(N_0B + P_pz_3)) f_{Z_2}(z_2) dz_2 dz_3 dz_1}_{\mathcal{L}_2},
\end{aligned}
\tag{2.28}
$$

where $f_{Z_1,Z_2,Z_3}(z_1,z_2,z_3)$ is the joint PDF of random variables Z_1, Z_2 and Z_3.

Focusing on multiple integral $\mathcal{L}_1$, by making use of [33, 3.352.2], we obtain

$$
\mathcal{L}_1 = \mathcal{L}_{1,1,1} + \mathcal{L}_{1,1,2} + \mathcal{L}_{1,2},
\tag{2.29}
$$

where, for the first term of (2.29), by using [33, 4.337.5], it can be shown that $\mathcal{L}_{1,1,1} = \mathcal{K}_{1,1}$. The derivation of term $\mathcal{L}_{1,1,2}$, leads to the following expression

$$
\mathcal{L}_{1,1,2} = \frac{e^{\frac{-\mathcal{I}}{P_s\sigma_{sp}^2}}}{\Gamma(M)} \int_0^\infty e^{-u} u^{M-1} e^{\frac{N_0B + P_s\sigma_{ss}^2 u}{P_p\sigma_{ps}^2}} E_1\left(\frac{N_0B + P_s\sigma_{ss}^2 u}{P_p\sigma_{ps}^2}\right) du,
\tag{2.30}
$$

which can be computed by applying [6, 25.4.45].

Term $\mathcal{L}_{1,2}$ is given by the following expression

$$
\mathcal{L}_{1,2} = \frac{1}{\Gamma(M)} \int_0^\infty e^{-u_1} \int_0^\infty e^{-u_3} u_1^{M-1} e^{\frac{\mathcal{I}\sigma_{ss}^2 u_1}{\sigma_{sp}^2(N_0B + P_p\sigma_{ps}^2 u_3)}} E_1\left(\frac{\mathcal{I}}{P_s\sigma_{sp}^2} + \frac{\mathcal{I}\sigma_{ss}^2 u_1}{\sigma_{sp}^2(N_0B + P_p\sigma_{ps}^2 u_3)}\right) du_3 du_1.
\tag{2.31}
$$

Since a closed form expression of the latter double integral cannot be derived, two dimensional numerical integration can be applied by employing twice, one for each dimension, the Laguerre quadrature rules [6, 25.4.45].

Moreover, one can compute multiple integral $\mathcal{L}_2$ by using [33, 3.352.2], giving

$$
\mathcal{L}_2 = e^{\frac{-\mathcal{I}}{P_s\sigma_{sp}^2}} \left(\ln\left(\frac{N_0B\mathcal{I}}{P_s}\right) + e^{\frac{N_0B}{P_s\sigma_{ps}^2}} E_1\left(\frac{N_0B}{P_s\sigma_{ps}^2}\right)\right) + E_1\left(\frac{\mathcal{I}}{P_s\sigma_{sp}^2}\right).
\tag{2.32}
$$

Finally, it can be observed that expectation $\mathbb{E}\{\mathcal{D}_2\}$ is the same with expecation $\mathbb{E}\{\mathcal{A}_2\}$, appearing in (2.10), thus we obtain

$$
\mathbb{E}\{\mathcal{D}_2\} = \mathbb{E}\{\mathcal{A}_2\}.
\tag{2.33}
$$

2.4.3 Power policy at the secondary link under ZF

In this case, BS p applies (as before) MRC BF with full power, P_p, while the BF vector applied at BS s is the following

$$\mathbf{w}_{s,ZF}^{und} = \sqrt{P_{s,ZF}^{und}} \, \tilde{\mathbf{h}}_{ZF}^{H}, \tag{2.34}$$

where $\tilde{\mathbf{h}}_{ZF}$ is a unit norm vector belonging to the null space of vector $\mathbf{h}_{sp}$. Since we consider perfect estimation of this channel at BS s, the interference created towards the PU will be equal to zero, thus, BS s is free to transmit with full power, as a result

$$P_{s,ZF}^{und} = P_s. \tag{2.35}$$

In the following, an expression for the outage probability of PU will be given in closed form, as well as an expression describing the achievable ergodic rate of the SU.

2.4.3.1 Outage probability of primary communication

As it has already been defined, an outage event occurs at the PU when the SINR of the PU is below threshold γ_0. Since, the use of a ZF BF vector at BS s creates zero interference towards the PU, then the primary system will suffer from outages due to the deep fades of channel $\mathbf{h}_{pp}$. Hence, it is easy to show that the outage probability of PU is described by the following expression

$$\mathcal{P}_{out,ZF}^{und} = \mathcal{P}\left\{ \frac{P_p \|\mathbf{h}_{pp}\|^2}{N_0 B} < \gamma_0 \right\} = \frac{\gamma\left(M, \frac{\gamma_0 N_0 B}{P_p \sigma_{pp}^2}\right)}{\Gamma(M)}. \tag{2.36}$$

2.4.3.2 Ergodic rate of secondary communication

Applying the above described BF and power allocation policy, the expression that describes the achievable ergodic rate of the SU is the one that follows

$$\mathbb{E}\{R_{s,ZF}^{und}\} = \mathcal{P}(\mathcal{H}_0) B \mathbb{E}\left\{ \underbrace{\log_2\left(1 + \frac{P_s |\mathbf{h}_{ss}\tilde{\mathbf{h}}_{ZF}^{H}|^2}{N_0 B}\right)}_{\mathcal{G}_1} \right\} + \mathcal{P}(\mathcal{H}_1) B \mathbb{E}\left\{ \underbrace{\log_2\left(1 + \frac{P_s |\mathbf{h}_{ss}\tilde{\mathbf{h}}_{ZF}^{H}|^2}{N_0 B + P_p |\mathbf{h}_{ps}\tilde{\mathbf{h}}_{pp}^{H}|^2}\right)}_{\mathcal{G}_2} \right\}.$$

$$\tag{2.37}$$

2.4.3.2.1 Deriving expectation $\mathbb{E}\{\mathcal{G}_1\}$

Random variable $V_1 = |\mathbf{h}_{ss}\tilde{\mathbf{h}}_{ZF}^{H}|^2$ is exponentially distributed with PDF $f_{V_1}(v_1) = \frac{1}{\sigma_{ss}^2} e^{\frac{-v_1}{\sigma_{ss}^2}}$, thus, the computation of expectation $\mathbb{E}\{\mathcal{G}_1\}$ gives

$$\mathbb{E}\{\mathcal{G}_1\} = \frac{1}{\ln(2)} \mathbb{E}\left\{ \ln\left(1 + \frac{P_s V_1}{N_0 B}\right) \right\} = \frac{1}{\ln(2)} \int_0^\infty \ln\left(1 + \frac{P_s v_1}{N_0 B}\right) f_{V_1}(v_1) dv_1 = \frac{1}{\ln(2)} e^{\frac{N_0 B}{P_s \sigma_{ss}^2}} E_1\left(\frac{N_0 B}{P_s \sigma_{ss}^2}\right),$$

$$\tag{2.38}$$

where integration by parts as well as [33, 3.352.4] were used for this derivation.

2.4.3.2.2 Deriving expectation $\mathbb{E}\{\mathcal{G}_2\}$

Working now on the derivation of $\mathbb{E}\{\mathcal{G}_2\}$, random variable $V_2 = Z_3 = |\mathbf{h}_{ps}\tilde{\mathbf{h}}_{pp}^{H}|^2$ is independent of V_1 and exponentially distributed with PDF $f_{V_2}(v_2) = \frac{1}{\sigma_{ps}^2} e^{\frac{-v_2}{\sigma_{ps}^2}}$, thus, one obtains

$$\mathbb{E}\{\mathcal{G}_2\} = \frac{1}{\ln(2)}\mathbb{E}\left\{\ln\left(1 + \frac{P_sV_1}{N_0B + P_pV_2}\right)\right\}, \tag{2.39}$$

with

$$\mathbb{E}\left\{\ln\left(1 + \frac{P_sV_1}{N_0B + P_pV_2}\right)\right\} = \int_0^\infty f_{V_1}(v_1)\int_0^\infty \ln\left(1 + \frac{P_sv_1}{N_0B + P_pv_2}\right)f_{V_2}(v_2)dv_2dv_1$$

$$= \underbrace{\int_0^\infty f_{V_1}(v_1)\int_0^\infty \ln(N_0B + P_pv_2 + P_sv_1)f_{V_2}(v_2)dv_2dv_1}_{\mathcal{M}_1} - \underbrace{\int_0^\infty f_{V_1}(v_1)\int_0^\infty \ln(N_0B + P_pv_2)f_{V_2}(v_2)dv_2dv_1}_{\mathcal{M}_2}.$$
$$\tag{2.40}$$

The computation of term $\mathcal{M}_1$ gives, after using integration by parts and [33, 3.352.4] the following

$$\mathcal{M}_1 = \mathcal{M}_{1,1} + \mathcal{M}_{1,2}, \tag{2.41}$$

where, by using again [33, 3.352.4], we obtain

$$\mathcal{M}_{1,1} = \ln(N_0B) + e^{\frac{N_0B}{P_s\sigma_{ss}^2}}E_1\left(\frac{N_0B}{P_s\sigma_{ss}^2}\right). \tag{2.42}$$

Considering term $\mathcal{M}_{1,2}$, after a simple variable transformation we obtain the following expression

$$\mathcal{M}_{1,2} = \int_0^\infty e^{-w}e^{\frac{N_0B + P_s\sigma_{ss}^2 w}{P_p\sigma_{ps}^2}}E_1\left(\frac{N_0B + P_s\sigma_{ss}^2 w}{P_p\sigma_{ps}^2}\right), \tag{2.43}$$

which can be computed by exploiting Laguerre quadrature rules [6, 25.4.45].

Finally, the computation of term $\mathcal{M}_2$, gives, after integrating by parts and using [33, 3.352.4], the following expression

$$\mathcal{M}_2 = \ln(N_0B) + e^{\frac{N_0B}{P_p\sigma_{ps}^2}}E_1\left(\frac{N_0B}{P_p\sigma_{ps}^2}\right). \tag{2.44}$$

In the following section, the criteria for a fair comparison between the abovementioned CRN approaches are defined and the generic design parameters of each CRN approach are optimized in a rate-optimal sense for the SU.

2.5 Optimizing Generic Design Parameters of the CRN Approaches

In this section, the generic design parameters of each of the two examined CRN approaches will be optimized in the sense of maximizing the ergodic rate of the SU, subject to an outage probability constraint for primary communication, denoted by $\mathcal{P}_o$. In what follows, we start with the interweaved CRN approach.

2.5.1 Optimizing generic design parameters of an interweaved CRN

Concentrating on the interweaved approach, the optimization problem to be solved is the following

$$
\begin{aligned}
(\epsilon^*, \tau^*) &= \arg \max_{\epsilon, \tau} \ \mathbb{E}\{R_s^{int}\} \\
s.t. \ \ \mathcal{P}_{out}^{int} &= \mathcal{P}_o, \ \ 0 \leq \tau \leq T, \ \ \epsilon \geq 0,
\end{aligned}
\tag{2.45}
$$

where, considering the outage constraint, bound $\mathcal{P}_{d,B}$, presented in (2.6), is used. By analyzing the outage constraint of (2.45), one can express the energy detection threshold, ϵ, as a function of sensing time, τ, as follows

$$
\epsilon = m_1 \left(\frac{\delta}{\sqrt{\tau f_s}} + 1 \right),
\tag{2.46}
$$

where m_1 and δ are quantities equal to $P_p \sigma_{00}^2 + N_0$ and $\mathcal{Q}^{-1}\left(\frac{\mathcal{P}_o - \mathcal{P}_1}{\mathcal{P}_2 - \mathcal{P}_1} \right)$, respectively and $\mathcal{Q}^{-1}(\cdot)$ is the inverse of $\mathcal{Q}$-function. It should be noted that target outage probability, $\mathcal{P}_o$, is feasible for a specific interval of SINR QoS threshold, such that the argument of function $\mathcal{Q}^{-1}(\cdot)$ belongs to interval $(0,1)$. As a result, problem (2.45) will be expressed as follows

$$
\begin{aligned}
(\epsilon^*, \tau^*) &= \arg \max_{\epsilon, \tau} \ \mathbb{E}\{R_s^{int}\} \\
s.t. \ \ \epsilon &= m_1 \left(\frac{\delta}{\sqrt{\tau f_s}} + 1 \right), \ \ 0 \leq \tau \leq T, \ \ \epsilon \geq 0.
\end{aligned}
\tag{2.47}
$$

With the aim of solving problem (2.47), the following proposition can be proved.

Proposition 3. Function $U(\tau) = \mathbb{E}\{R_s^{int}\}(\tau)$, which is obtained by substituting the outage probability constraint to the objective function of (2.47) is concave for $\tau \in [0, T]$.

Proof. See Appendix .3. □

Capitalizing on Proposition 3, problem (2.47) can be solved by applying a gradient ascent method, which is described in Algorithm 1.

Algorithm 1 Optimizing ϵ and τ for a given $\mathcal{P}_o$

---

1. Initialization $(n = 0)$. Select a $\tau_0 \in [0, T]$ and increase counter by one.

2. For the n-th iteration, compute value τ_n as follows

$$\tau_n = \tau_{n-1} + \lambda \frac{\partial U(\tau)}{\partial \tau}\bigg|_{\tau = \tau_{n-1}}, \tag{2.48}$$

   where λ stands for the step of the algorithm.

3. Increase counter n by one and if $n > N_{max,1}$, where $N_{max,1}$ is a maximum number of iterations, stop, otherwise go to Step 2.

4. Having found τ^* compute the corresponding
   $\epsilon^* = m_1 \left(\frac{\delta}{\sqrt{\tau^* f_s}} + 1 \right).$

In what follows, the level of interference power received at the PU, $\mathcal{I}$, corresponding to the same target outage probability, $\mathcal{P}_o$, will be derived for the underlay CRN approach when MRC BF is applied at $BS\ s$.

2.5.2 Optimizing generic design parameters of an underlay CRN when MRC-based precoding is applied at BS_s

In this case, the interference temperature, $\mathcal{I}^*$, corresponding to the same target outage level, $\mathcal{P}_o$, can be found by setting $\mathcal{P}_{out,MRC}^{und} = \mathcal{P}_o$, which leads to equation $f(\mathcal{I}^*) = 0$. Function $f(\mathcal{I})$ has the expression that follows

$$f(\mathcal{I}) = \mathcal{P}_{out,MRC}^{und} - \mathcal{P}_o, \tag{2.49}$$

where the expression of $\mathcal{P}_{out,MRC}^{und}$ is given in (2.18).

Algorithm 2 Determine $\mathcal{I}^*$ for a given $\mathcal{P}_o$

---

1. Initialization $(n = 0)$. Select an $\mathcal{I}_0 \geq 0$ and increase counter by one.

2. For the n-th iteration, compute value $\mathcal{I}_n$ as follows

$$\mathcal{I}_n = \mathcal{I}_{n-1} - f(\mathcal{I}_{n-1}) \left(\frac{df(\mathcal{I})}{d\mathcal{I}}\bigg|_{\mathcal{I} = \mathcal{I}_{n-1}} \right)^{-1}. \tag{2.50}$$

3. Increase counter n by one and if $n > N_{max,2}$, where $N_{max,2}$ is a maximum number of iterations, stop, otherwise go to Step 2.

As PU outage probability is monotonically increasing with $\mathcal{I}$, it is implied that there exists a single $\mathcal{I}^* \geq 0$ to search for and this can be accomplished by applying Newton's method as it is described in Algorithm 2.

Considering an underlay CRN, where ZF BF is applied at BS s, since zero interference will be created towards the PU, the throughput performance at the SU will be invariant of the outage probability constraint posed by the primary network.

In the section that follows, the throughput performance of the studied CRN approaches will be evaluated.

2.6 Numerical Evaluation

In order to evaluate the performance of the examined CRN approaches under different conditions, extensive Monte Carlo (MC) simulations have been performed, with the aim of confirming the validity of the theoretical expressions derived. More specifically, 5000 MAC frames were simulated. According to the scenario, the strengths of the involved channels are: $\sigma_{pp}^2 = \sigma_{ss}^2 = 10$ dB for the direct links, $\sigma_{ps}^2 = \sigma_{sp}^2 = 9$ dB for the cross-links and $\sigma_{00}^2 = 6$ dB for the link between BS p and BS s, which is devoted to spectrum sensing. Moreover, we set $B = 1$Hz, $f_s = 6$MHz and T=100ms. Also, we consider unit noise variance in the system. In addition, the SINR level of the PU, γ_0, below which an outage occurs is chosen such that only a 10% rate loss, compared to the interference-free case, can be tolerated at the PU.
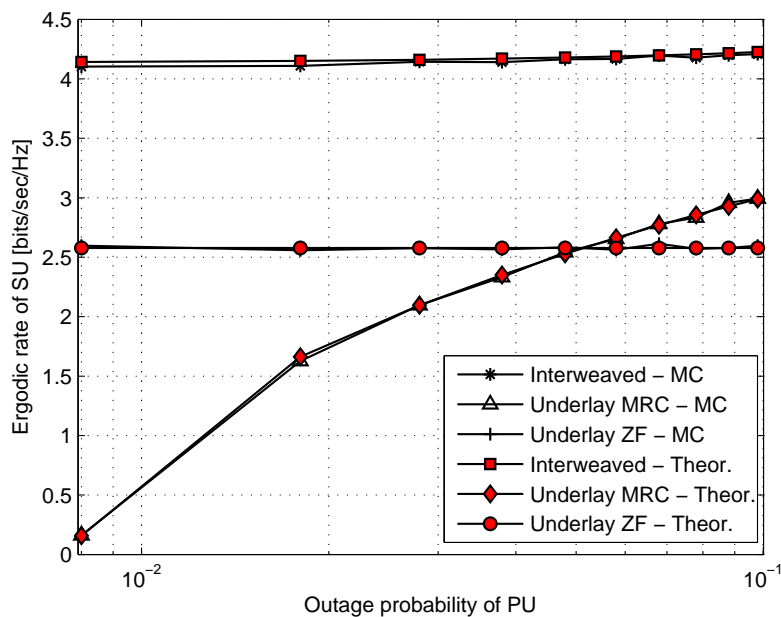
Figure 2.3: Ergodic SU capacity vs. PU outage probability, M=4 antennas, $\mathcal{P}(\mathcal{H}_1) = 0.2$.

In Fig. 2.3, the ergodic rate of the SU, considering an interweaved CRN is illustrated as a function of the primary system's outage probability and compared with the ergodic rate achieved at the SU when the underlay approach (concerning both BF schemes) is adopted. Both MC and theoretical curves are depicted. In the examined scenario, the primary system is sporadically active with probability $\mathcal{P}(\mathcal{H}_1)$= 0.2 and the BSs are equipped with $M = 4$ antennas, each. The curves shown demonstrate a clear rate gain to the benefit of the interweaved CRN approach for the whole examined interval of PU outage probability. However, the SU throughput in the underlay approach, when MRC precoding is applied at BS s, is fastly increasing with the outage

probability level, resulting to a reduced throughput gain in favour of the interweaved approach
for relatively high outage probabilities of the PU. Also, considering the performance of the
underlay approach, when ZF precoding is applied at $BS\ s$, it is observed that it outperforms
the MRC-based one for low PU outage probabilities, while this behavior changes for PU outage
probabilities higher than 5%.
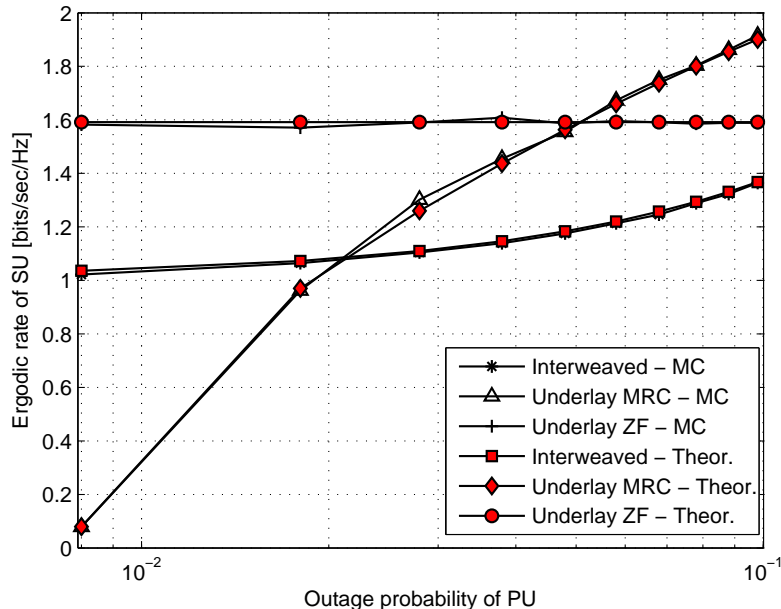
Figure 2.4: Ergodic SU rate vs. PU outage probability, $M=4$ antennas, $\mathcal{P}(\mathcal{H}_1) = 0.8$.

In Fig. 2.4, the achievable average rate of the SU, is depicted as a function of the outage
probability of the PU, with the only difference lying in the fact that the primary system is
characterized by a high activity profile ($\mathcal{P}(\mathcal{H}_1)$=0.8). One can observe that, for low target outage
probabilities at the PU, the ZF-based underlay CRN approach, outperforms the other two, while,
as the outage probability of PU increases, the MRC-based underlay approach starts to show a
performance gain, first in comparison with the interweaved one (when $\mathcal{P}_o$ becomes higher than
2%) and then in comparison with the ZF-based underlay one (when $\mathcal{P}_o$ becomes higher than
5%).

The same performance metric is depicted in Fig. 2.5, as a function of primary system's
activity profile when the target PU outage probability is 1% and for two different numbers of
transmit antennas, $M = 4$ and $M = 8$, respectively. It can be observed that, regardless of
the CRN approach followed, the ergodic rate of the SU is a decreasing function of the activity
rate of primary communication. This can be justified because as the primary network becomes
highly active, the average interference (over time) received at the SU will be increasing. It is
also worth noticing that the rate gain achieved when the number of BS antennas is doubled is
much larger in the MRC-based underlay approach, in comparison with the rate gain achieved
in the interweaved approach, while this gain is zero for the ZF-based underlay approach. Also,
it is interesting to mention that when $M = 8$, the performance of the underlay approach with
MRC BF overcomes the performance of the interweaved one for all levels of primary activity.

In Fig. 2.6, the throughput performance of the SU is illustrated with reference to the number

30
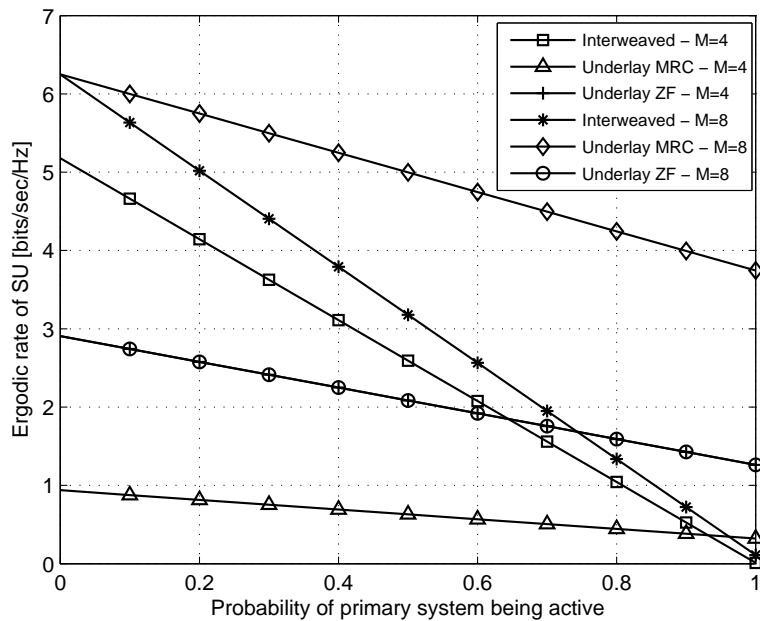
Figure 2.5: Ergodic SU rate vs. primary system's activity profile, target PU outage probability $\mathcal{P}_o = 0.01$.
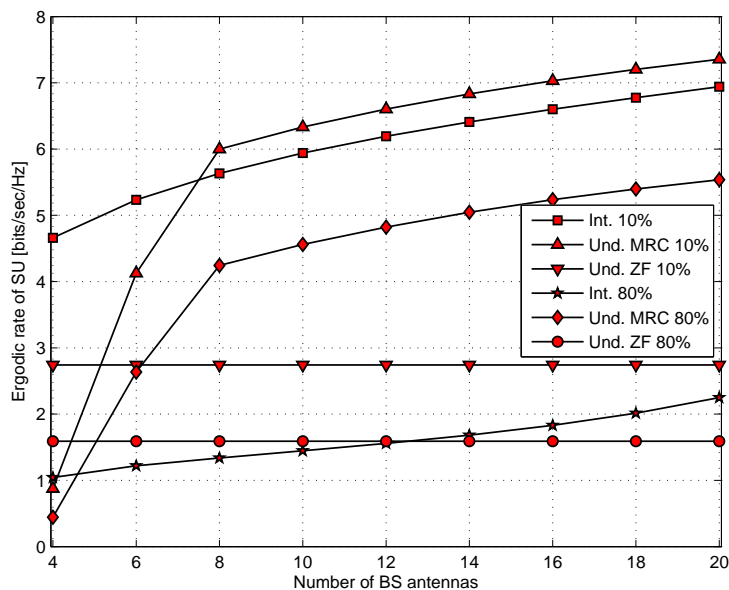
Figure 2.6: Ergodic SU rate vs. number of transmit antennas, M, target PU outage probability $\mathcal{P}_o = 0.01$.

of transmitting antennas, M, for two different levels of primary activity, i.e., for primary systems that are transmitting for the 10% and 80% of the time. Also, the comparison is made for a common PU outage probability level of 1%. In this case, it is clear that an increase in the

number of BS antennas enhances the ergodic rate of the SU, with a large rate gain appearing in
favour of the MRC-based underlay approach, as it was seen in Fig. 2.5.
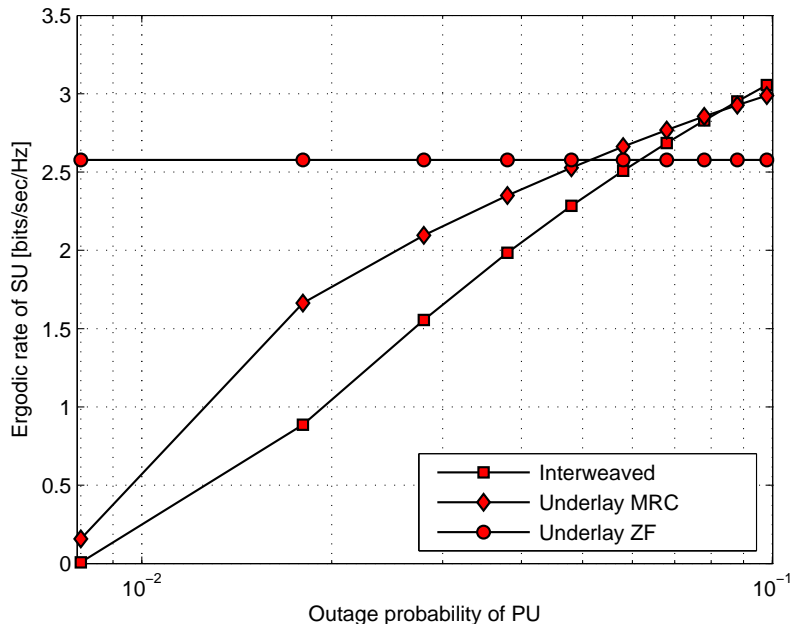
Figure 2.7: Ergodic SU rate vs. PU outage probability, $\mathcal{P}(\mathcal{H}_1) = 0.2$, weak $BS\ p - BS\ s$ link
with strength $\sigma_{00}^2 = -17$ dB.

Moreover, it can be seen that the number of BS antennas over which the MRC-based underlay
approach outperforms the interweaved one in terms of ergodic SU rate, depends on the activity
profile of the primary network. More concretely, this change occurs when $M = 5$ antennas for
a highly active primary network, whereas it is observed when $M = 8$ antennas for a primary
network characterized by low activity.

Finally, in Fig. 2.7 the same metric is depicted as a function of the outage probability of
the PU, when $\mathcal{P}(\mathcal{H}_1) = 0.2$, with the difference that channel $\mathbf{h}_{00}$, is much weaker than before
($\sigma_{00}^2 = -17$ dB). As one would expect, the throughput performance of the interweaved approach
is much more degraded in comparison with the one shown in Fig. 2.3. This occurs because as
the channel useful for spectrum sensing becomes weaker, the secondary transmitter spends a
considerable amount of secondary communication resources towards sensing, which leads to a
degraded ergodic rate at the SU.

2.7 Conclusions

In this chapter, the interweaved CRN approach was examined and compared with the under-
lay CRN approach in terms of the ergodic throughput of the SU for a common PU outage
level. Expressions for the ergodic rate of the SU as well as for the outage probability of primary
communication, were derived for both approaches and it was shown that the performance com-
parison results are driven by a set of key system parameters which are: (a) the activity profile
of the primary system, (b) the number of transmit antennas, as well as (c) the quality of the
sensed channel in the interweaved CRN approach.

In the following part, we focus on the design and evaluation of signal processing algorithms for unprioritized and underlay multi-antenna CRNs, in the presence of mixed instantaneous and statistical CSI. The reason for concentrating on underlay rather than on interweaved CRNs is the observed throughput gain in favour of the underlay approach, in scenarios where multiple antennas are used at the transmitters, especially in the case of highly active primary systems.

Part III

Coordinated CRN BF Schemes with Mixed CSI

Chapter 3

Rate Optimal BF and User Selection for Unprioritized SIMO CRNs

3.1 Introduction

The study of optimal transmission schemes over the interference channel (IC), has attracted significant attention in the recent years. While the capacity achieving scheme remains unknown for the general case, much progress has been reached when it comes to describing optimal strategies in specific settings, one example among others being the Pareto optimal linear transmit BF under single user decoding capability [35]. While rate-optimal BF investigations are typically carried out with little limitations regarding available CSI, practical networks do pose constraints as to how much instantaneous CSI can be acquired, via feedback or pilot schemes. A classical approach for circumventing the practical CSI limitations consists in assuming a quantization scheme with a finite number of bits [36] or in deriving BF solutions from channel statistics alone. BF solutions based on covariance information were reported in [37–41] as well as in [42–47]. More recently, an optimal BF scheme suited to the downlink of a two-user IC based solely on covariance information was derived in [48]. There, the optimal BF vector, based on the covariance matrices of the desired and interfering channels, is shown to be in the form of a generalized eigenvector.

In this chapter, we argue that in the light of current standardization discussions, the assumptions of a CSI setting where only instantaneous (resp. only statistical) channel information is available to all interfering devices is overly optimistic (resp. pessimistic). In fact, forthcoming standard releases for fourth generation (4G) wireless systems stipulate that a given user is allowed to report instantaneous CSI to its home BS, while it cannot report such information to interfering BSs (at least not directly). Such a constraint motivates the use of a "mixed" CSI scenario, where direct (useful) CSI is made available in instantaneous form, while the interfering channels will be known only based on their second order statistics.

In such a setting, we propose to revisit the optimal BF problem for a two-transmitter unprioritized CRN, in the uplink. More specifically, our contributions are as follows:

- We derive a closed form expression for the user rates under single user decoding capability. This expression is a function of the instantaneous desired channel vectors and the covariance matrices of interfering channels.

- By focusing on interference dominated systems, i.e., assuming that interference is the dominant, as compared to noise, source of signal degradation, we derive a novel, simple approximation for the ergodic rate, which leads to a simplified formulation of an optimal receive BF design.

- We derive the optimal receive BF vector in the sense of the ergodic rate for the aforementioned interference dominated regime.

- We make use of the optimal BF design in order to suggest new, coordinated, low complexity multi-user selection schemes. The new schedulers allow to reduce the impact of interference substantially as the number of users increases.

3.2   System Model
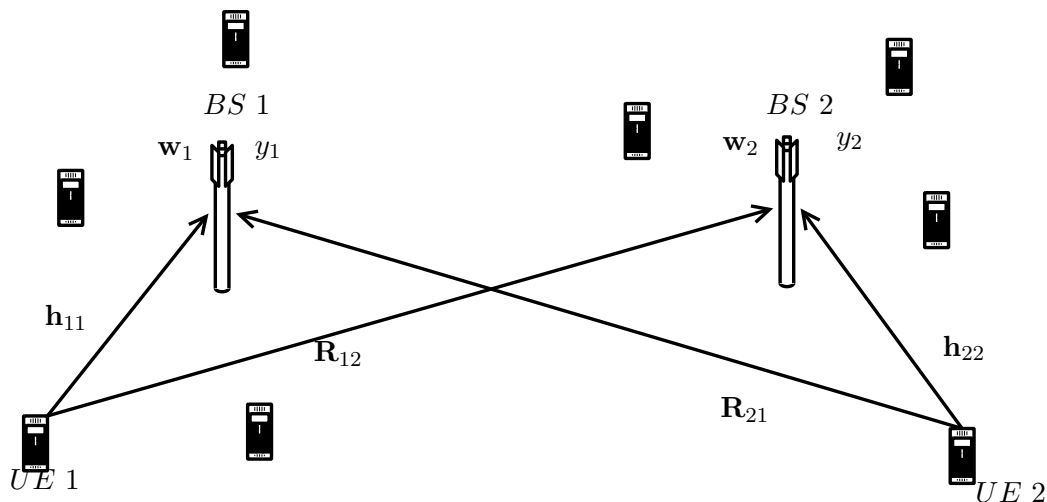
Figure 3.1: Topology of a two-transmitter, unprioritized multiuser network in the uplink.

An unprioritized CRN, consisting of two BSs employing the same frequency resources, as shown in Fig. 3.1, is considered. Both BSs, BS 1 and BS 2, are equipped with M receive antennas, whereas, for the two user equipment (UE) operating in the same frequency slot, i.e., UE 1, UE 2, served by BS 1 and BS 2 respectively, the use of single antenna terminals is assumed. Focusing on the uplink, the signal received at the i-th BS area, $i = 1, 2$ can be written as

$$y_i = \mathbf{w}_i \mathbf{h}_{1i} s_1 + \mathbf{w}_i \mathbf{h}_{2i} s_2 + \mathbf{w}_i \mathbf{z}_i, \tag{3.1}$$

where $\mathbf{h}_{ji}$, $j = 1, 2$ is the $M \times 1$ SIMO Rayleigh fading channel between UE j and BS i undergoing correlation due to the finite multipath angle spread at the BS, $\mathbf{w}_i \in \mathbb{C}^{1 \times M}, i = 1, 2$ is the unit norm, i.e., $\|\mathbf{w}_i\| = 1$, receive BF vector at BS i and $\mathbf{z}_i$ is the $M \times 1$ noise vector, the elements of which are, without loss of generality, assumed to be i.i.d. standard CSCG random variables, i.e., $\mathbf{z}_i \sim \mathcal{CN}(\mathbf{0}, \mathbf{I}_M)$.[1] Assuming that Gaussian codebooks are used for both users' information signals, s_i, it holds that $s_i \sim \mathcal{CN}(0, 1), i = 1, 2$.

---

[1]For the rest of the analysis, we will assume that noise power is equal to one.

Channel vector $\mathbf{h}_{ji}, \quad i, j \in \{1, 2\}$, can be written as

$$\mathbf{h}_{ji} = \mathbf{R}_{ji}^{\frac{1}{2}} \mathbf{h}_{ji}^{(w)}, \tag{3.2}$$

where $\mathbf{R}_{ji}^{\frac{1}{2}}$ is the symmetric square root of the covariance matrix $\mathbf{R}_{ji}$ of channel vector $\mathbf{h}_{ji}$, and $\mathbf{h}_{ji}^{(w)} \sim \mathcal{CN}(\mathbf{0}, \mathbf{I}_M)$. Moreover, it is assumed that the covariance matrix encompasses the transmit power P_i, $i = 1, 2$ of both users as well as the deterministic path loss induced by the wireless channels. Based on (3.1), it is easy to show that the achievable rate for communication of UE i with BS i is defined as [49] [2]

$$R_i = \log \left(1 + \frac{|\varsigma_i|^2}{1 + |\pi_i|^2} \right), \tag{3.3}$$

where $\varsigma_i = \mathbf{w}_i \mathbf{h}_{ii}$ and $\pi_i = \mathbf{w}_i \mathbf{h}_{ji}$, with $\mathbf{h}_{ji}, j \neq i$ denoting the interfering channel vector. From (3.2), quantity π_i is written as

$$\pi_i = \mathbf{w}_i \mathbf{R}_{ji}^{\frac{1}{2}} \mathbf{h}_{ji}^{(w)}. \tag{3.4}$$

By defining the quantity $\alpha_i = 1 + |\varsigma_i|^2$, (3.3) is readily expressed as

$$R_i = \log(\alpha_i + |\pi_i|^2) - \log(1 + |\pi_i|^2). \tag{3.5}$$

One of the most commonly adopted criteria for user selection and BF design in the presence of interfering users is the sum rate maximization criterion given instantaneous CSI for all, direct and interfering, channels [50–54]. In the system model that we investigate, the use of such user selection and BF criteria would require acquiring and exchanging instantaneous CSI that, among others, presumes high rate communication links for the cooperation of BSs and thus, increases the cost of the network. Therefore, in our analysis we investigate a realistic scheme that is based on the exchange of statistical CSI between the BSs and, specifically the covariance of channel $\mathbf{h}_{ji}$. Since such statistics are expected to vary slowly with time, the information exchange required in order to obtain $\mathbf{R}_{ji}$ is significantly smaller as compared to the case of exchanging instantaneous CSI. Hence, we assume knowledge of $\mathbf{R}_{ji}$, $j \neq i$ at BS i, and we pose and solve the receive BF problem at BS i with the aim of maximizing its expected rate, given the instantaneous direct channel $\mathbf{h}_{ii}$, denoted as $\mathbb{E}_{|\mathbf{h}_{ii}} \{R_i\}$. To do so, we calculate the statistical distribution of interference term $|\pi_i|^2$ and then $\mathbb{E}_{|\mathbf{h}_{ii}} \{R_i\}$. In the sequel, an approximation of $\mathbb{E}_{|\mathbf{h}_{ii}} \{R_i\}$ for an interference dominated system is derived. Following that, an analytical method is given for optimal receive BF design in terms of maximizing $\mathbb{E}_{|\mathbf{h}_{ii}} \{R_i\}$. These two steps are further described in the two following sections.

3.3   Calculation of the conditional expected sum rate

In order to calculate $\mathbb{E}_{|\mathbf{h}_{ii}} \{R_i\}$, first the PDF of the interference term $|\pi_i|^2$ is derived as shown in the following analysis.

---

[2]Throughout the chapter, information rates will be measured in nats/sec/Hz.

3.3.1 Distribution of the interference term

Using standard properties of complex Gaussian random variables, it is easy to prove that π_i for a given $\mathbf{w}_i$ is a complex Gaussian random variable with variance equal to $\sigma_{\pi_i}^2 = ||\mathbf{w}_i \mathbf{R}_{ji}^{\frac{1}{2}}||^2$. As a result, random variable $\beta_i = |\pi_i|^2$ follows a chi-squared distribution of the form

$$p_{\beta_i}(x) = \frac{1}{\sigma_{\pi_i}^2} \exp\left(-\frac{x}{\sigma_{\pi_i}^2}\right). \tag{3.6}$$

In what follows, (3.6) is employed in order to calculate $\mathbb{E}_{|\mathbf{h}_{ii}}\{R_i\}$.

3.3.2 Calculation of $\mathbb{E}_{|\mathbf{h}_{ii}}\{R_i\}$

Combining (3.5) and (3.6), $\mathbb{E}_{|\mathbf{h}_{ii}}\{R_i\}$ is written as

$$\mathbb{E}_{|\mathbf{h}_{ii}}\{R_i\} = \int_0^\infty \left(\log(\alpha_i + \beta_i) - \log(1 + \beta_i)\right) p_{\beta_i}(\beta_i) d\beta_i. \tag{3.7}$$

The following theorem states the result.

Theorem 1. The expected rate $\mathbb{E}_{|\mathbf{h}_{ii}}\{R_i\}$ defined in (3.7) for the system model in Fig. 3.1 is expressed as

$$\mathbb{E}_{|\mathbf{h}_{ii}}\{R_i\} = \log(\alpha_i) + e^{\frac{\alpha_i}{\sigma_{\pi_i}^2}} E_1\left(\frac{\alpha_i}{\sigma_{\pi_i}^2}\right) - e^{\frac{1}{\sigma_{\pi_i}^2}} E_1\left(\frac{1}{\sigma_{\pi_i}^2}\right). \tag{3.8}$$

Proof. Using integration by parts along with [6, 5.1.28], it is easy to prove that for any positive α and δ

$$\int_0^\infty \frac{1}{\delta} e^{-\frac{\beta}{\delta}} \log(\alpha + \beta) d\beta = \log(\alpha) + e^{\frac{\alpha}{\delta}} E_1\left(\frac{\alpha}{\delta}\right). \tag{3.9}$$

Therefore, by substituting (3.9) in (3.7), (3.8) is derived. □

Focusing on the behavior of (3.8) in the case of interference dominated systems, the following proposition can be proved.

Proposition 4. For an interference dominated system, the (conditional) expected rate (3.8) can be closely approximated as

$$\mathbb{E}_{|\mathbf{h}_{ii}}\{R_i\} \approx \log\left(\frac{\alpha_i}{\sigma_{\pi_i}^2}\right) + e^{\frac{\alpha_i}{\sigma_{\pi_i}^2}} E_1\left(\frac{\alpha_i}{\sigma_{\pi_i}^2}\right) + \gamma, \tag{3.10}$$

where $\gamma \approx 0.5772$ is the Euler-Mascheroni constant.

Proof. Assuming that interference is the dominant degradation factor, or equivalently that interference power is sufficiently larger than noise power, it holds that $\sigma_{\pi_i}^2 \gg 1$. Hence, the last term on the right hand side of (3.8) asymptotically converges to [6, 5.1.11]

$$e^{\frac{1}{\sigma_{\pi_i}^2}} E_1\left(\frac{1}{\sigma_{\pi_i}^2}\right) \xrightarrow{\sigma_{\pi_i}^2 \gg 1} -\gamma + \log\left(\sigma_{\pi_i}^2\right). \tag{3.11}$$

Consequently, one can approximate (3.8) by

$$\mathbb{E}_{|\mathbf{h}_{ii}}\{R_i\} \approx \log\left(\frac{\alpha_i}{\sigma_{\pi_i}^2}\right) + e^{\frac{\alpha_i}{\sigma_{\pi_i}^2}} E_1\left(\frac{\alpha_i}{\sigma_{\pi_i}^2}\right) + \gamma. \tag{3.12}$$

□

In the following, a receive BF design is proposed based on maximizing the expected rates $\mathbb{E}_{|\mathbf{h}_{ii}}\{R_i\}, i = \{1,2\}$ as calculated by employing (3.10).

3.4 Optimal Receive BF

Capitalizing on the simple closed form expression (3.10), one can explicitly derive the optimal BF vector for interference dominated systems, i.e., the BF vector that maximizes (3.10). This is illustrated in the following proposition

Proposition 5. The optimal receive BF vector at BS i is the unit-norm dominant generalized eigenvector (DGE) [3] of the pair $((\mathbf{I}_M + \mathbf{h}_{ii}\mathbf{h}_{ii}^H), \mathbf{R}_{ji}), i \neq j$.

Proof. The optimal solution is reached by solving the following optimization problem at BS i

$$\mathbf{w}_i^{opt} = \arg\max_{\mathbf{w}_i} \mathbb{E}_{|\mathbf{h}_{ii}}\{R_i\}, i \in \{1,2\}. \tag{3.13}$$

To start, one can rewrite $\mathbb{E}_{|\mathbf{h}_{ii}}\{R_i\}$ as

$$\mathbb{E}_{|\mathbf{h}_{ii}}\{R_i\} = \mathcal{U}(\lambda_{\mathbf{w}_i}), \text{ where } \lambda_{\mathbf{w}_i} = \frac{1 + \mathbf{w}_i\mathbf{h}_{ii}\mathbf{h}_{ii}^H\mathbf{w}_i^H}{\mathbf{w}_i\mathbf{R}_{ji}\mathbf{w}_i^H}, \quad i \in \{1,2\}. \tag{3.14}$$

The function $\mathcal{U}(\cdot)$ is defined as

$$\mathcal{U}(\lambda) = \log(\lambda) + e^\lambda E_1(\lambda) + \gamma, \tag{3.15}$$

where λ is a dummy variable. Since $\|\mathbf{w}_i\| = 1$, $\lambda_{\mathbf{w}_i}$ can be expressed as

$$\lambda_{\mathbf{w}_i} = \frac{\mathbf{w}_i(\mathbf{I}_M + \mathbf{h}_{ii}\mathbf{h}_{ii}^H)\mathbf{w}_i^H}{\mathbf{w}_i\mathbf{R}_{ji}\mathbf{w}_i^H}, \quad i \in \{1,2\}. \tag{3.16}$$

By differentiating $\mathcal{U}(\lambda)$ and using [6, eq. 5.1.26], one can prove that $\mathcal{U}(\lambda)$ is an increasing function of λ. Thus, the optimization problem (3.13) is equivalent to the Rayleigh - Ritz ratio maximization problem

$$\mathbf{w}_i^{opt} = \arg\max_{\mathbf{w}_i} \lambda_{\mathbf{w}_i}, i \in \{1,2\}. \tag{3.17}$$

By setting the derivative of (3.16) equal to zero, it can be seen that the optimal BF vector is the one that satisfies the equation

$$(\mathbf{I}_M + \mathbf{h}_{ii}\mathbf{h}_{ii}^H)\mathbf{w}_i^H = \lambda_{\mathbf{w}_i}\mathbf{R}_{ji}\mathbf{w}_i^H. \tag{3.18}$$

As a result, by inspecting (3.18) it can be seen that the optimal BF vector for BS i is the eigenvector corresponding to the maximum eigenvalue of matrix $\mathbf{R}_{ji}^{-1}(\mathbf{I}_M + \mathbf{h}_{ii}\mathbf{h}_{ii}^H)$, that is, the DGE of matrix pair $((\mathbf{I}_M + \mathbf{h}_{ii}\mathbf{h}_{ii}^H), \mathbf{R}_{ji})$. $\square$

The above solution is reminiscent of the one in [48], with the key difference lying in the fact that the left hand side of (3.18) uses an instantaneous "estimate" of the covariance $\mathbf{R}_{ii}$ exploited in [48]. Moreover, unlike [48], the obtained solution is independent of the number of receive antennas. In the following, new, low complexity user selection algorithms are introduced that exploit the derived BF solution.

---

[3]We define the DGE of a pair of matrices $(\mathbf{A}, \mathbf{B})$ as the eigenvector corresponding to the maximum eigenvalue of the matrix $\mathbf{C} = \mathbf{B}^{-1}\mathbf{A}$.

3.5   Coordinated User Selection Algorithm

Given $N_i, i = 1, 2$, users within the coverage area (CA) of BS i, optimal user selection with respect to the criterion adopted for BF design, would involve searching over all the $N_1 \times N_2$ possible user pairs in order to find the pair $\{\kappa_1, \kappa_2\}$, $\kappa_1 \in [1, N_1], \kappa_2 \in [1, N_2]$ that maximizes the sum of conditional expected rates, i.e., the pair

$$\{\kappa_1, \kappa_2\} = \arg\max_{k_1, k_2} \mathbb{E}_{|\mathbf{h}_{11}}\{R_1(k_1, k_2)\} + \mathbb{E}_{|\mathbf{h}_{22}}\{R_2(k_1, k_2)\}, \tag{3.19}$$

where $R_i(k_1, k_2)$ denotes the instantaneous information rate at BS i, $i = 1, 2$, when users indexed by k_1 and k_2 are scheduled by BS 1 and BS 2 respectively. To overcome the increased complexity of this *exhaustive coordinated* approach, motivated by [55], we propose a novel greedy user selection algorithm. The algorithm is based on an iterative optimization procedure where, on each iteration, BS i decides in favour of user κ_i that maximizes the sum of conditional expected rates $\mathbb{E}_{|\mathbf{h}_{11}}\{R_1(\cdot, \cdot)\} + \mathbb{E}_{|\mathbf{h}_{22}}\{R_2(\cdot, \cdot)\}$, given that BS j, $j \neq i$ has decided upon user κ_j. In what follows, this algorithm, henceforth characterized as the *centralized coordinated* algorithm, is summarized.

Algorithm 3 Centralized coordinated user selection algorithm

Initialization:

- Randomly select a user κ_2 in the CA of BS 2
- Set the iteration number, $\nu = 0$.

Step 1:

- Set $\nu = \nu + 1$
- Select the user with index κ_1 in the CA of BS 1 that satisfies

$$\kappa_1 = \arg\max_{k1} \mathbb{E}_{|\mathbf{h}_{11}}\{R_1(k_1, \kappa_2)\} + \mathbb{E}_{|\mathbf{h}_{22}}\{R_2(k_1, \kappa_2)\}. \tag{3.20}$$

Step 2:

- Select the user with index κ_2 in the CA of BS 2 that satisfies

$$\kappa_2 = \arg\max_{k2} \mathbb{E}_{|\mathbf{h}_{11}}\{R_1(\kappa_1, k_2)\} + \mathbb{E}_{|\mathbf{h}_{22}}\{R_2(\kappa_1, k_2)\}. \tag{3.21}$$

Step 3:

- If the number of iterations, ν, is smaller than a predefined threshold, go back to Step 1 and iterate.

With the proposed algorithm, at each iteration the decision of BS j, given the previous decision of BS i, leads to the selection of a user that increases, or, in the worst case, preserves the expected sum rate obtained from the previous iteration. Thus, the algorithm always converges to a solution. However, a drawback of this algorithm is the fact that apart from slow-varying covariance information, also instantaneous CSI needs to be exchanged between the BSs. As a result,

in addition to the centralized coordinated algorithm, we propose an iterative *distributed coordinated* user selection approach, in which at each iteration, BS i selects user κ_i that maximizes the expected rate of its own CA rather than the expected sum rate, that is

$$\kappa_i = \arg\max_{k_i} \mathbb{E}_{|\mathbf{h}_{ii}}\{R_i(k_i, \kappa_j)\}, \quad i \in \{1, 2\}, \quad j \neq i, \tag{3.22}$$

where κ_j is the user already selected by BS j.

3.6   Numerical Results

In order to evaluate the performance of the proposed receive BF and user selection schemes, extensive MC simulations of a two-BS, unprioritized CRN have been performed. In the simulations setup, a spectrum sharing scenario is considered, in which two BSs are located in such a way that the two CAs overlap with each other (by a factor of 50% in our scenario). In this scenario it has been assumed that the users in each CA were uniformly distributed and that both BS CAs have common signal-to-noise ratio (SNR) characteristics, i.e., the same transmit power and BS CA radius. Some further simulation parameters are given in Table 3.1.

Table 3.1: Basic simulation parameters

BS CA radius	1 km
Number of BS antennas	2
Path loss exponent	3
Carrier frequency	2 GHz
Antenna spacing	$\lambda/2$
AOA distribution	Gaussian
Multipath angle spread	30 degrees

The coefficients of covariance matrices $\mathbf{R}_{ji}, \quad i, j \in \{1, 2\}$ are computed as in [18]

$$\mathbf{R}_{ji}(m, n) = \frac{\beta_{ji}}{\sqrt{2\pi}\sigma} \int_{-\infty}^{\infty} e^{j2\pi \frac{D}{\lambda}(n-m)cos(\theta+\bar{\theta}_{ji})-\frac{\theta^2}{2\sigma^2}} \mathrm{d}\theta, \tag{3.23}$$

where β_{ji} is the distance-based path loss between the user scheduled by BS j and BS i, σ is the multipath angle spread, considered to be the same for both desired and interference channels, D is the antenna spacing at BS side, λ is the wavelength of the signal and $\bar{\theta}_{ji}$ is the mean angle of arrival (AOA) between the user scheduled by BS j and BS i. The distance-based path loss is defined as:

$$\beta_{ji} = \frac{\alpha}{d_{ji}^{\gamma_{path}}} \tag{3.24}$$

where α stands for a constant which depends on the prescribed average SNR at the BS CA edge, d_{ji} is the geographical distance between the user scheduled by BS j and BS i and γ_{path} denotes the path loss exponent.

In Fig. 3.2 the achievable expected sum rate of the proposed BF scheme is depicted as a function of the average SNR at the BS CA edge and compared with the expected sum rate of the MRC BF scheme. The results correspond to the case that $N_1 = N_2 = 1$ user/BS CA.
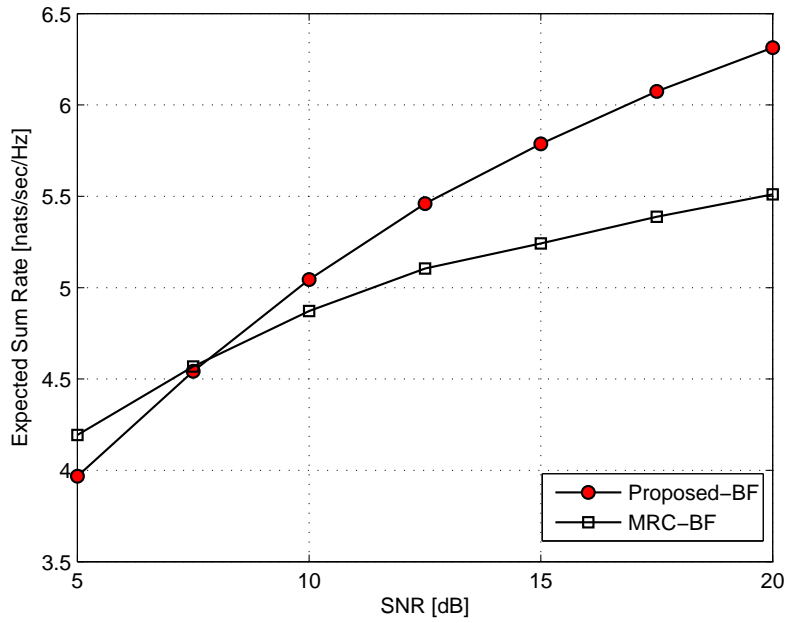
Figure 3.2: Expected sum rate vs. SNR for the two examined BFs, for 1 user/BS CA.
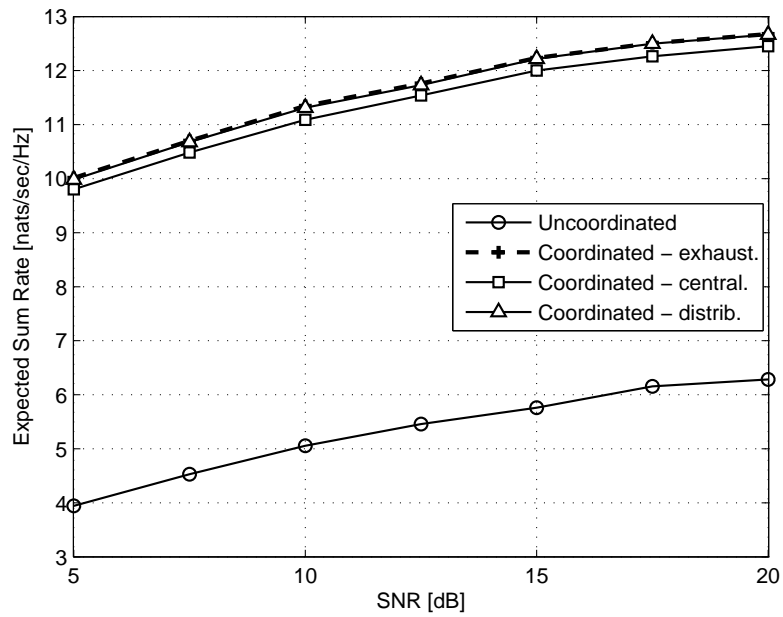
Figure 3.3: Expected sum rate vs. SNR for 10 users/BS CA.

MC averaging is performed with respect to the two users' positions/covariance structure and instantaneous channel realizations. The motivation behind this comparison is the fact that MRC is perhaps the closest, in terms of required CSI, to the proposed BF scheme. The sum rate curves

44
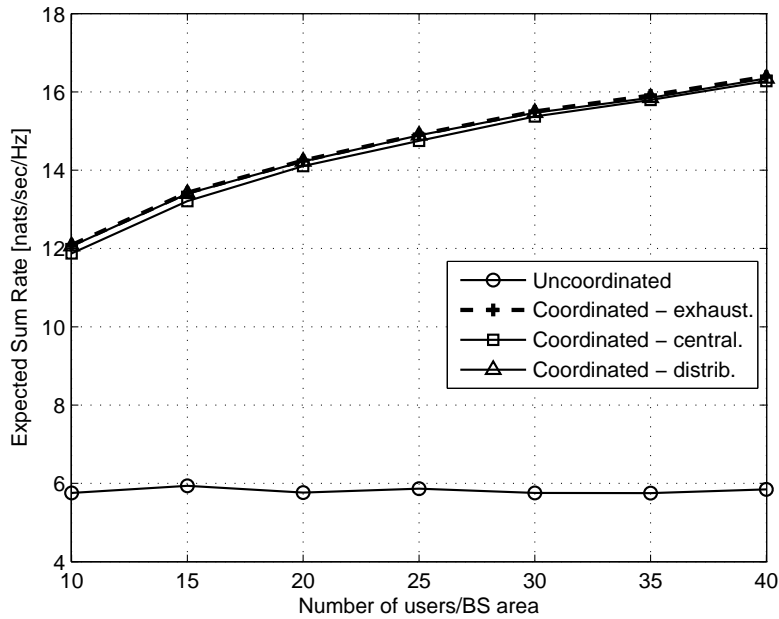
Figure 3.4: Expected sum rate vs. N, SNR=15dB.

demonstrate the superiority of the proposed BF scheme for almost all the examined SNR levels.

In Fig. 3.3 the expected sum rate for systems employing the proposed BF and user selection schemes is depicted as a function of the average SNR at the CA edge for the case that $N_1 = N_2 = 10$ users/BS CA. Specifically, four different user selection scenarios are compared: the uncoordinated one (random user selection), the exhaustive coordinated one, the centralized coordinated one as well as the distributed coordinated one (one iteration). It is evident that both the centralized and distributed greedy approaches achieve a performance which is marginally lower than the exhaustive one. Additionally, the coordination gain is evident for the whole SNR range.

In Fig. 3.4, the expected sum rate of the system is depicted with respect to the number of users per BS CA, assuming that $N_1 = N_2 = N$ users/BS CA. The average SNR level at the BS CA edge for our simulation setup was set equal to 15dB. We observe that both the centralized and the distributed (with only one iteration) low complexity approaches achieve a slightly inferior performance with respect to the coordinated exhaustive approach. Moreover, both the proposed and the coordinated exhaustive algorithms, offer a clear multi-user diversity gain that increases with respect to N.

3.7   Conclusions

In this chapter, the uplink of a two-transmitter, unprioritized CRN has been investigated. Closed form expressions for the expected rate, conditioned on instantaneous CSI for the direct channels have been derived. By examining the asymptotic behavior of the derived expression with respect to interference dominated systems, an optimal receive BF scheme has been developed that exploits both instantaneous (for direct channels) and statistical (for interfering channels)

45

CSI. Finally, novel low complexity user selection algorithms have been proposed, that achieve performance similar to the optimum, with respect to the available CSI, user selection policy.

In the following chapter, we investigate the problem of optimizing multiple antenna combining at the transmitters in the downlink of an underlay CRN, considering exchange of only statistical CSI.

Chapter 4

Team Decisional BF for Underlay MISO CRNs

4.1 Introduction

The problem of optimizing the coexistence of spectrum sharing devices in radio networks is emerging as an important one in view of improving the efficiency of future mobile communications systems. In the classical underlay CR context, a primary operator allows the reuse of its spectral resources by a newcoming secondary system under a maximum tolerated interference level generated by the secondary transmitter [10] [12]. Under this setup, several approaches have been considered to optimize a BF vector at the transmitter side so as to strike a balance between maximizing the SNR at the served users and reducing the generated interference from the secondary transmitter [56–60].

In this chapter, we take on the problem of optimizing multiple antenna combining at the transmitters in the downlink of an underlay CRN, however a meaningful revision of proposals is suggested, considering the classical underlay model so far adopted in much of the literature. First, we propose to use a QoS constraint at the primary terminal in the form of a minimum data rate target. This is an alternative to the traditional interference power constraint which has the drawback of neglecting the strength of the primary link, hence oversimplifying the actual impact that the secondary link has over the performance of the primary system. Secondly, we place emphasis on more realistic CSI scenarios at the transmitter (CSIT), whereby only a "mixed" form of CSIT is available at the primary and secondary transmitters. More precisely, one assumes that direct channels between a serving transmitter to a served terminal are known in instantaneous form, while other channels are only known through second order statistics (covariance) information. Under this scenario, we consider the problem of BF design at both the primary and secondary transmitters so as to maximize secondary rate performance under a QoS target on the primary terminal. Thirdly, we are emphasizing *distributed* techniques, where each transmitter makes a BF decision under its *locally* available CSIT together with channel covariance information. We highlight the connection with *team decision theory*, i.e., distributed multi-agent decision making [61]. More concretely, our contributions are the following:

- We derive a closed-form expression for the achievable expected user rates, conditioned on the knowledge of the instantaneous direct channels, as well as a simple approximation of this expression by focusing on interference-limited systems, i.e., systems in which

47

interference is the dominant factor of signal degradation, compared to noise.

- We formulate the problem of optimal distributed transmit BF, with respect to a MISO underlay CRN with distributed CSIT. We show an algorithm inspired from team decisional methods. The BF solutions are reached by solving semidefinite programs (SDPs). Finally, we numerically evaluate its performance by making a comparison with known precoding solutions.

4.2 System Model - Derivation of the Conditional Expected Rates

The system under investigation is shown in Fig. 4.1. It consists of a primary BS, $BS\ p$, that communicates with a PU, $UE\ p$, in the presence of a secondary BS, $BS\ s$ that communicates with a SU, $UE\ s$. Assuming an underlay scenario, both $BS\ p$ and $BS\ s$ are sharing the same frequency resources, while they are both equipped with M antennas, whereas the two users use single antenna terminals. For such a system, a distributed CSIT architecture is examined with emphasis on downlink communication.
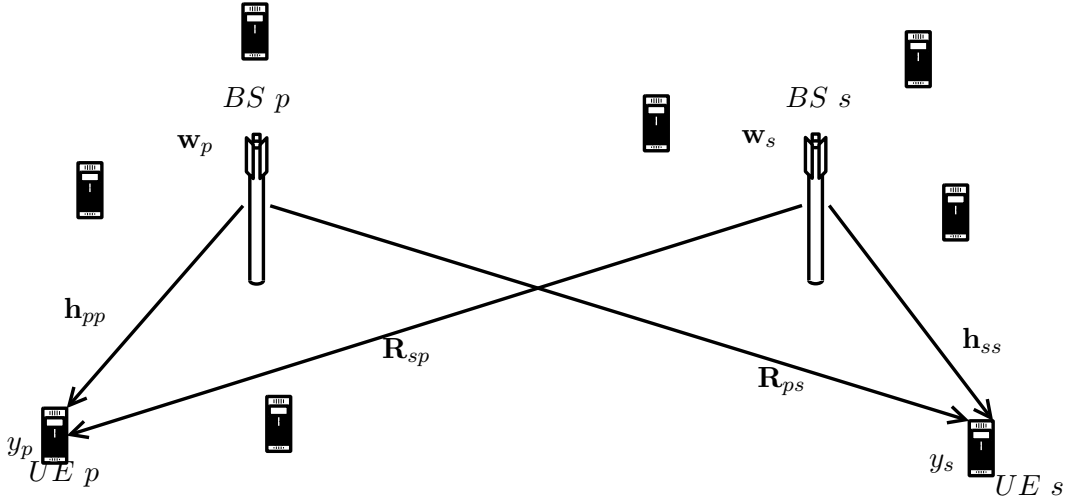
Figure 4.1: Topology of a MISO CRN.

The signal received at user $UE\ i$ can be expressed as

$$y_i = \mathbf{h}_{ii}^H \mathbf{w}_i s_i + \mathbf{h}_{ji}^H \mathbf{w}_j s_j + n_i,\ i,j = \{p,s\},\ j \neq i, \tag{4.1}$$

where $\mathbf{h}_{ii}$, $i = \{1,2\}$ is the direct $M \times 1$ MISO Rayleigh fading channel between $BS\ i$ and $UE\ i$, $\mathbf{h}_{ji}$, $j \neq i$ is the $M \times 1$ interfering Rayleigh fading channel between $BS\ j$ and $UE\ i$, whereas $\mathbf{w}_p$ and $\mathbf{w}_s$ are the $M \times 1$ complex transmit BF vectors at $BS\ p$ and $BS\ s$, respectively, with $\|\mathbf{w}_p\|^2 = P_p^{max}$ and $\|\mathbf{w}_s\|^2 \leq P_s^{max}$, P_p^{max} and P_s^{max} being the maximum available power levels at $BS\ p$ and $BS\ s$. Additionally, $n_i \sim \mathcal{CN}(0, N_0)$ is the additive Gaussian noise at the receiver side[1] and s_i, s_j are the information symbols, for the transmission of which, Gaussian codebooks

---

[1]For the rest of our analysis and without any loss of generality, we will assume that noise density, N_0, is equal to one.

are used, i.e., $s_i \sim \mathcal{CN}(0,1)$, $i = \{p, s\}$.

Correlated Rayleigh fading is assumed for both direct and interfering channels. As a result, channel vector $\mathbf{h}_{ji}$, $i, j \in \{p, s\}$ can be expressed as

$$\mathbf{h}_{ji} = \mathbf{R}_{ji}^{\frac{1}{2}} \mathbf{h}_{ji}^{(w)}, \tag{4.2}$$

where $\mathbf{R}_{ji}^{\frac{1}{2}}$ is the symmetric square root of the covariance matrix $\mathbf{R}_{ji}$ of vector $\mathbf{h}_{ji}$, and $\mathbf{h}_{ji}^{(w)} \sim \mathcal{CN}(\mathbf{0}, \mathbf{I}_M)$. It should be noted that the covariance matrix includes the parameters determining the SNR, such as the deterministic path loss. By analyzing (4.1), one can easily show that the achievable instantaneous rate for communication between $BS\ i$ and $UE\ i$ is defined as

$$R_i = \log\left(1 + \frac{|\eta_i|^2}{1 + |\zeta_i|^2}\right), \tag{4.3}$$

where $\eta_i = \mathbf{h}_{ii}^H \mathbf{w}_i$ and $\zeta_i = \mathbf{h}_{ji}^H \mathbf{w}_j$, $j \neq i$. A realistic assumption that can be made is that $BS\ i$ collects instantaneous CSI for its direct channel $\mathbf{h}_{ii}$, $i = p, s$, as well as statistical CSI for all links i.e., the covariance matrices $\mathbf{R}_{ji}$, $i, j = \{p, s\}^2$. Assuming that BF vectors $\mathbf{w}_p, \mathbf{w}_s$ are functions of this information, given any pair of such BF vectors, one can calculate the expected rates, conditioned on the instantaneous direct channels, i.e., expectation is taken over the interference terms, in closed form. Specifically, by following the proof steps of Theorem 1 in the previous chapter, it is easy to prove that the expected rate of $UE\ i$, hereby denoted as $\mathbb{E}_{|\mathbf{h}_{ii}}\{R_i\}$, $i = \{p, s\}$, conditioned on the instantaneous direct channel is expressed as

$$\mathbb{E}_{|\mathbf{h}_{ii}}\{R_i\} = \log(\alpha_i) + e^{\frac{\alpha_i}{\sigma_{\zeta_i}^2}} E_1\left(\frac{\alpha_i}{\sigma_{\zeta_i}^2}\right) - e^{\frac{1}{\sigma_{\zeta_i}^2}} E_1\left(\frac{1}{\sigma_{\zeta_i}^2}\right), \tag{4.4}$$

where $\alpha_i = 1 + |\eta_i|^2$ and $\sigma_{\zeta_i}^2 = \|\mathbf{w}_j^H \mathbf{R}_{ji}^{\frac{1}{2}}\|^2$, $j \neq i$. Moreover, for interference dominated systems in which $\sigma_{\zeta_i}^2 \gg N_0$, following an approach similar to Proposition 4, it can be shown that (4.4) can be effectively approximated as

$$\mathbb{E}_{|\mathbf{h}_{ii}}\{R_i\} = \log\left(\frac{\alpha_i}{\sigma_{\zeta_i}^2}\right) + e^{\frac{\alpha_i}{\sigma_{\zeta_i}^2}} E_1\left(\frac{\alpha_i}{\sigma_{\zeta_i}^2}\right) + \gamma. \tag{4.5}$$

In the following section, by taking into account expression (4.5), the problem of joint optimal design of transmit BF vectors with limited CSIT, for both primary and secondary communication is presented and a distributed method for solving this problem is developed. The proposed design is based on the maximization of transmission rate $\mathbb{E}_{|\mathbf{h}_{ss}}\{R_s\}$, while satisfying a QoS constraint for rate $\mathbb{E}_{|\mathbf{h}_{pp}}\{R_p\}$.

4.3 Transmit CR BF with Distributed CSIT

With the assumption that BSs are allowed to exchange the available CSIT, the problem of maximizing rate $\mathbb{E}_{|\mathbf{h}_{ss}}\{R_s\}$ at the SU, subject to a QoS constraint for rate $\mathbb{E}_{|\mathbf{h}_{pp}}\{R_p\}$ achieved

---

[2]Note that this assumption slightly extends the mixed CSI scenario presented in the previous chapter, by also considering knowledge of covariance information regarding direct channels.

at the PU, is mathematically formulated as

$$
\begin{aligned}
&\underset{\mathbf{w}_p, \mathbf{w}_s \in \mathbb{C}^M}{\text{maximize}} && \mathbb{E}_{|\mathbf{h}_{ss}}\{R_s\} \\
&\text{subject to} && \mathbb{E}_{|\mathbf{h}_{pp}}\{R_p\} \geq T, \\
& && \|\mathbf{w}_p\|^2 = P_p^{max}, \quad \|\mathbf{w}_s\|^2 \leq P_s^{max},
\end{aligned}
\tag{4.6}
$$

where T stands for the QoS threshold at UE p and the expected rates are obtained from (4.5). Examining an interference dominated scenario, i.e., employing expression (4.5) and the fact that function $f(x) = \log(x) + e^x E_1(x) + \gamma$, is a monotonically increasing function of x, it is easy to show that problem (4.6) is equivalent to the following one

$$
\begin{aligned}
&\underset{\mathbf{w}_p, \mathbf{w}_s \in \mathbb{C}^M}{\text{maximize}} && \frac{1 + \mathbf{w}_s^H \mathbf{h}_{ss} \mathbf{h}_{ss}^H \mathbf{w}_s}{\mathbf{w}_p^H \mathbf{R}_{ps} \mathbf{w}_p} \\
&\text{subject to} && \frac{1 + \mathbf{w}_p^H \mathbf{h}_{pp} \mathbf{h}_{pp}^H \mathbf{w}_p}{\mathbf{w}_s^H \mathbf{R}_{sp} \mathbf{w}_s} \geq \tau \\
& && \|\mathbf{w}_p\|^2 = P_p^{max}, \quad \|\mathbf{w}_s\|^2 \leq P_s^{max},
\end{aligned}
\tag{4.7}
$$

where τ is the solution to the equation $T = f(\tau)$. However, in our analysis we consider a distributed architecture where we assume that no instantaneous CSI exchange is allowed between BSs. Thus, each BS tries to solve the BF problem by exploiting only its locally available CSIT by applying the approach presented in the following section.

4.3.1 Distributed information structure and BF

Since the two BSs have different views (instantaneous or statistical) of the same global downlink channel, the optimal transmit BF problem can be examined within the framework of team decision theory [61–63]. Following a team decisional approach, we can then define the distributed BF design problem by means of the following components [61]:

1. The **observations** (available CSIT) at BS p and BS s, denoted as $\mathbf{z}_p = [\mathbf{h}_{pp}, \mathbf{R}_{pp}, \mathbf{R}_{ps}, \mathbf{R}_{sp}, \mathbf{R}_{ss}]$ and $\mathbf{z}_s = [\mathbf{h}_{ss}, \mathbf{R}_{ss}, \mathbf{R}_{ps}, \mathbf{R}_{sp}, \mathbf{R}_{pp}]$, respectively.

2. A **transmission strategy** $g_i(\cdot), i = \{p, s\}$ available at BS i that is used in order to calculate BF vector $\mathbf{w}_i = g_i(\mathbf{z}_i)$.

3. An estimated **model** $\hat{g}_i(\cdot), i = \{p, s\}$ of strategy $g_i(\cdot), i = \{p, s\}$ available at BS j, $j \neq i$. In our case this model is based on a weighted linear combination of MRC and Statistical Zero-Forcing (SZF) BF[3]. The reasoning for using such a model is based on the fact that in [35] it was shown that for the two-user case, any point of the Pareto boundary of the achievable rate region of the MISO interference channel corresponds to BF vectors that are linear combinations of the MRC and ZF BF schemes. Thus, since the interference channels are statistically known at each BS, one could argue that a linear combination of MRC and SZF is a meaningful approximation to strategies corresponding to the Pareto boundary.

4. A **utility criterion** for the problem, which, in our case, is the expected rate of SU, $\mathbb{E}\{R_s\}$.

---

[3]In the case of SZF, we assume that the selected BF vector is perpendicular to the dominant eigenvector of the interfering channel's covariance matrix.

Given the above components, the target of the team decisional BF approach is to maximize the utility criterion subject to a QoS constraint for the PU as well as power constraints for the two BFs. To this end, our proposed BF approach is based on an iterative procedure applied at each BS, where at each iteration, $BS\ i$ redefines its strategy as well as the model for the strategy of $BS\ j,\ \ j \neq i$, based solely on its own CSI. The key principle of the iterative procedure applied by $BS\ i, i = p, s$ can be summarized as follows.

Algorithm 4 Team decisional CRN precoding

Initialization: Set the iteration counter n to 1 and initialize model $\hat{g}_j(\mathbf{z}_j)$ for the strategy followed by $BS\ j, j \neq i$.

Step 1: Given the model $\hat{\mathbf{w}}_j(n - 1) = \hat{g}_j(\mathbf{z}_j)$ for the strategy followed by $BS\ j, j \neq i$, estimate the optimum $\mathbf{w}_i(n) = g_i(\mathbf{z}_i)$ that maximizes an "analogous" to the utility criterion based on the available CSIT at $BS\ i$.

Step 2: Using the derived $\mathbf{w}_i(n)$, formulate a new model $\hat{g}_j(\mathbf{z}_j)$ for the BF strategy applied by $BS\ j$, based again on the utility maximization criterion and the available CSIT.

Step 3: Increase the iteration counter n by one and if $n \leq N_{max}$, where N_{max} is a predefined maximum number of iterations, go back to Step 1, otherwise stop.

This generic procedure is applied as follows by the two BSs.

Transmit BF design at $BS\ p$ Following the developed team decisional approach described in Algorithm 4, $BS\ p$ tries to find optimal values for $\mathbf{w}_p$ and for $\hat{\mathbf{w}}_s = g_s^{(p)}(\mathbf{z}_s)$. To this end, in the n-th iteration, $BS\ p$ uses the estimated model from step $n - 1$ i.e., $\hat{\mathbf{w}}_s(n-1) = \sqrt{P_s^{max}} \frac{\hat{\mathbf{w}}_s(n-1)}{\|\hat{\mathbf{w}}_s(n-1)\|}$ with $\hat{\mathbf{w}}_s(n-1) = \alpha(n-1)\mathbf{v} + (1 - \alpha(n-1))\tilde{\mathbf{h}}_{ss}$[4], where $\mathbf{v} \perp \mathbf{u}_{\mathbf{R}_{sp}}(1)$, $\tilde{\mathbf{h}}_{ss} = \frac{\mathbf{h}_{ss}}{\|\mathbf{h}_{ss}\|}$ and $\alpha(n) \in [0, 1]$ in order to find an optimum $\mathbf{w}_p(n)$ that exploits the available CSI to solve the problem

$$
\begin{aligned}
\underset{\mathbf{w}_p \in \mathbb{C}^M}{\text{maximize}} \quad & \frac{1 + \mathbb{E}_{|\mathbf{z}_p}\{\hat{\mathbf{w}}_s^H(n - 1)\mathbf{h}_{ss}\mathbf{h}_{ss}^H\hat{\mathbf{w}}_s(n - 1)\}}{\mathbf{w}_p^H \mathbf{R}_{ps} \mathbf{w}_p} \\
\text{subject to} \quad & \frac{1 + \mathbf{w}_p^H \mathbf{h}_{pp} \mathbf{h}_{pp}^H \mathbf{w}_p}{\mathbb{E}_{|\mathbf{z}_p}\{\hat{\mathbf{w}}_s^H(n - 1)\mathbf{R}_{sp}\hat{\mathbf{w}}_s(n - 1)\}} \geq \tau \\
& \|\mathbf{w}_p\|^2 = P_p^{max}.
\end{aligned}
\tag{4.8}
$$

One can show that the following optimization problem is formed

$$
\begin{aligned}
\underset{\mathbf{w}_p \in \mathbb{C}^M}{\text{minimize}} \quad & \mathbf{w}_p^H \mathbf{R}_{ps} \mathbf{w}_p \\
\text{subject to} \quad & \mathbf{w}_p^H \mathbf{H}_{pp} \mathbf{w}_p \geq \tau K(n - 1) - 1 \\
& \|\mathbf{w}_p\|^2 = P_p^{max},
\end{aligned}
\tag{4.9}
$$

where $\mathbf{H}_{pp} \triangleq \mathbf{h}_{pp}\mathbf{h}_{pp}^H$ is a rank-one positive semidefinite matrix and $K(n - 1) = \mathbb{E}_{|\mathbf{z}_p}\{\hat{\mathbf{w}}_s^H(n - 1)\mathbf{R}_{sp}\hat{\mathbf{w}}_s(n-1)\}$ can be numerically approximated via MC iterations exploiting knowledge of $\mathbf{R}_{sp}$

---

[4]Recall that $BS\ i$ assumes that $BS\ j$ uses a BF that is a linear combination of MRC and SZF BF.

and $\mathbf{R}_{ss}$. Problem (4.9) is a non-convex quadratically constrained quadratic problem (QCQP), which by introducing $\mathbf{W}_p \triangleq \mathbf{w}_p \mathbf{w}_p^H$ can be expressed as follows

$$
\begin{aligned}
\underset{\mathbf{W}_p \in \mathbb{C}^{M \times M}}{\text{minimize}} \quad & \text{tr}(\mathbf{R}_{ps}\mathbf{W}_p) \\
\text{subject to} \quad & \text{tr}(\mathbf{H}_{pp}\mathbf{W}_p) \geq \tau K(n-1) - 1, \\
& \text{tr}(\mathbf{W}_p) = P_p^{max}, \quad \mathbf{W}_p \succeq 0, \\
& rank(\mathbf{W}_p) = 1.
\end{aligned}
\tag{4.10}
$$

Solving (4.10) with the rank-one restriction, proves to be cumbersome. To overcome this problem, the rank-one constraint can be dropped by applying semidefinite relaxation (SDR) [64]. The resulting problem is

$$
\begin{aligned}
\underset{\mathbf{W}_p \in \mathbb{C}^{M \times M}}{\text{minimize}} \quad & \text{tr}(\mathbf{R}_{ps}\mathbf{W}_p) \\
\text{subject to} \quad & \text{tr}(\mathbf{H}_{pp}\mathbf{W}_p) \geq \tau K(n-1) - 1, \\
& \text{tr}(\mathbf{W}_p) = P_p^{max}, \quad \mathbf{W}_p \succeq 0,
\end{aligned}
\tag{4.11}
$$

that can be solved by using well known optimization packages such as CVX [65]. The optimal BF vector, $\mathbf{w}_p(n)$, can then be approximated by the eigenvector corresponding to the dominant eigenvalue of the solution obtained from (4.11).

Having calculated $\mathbf{w}_p(n)$, $BS\ p$ then produces a new model $\hat{\mathbf{w}}_s(n)$ that can be seen as the optimum "response" to the selection of $\mathbf{w}_p(n)$. This is achieved by setting $\alpha(n)$ to be the solution of the following problem[5]

$$
\begin{aligned}
\underset{\alpha \in \mathbb{R}}{\max} \quad & \mathbb{E}_{|\mathbf{z}_p} \left\{ \log \left(1 + \frac{|\hat{\mathbf{w}}_s^H \mathbf{h}_{ss}|^2}{1 + \mathbf{w}_p^H(n)\mathbf{h}_{ps}\mathbf{h}_{ps}^H\mathbf{w}_p(n)} \right) \right\} \\
\text{subject to} \quad & \mathbb{E}_{|\mathbf{z}_p} \{ \| \hat{\mathbf{w}}_s^H \mathbf{R}_{sp}^{\frac{1}{2}} \|^2 \} \leq \frac{1}{\tau}(\mathbf{w}_p^H(n)\mathbf{H}_{pp}\mathbf{w}_p(n) + 1), \\
& 0 \leq \alpha \leq 1,
\end{aligned}
\tag{4.12}
$$

where $\hat{\mathbf{w}}_s$ is a function of α.

It is easy to observe that the objective function in (4.12) is increasing as α decreases. Thus, one can solve problem (4.12) simply by finding the minimum possible value of α that satisfies the QoS-related inequality constraint in (4.12). The expectations involved in (4.12), can be computed by means of MC simulations. The value α that is calculated through this procedure at the n-th iteration, is selected to be the value $\alpha(n)$ that updates the model $\hat{\mathbf{w}}_s(n)$ that should be used in iteration $n+1$.

A case that requires special treatment appears when problem (4.11) is infeasible. Such an event can occur due to strict primary communication QoS constraints and/or deep fades for primary communication. In this case, in an attempt to protect the PU, a minimal information exchange is allowed between the BSs. Specifically, $BS\ p$ reports the infeasibility to $BS\ s$. $BS\ s$ then decides upon using SZF, i.e., employs a BF vector orthogonal to the dominant eigenvector of $\mathbf{R}_{sp}$ such as to minimize the interference towards the PU, while at the same time $BS\ p$ decides upon using MRC such as to maximize its SNR.

---

[5]Given that different CSIT is availabe at $BS\ p$ and $BS\ s$, one can see this problem as the "analogous" to the problem that $BS\ s$ is trying to solve.

Transmit BF design at *BS s*   In a similar fashion with *BS p*, *BS s* starts its *n*-th iteration using an estimate $\hat{\mathbf{w}}_p(n-1) = \sqrt{P_p^{max}}\frac{\hat{\bar{\mathbf{w}}}_p(n-1)}{\|\hat{\bar{\mathbf{w}}}_p(n-1)\|}$ with $\hat{\bar{\mathbf{w}}}_p(n-1) = \beta(n-1)\mathbf{u} + (1-\beta(n-1))\tilde{\mathbf{h}}_{pp}$, where $\mathbf{u} \perp \mathbf{u}_{\mathbf{R}_{ps}}(1), \tilde{\mathbf{h}}_{pp} = \frac{\mathbf{h}_{pp}}{\|\mathbf{h}_{pp}\|}$ and $\beta(n) \in [0,1]$, and given its set of observations, $\mathbf{z}_s$, it forms the following optimization problem

$$
\begin{aligned}
\underset{\mathbf{w}_s \in \mathbb{C}^M}{\text{maximize}} \quad & \frac{1 + \mathbf{w}_s^H \mathbf{H}_{ss} \mathbf{w}_s}{\mathbb{E}_{|\mathbf{z}_s}\{\hat{\mathbf{w}}_p^H(n-1)\mathbf{R}_{ps}\hat{\mathbf{w}}_p(n-1)\}} \\
\text{subject to} \quad & \frac{1 + \mathbb{E}_{|\mathbf{z}_s}\{\hat{\mathbf{w}}_p^H(n-1)\mathbf{h}_{pp}\mathbf{h}_{pp}^H\hat{\mathbf{w}}_p(n-1)\}}{\mathbf{w}_s^H \mathbf{R}_{sp}\mathbf{w}_s} \geq \tau, \\
& \|\mathbf{w}_s\|^2 \leq P_s^{max},
\end{aligned}
\tag{4.13}
$$

where $\mathbf{H}_{ss} \triangleq \mathbf{h}_{ss}\mathbf{h}_{ss}^H$, $\mathbf{H}_{ss} \succeq 0$. Problem (4.13) is equivalent to

$$
\begin{aligned}
\underset{\mathbf{w}_s \in \mathbb{C}^M}{\text{maximize}} \quad & \mathbf{w}_s^H \mathbf{H}_{ss} \mathbf{w}_s \\
\text{subject to} \quad & \mathbf{w}_s^H \mathbf{R}_{sp}\mathbf{w}_s \leq \frac{1}{\tau}(L(n-1)+1), \\
& \|\mathbf{w}_s\|^2 \leq P_s^{max},
\end{aligned}
\tag{4.14}
$$

where $L(n-1) = \mathbb{E}_{|\mathbf{z}_s}\{\hat{\mathbf{w}}_p^H(n-1)\mathbf{h}_{pp}\mathbf{h}_{pp}^H\hat{\mathbf{w}}_p(n-1)\}$ can be numerically evaluated, since *BS s* has knowledge of covariance matrices $\mathbf{R}_{ps}$ and $\mathbf{R}_{pp}$. Following the same steps as before, the optimization problem becomes

$$
\begin{aligned}
\underset{\mathbf{W}_s \in \mathbb{C}^{M \times M}}{\text{maximize}} \quad & \text{tr}(\mathbf{H}_{ss}\mathbf{W}_s) \\
\text{subject to} \quad & \text{tr}(\mathbf{R}_{sp}\mathbf{W}_s) \leq \frac{1}{\tau}(L(n-1)+1), \\
& \text{tr}(\mathbf{W}_s) \leq P_s^{max}, \quad \mathbf{W}_s \succeq 0,
\end{aligned}
\tag{4.15}
$$

where $\mathbf{W}_s \triangleq \mathbf{w}_s\mathbf{w}_s^H$. This optimization problem can be also efficiently solved by using the CVX package. Having obtained an optimal $\mathbf{w}_s(n)$ for a given $\beta(n-1)$, *BS s* reestimates the strategy followed by *BS p*, by exploiting its available observations $\mathbf{z}_s$ and finding an optimal $\beta(n)$ for the obtained $\mathbf{w}_s(n)$. Thus, the problem to be solved is the following

$$
\begin{aligned}
\underset{\beta \in \mathbb{R}}{\max} \quad & \mathbb{E}_{|\mathbf{z}_s}\left\{ \log\left(1 + \frac{\mathbf{w}_s^H(n)\mathbf{H}_{ss}\mathbf{w}_s(n)}{1 + |\hat{\mathbf{w}}_p^H\mathbf{h}_{ps}|^2}\right)\right\} \\
\text{subject to} \quad & \mathbb{E}_{|\mathbf{z}_s}\{|\hat{\mathbf{w}}_p^H\mathbf{h}_{pp}|^2\} \geq \tau\mathbf{w}_s^H(n)\mathbf{R}_{sp}\mathbf{w}_s(n) - 1, \\
& 0 \leq \beta \leq 1,
\end{aligned}
\tag{4.16}
$$

where $\hat{\mathbf{w}}_p$ is a function of β. The resulting approximate solution of (4.16) that can be reached by discretizing the search space for β is the new estimate $\beta(n)$ that should be used to determine the model $\hat{\mathbf{w}}_p(n)$ that should be used in iteration $n+1$, leading towards an iterative process of solving problems (4.15) and (4.16).

4.4 Numerical Results

With the aim of evaluating the performance of the proposed BF scheme, extensive MC simulations have been performed for the studied system model. A CRN scenario is considered, in which the two BS CAs overlap with each other by a factor of 50%. We assume that $P_p^{max} = P_s^{max}$ and that both CAs have the same radius. The covariance matrices are computed as a function of angle spread, antenna spacing and wavelength, according to [18]. In Table 4.1, further simulation parameters are provided.

Table 4.1: Basic simulation parameters

BS CA radius	1 km
Number of BS antennas	2
Path loss exponent	3
Carrier frequency	2 GHz
Antenna spacing	$\lambda/2$
AOA distribution	Gaussian
Multipath angle spread	20 degrees
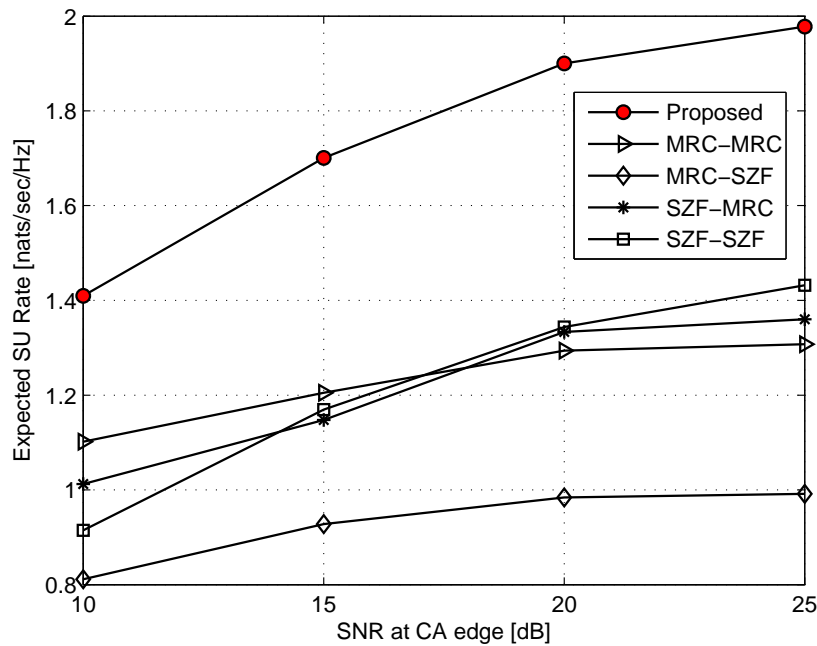
Figure 4.2: Expected SU rate vs. average SNR at CA edge, T=1nat/sec/Hz.

In Fig. 4.2, the expected rate of the SU is depicted as a function of the prescribed average SNR at the CA edge for a QoS level, $T = 1$ nat/sec/Hz, considering the PU. We choose to compare our novel method ($N_{max} = 2$) with other distributed BF methods exploiting the same combined CSIT available here. Specifically, we compare our proposed BF solution with BFs based on MRC and SZF BF. The four reference schemes are then given by MRC-MRC, MRC-

SZF, SZF-MRC and SZF-SZF, where the first (resp. second) acronym in each pair denotes the BF solution implemented at *BS p* (resp. *BS s*). The BF solutions obtained by applying our iterative method are such that a clear rate gain appears, compared with the classical BF solutions.
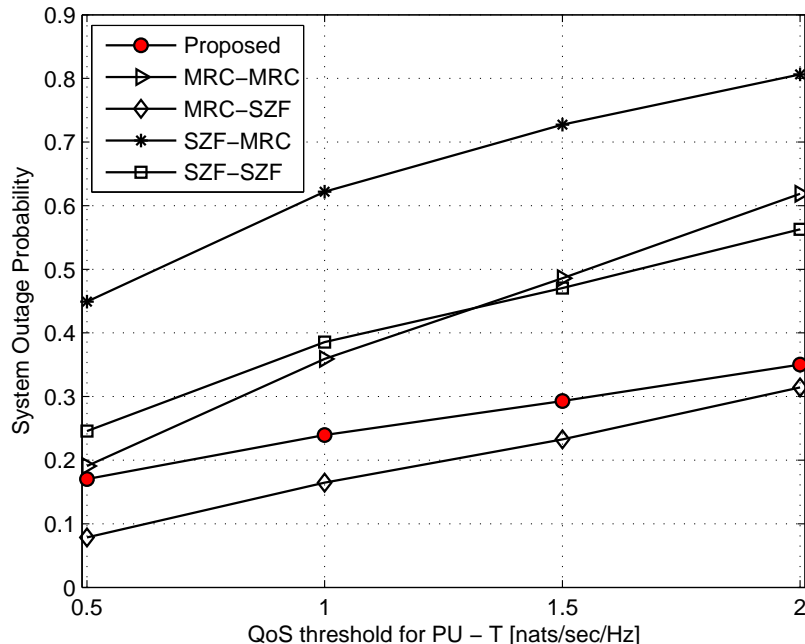
Figure 4.3: System outage probability vs. QoS threshold, T for PU, SNR=20 dB.

In Fig. 4.3, the outage probability of the system is depicted for all the abovementioned BF design approaches, as a function of the QoS threshold, T, posed at the PU, for an SNR at the CA edge equal to 20dB. An outage event is declared when the initial QoS constraint in (4.6) is not satisfied for the PU. It is evident that as the value of T increases, the probability of the system being in outage will increase for all the examined BF approaches. Also, only the MRC-SZF BF method outperforms our method, since it is mostly focused on protecting the PU. It is worth mentioning that with a QoS value, $T = 1$ nat/sec/Hz for the PU, and for an SNR value of 20dB at the CA edge, the new BF scheme gives 37% rate increase over SZF-SZF BF and 33% outage probability decrease over the same BF method.

4.5   Conclusions

In this chapter, a distributed MISO BF method was proposed, with respect to an underlay CRN setup, when the available CSIT is both instantaneous and statistical. First, expressions for the conditional expected rates of the users were derived, and then the problem of rate-optimal MISO BF was studied in the presence of local CSIT at each BS, leading to the solution of a team decisional problem. Substantial gains were depicted in comparison with other known distributed precoding solutions.

In the chapter that follows, a low complexity, non-iterative, statistically coordinated precoding scheme for the examined underlay CRN scenario, will be described.

Chapter 5

Underlay MISO CRN Precoding with Statistical Coordination

5.1 Introduction

Cognitive radio has been lately suggested as a promising technology in view of increasing spectral efficiency in wireless communications [12]. As we have seen before, in the *underlay* CR approach, a primary operator allows the simultaneous use of its spectral resources by an unlicensed secondary system, on condition that harmful interference emitted by the secondary transmitter will not exceed a prescribed maximum tolerated level [10]. Under such a setup, efficient schemes have been developed in multiple-input-multiple-output (MIMO) settings with the aim of maximizing the rate of the SUs, subject to given constraints over the interference suffered by the PUs [3, 66, 67]. In practice, it is expected to be difficult for the secondary transmitter to obtain accurately the multi-user CSI. In particular, the CSI exchange between transmitters (if possible) is likely to introduce delays, which impact significantly the performance of the followed precoding scheme [68].

Therefore, an extensive literature has emphasized on designing iterative distributed approaches being robust to imperfect CSI or requiring only local CSI [See [60] and references therein]. Game theoretic iterative approaches have been also suggested as a way to avoid the need for exchanging the global multi-user CSI for spectrum sharing approaches [69] as well as for underlay CRNs [70, 71].

These approaches, however, assume that the primary transmitter should be *unaware* of the presence of a secondary transmitter, an assumption which might be too pessimistic. In contrast, we propose a new coordination scheme, where the primary transmitter exploits its locally available CSI and the statistical information of the multi-user channel to coordinate with the secondary transmitter.

More specifically, we consider that each transmitter knows only the realization of the direct channel but cooperates with the other transmitter *without any exchange of instantaneous information*. The described scenario falls in the category of *team decisional* problems discussed in other wireless settings in [62, 72]. A similar scenario was already investigated in the previous chapter, however, the team decisional scheme developed there, is characterized by high complexity (it requires multiple iterations of MC averaging) and has to be run for each channel realization.

In particular, our main contributions are the following:

- Following the justifications of the previous chapter, we study a practical CRN setting with a rate constraint for the PU.

- In that setting, we develop a *statistically coordinated precoding* scheme, which outperforms conventional approaches from the literature without requiring any instantaneous CSI exchange between the transmitters and can be run off-line on the basis of statistical information only.

5.2 System and Channel Model

The cognitive setting studied consists of a primary BS, $BS\ p$, communicating with a PU, denoted by $UE\ p$, while a secondary BS, $BS\ s$, transmits to a SU, denoted by $UE\ s$. Assuming an underlay approach, both $BS\ p$ and $BS\ s$ share the same bandwidth. Each transmitter is equipped with M antennas while the receivers have a single antenna, each.

The signal received at $UE\ i$ is written as

$$y_i = \mathbf{h}_{ii}^H \mathbf{w}_i s_i + \mathbf{h}_{\bar{i}i}^H \mathbf{w}_{\bar{i}} s_{\bar{i}} + n_i, \qquad i \in \{p, s\}, \tag{5.1}$$

where $\mathbf{h}_{ji} \in \mathbb{C}^{M \times 1}, i, j \in \{p, s\}$ are distributed as $\mathcal{CN}(\mathbf{0}_M, \mathbf{R}_{ji})$ to model a Rayleigh fading scenario. The vector $\mathbf{w}_i \in \mathbb{C}^{M \times 1}$ denotes the BF vector at BS_i and it is assumed that $\mathbf{w}_i = \sqrt{P_i} \mathbf{u}_i$ with $\|\mathbf{u}_i\| = 1$. Finally, we consider Gaussian noise $n_i \sim \mathcal{CN}(0, N_0), i = \{p, s\}$ and we assume that the data symbols for transmission are also Gaussian distributed.

The instantaneous rate of user i is then given by the following expression

$$R_i(\mathbf{w}_p, \mathbf{w}_s) = \log_2 \left(1 + \frac{P_i |\mathbf{h}_{ii}^H \mathbf{u}_i|^2}{N_0 + P_{\bar{i}} |\mathbf{h}_{\bar{i}i}^H \mathbf{u}_{\bar{i}}|^2} \right). \tag{5.2}$$

5.3 Problem Formulation

We consider in this work a practical and realistic CSI configuration where $BS\ i$ has instantaneous knowledge of direct channel $\mathbf{h}_{ii}$, as well as statistical knowledge of all links, i.e., covariance matrices $\mathbf{R}_{ji}$, $i \in \{p, s\}$, $j \in \{i, \bar{i}\}$. We consider, then, the problem of maximizing the average rate of the SU, subject to a constraint for the average rate of the PU. This is mathematically formulated as

$$
\begin{aligned}
(\mathbf{w}_p^\star, \mathbf{w}_s^\star) &= \operatorname{argmax} \mathbb{E}\{R_s(\mathbf{w}_p(\mathbf{h}_{pp}), \mathbf{w}_s(\mathbf{h}_{ss}))\} \\
&\text{subject to} \quad \mathbb{E}\{R_p(\mathbf{w}_p(\mathbf{h}_{pp}), \mathbf{w}_s(\mathbf{h}_{ss}))\} \geq \tau > 0, \\
&0 \leq \|\mathbf{w}_p\|^2 \leq P_p^{\max}, 0 \leq \|\mathbf{w}_s\|^2 \leq P_s^{\max}.
\end{aligned} \tag{P1}
$$

Remark 1. This is a functional optimization problem as $\mathbf{w}_p$ and $\mathbf{w}_s$ are functions from $\mathbb{C}^M$ to $\mathbb{C}^M$. It should be noted that the precoder depends also on the statistical parameters of the channel, but this dependency is omitted for clarity. In the rest of the chapter we will not mention the dependencies of the BFs in an explicit manner, as it is outside of the scope of this chapter. □

This functional optimization is made especially difficult due to the expectations of the logarithm. Hence, we will consider an approximated problem to develop practical solutions, while

keeping the important features of optimization problem (P1). Our first step consists in applying Jensen's inequality to the expectations over the interfering channel which are instantaneously known at none of the transmitters. We hence obtain

$$
\mathbb{E}\{R_i(\mathbf{w}_p, \mathbf{w}_s)\} \geq \mathbb{E}\left\{ \log_2\left(1 + \frac{|\mathbf{h}_{ii}^H \mathbf{w}_i|^2}{N_0 + \mathrm{E}_{\mathbf{h}_{\bar{i}i}}[|\mathbf{h}_{ii}^H \mathbf{w}_{\bar{i}}|^2]} \right) \right\}
$$

$$
= \mathbb{E}\left\{ \log_2\left(1 + \frac{P_i|\mathbf{h}_{ii}^H \mathbf{u}_i|^2}{N_0 + P_{\bar{i}}\mathbf{u}_{\bar{i}}^H \mathbf{R}_{\bar{i}i}\mathbf{u}_{\bar{i}}} \right) \right\} \tag{5.3}
$$

$$
\triangleq \mathbb{E}\{\tilde{R}_i(\mathbf{w}_p, \mathbf{w}_s)\}.
$$

Remark 2. It is possible to apply Jensen's inequality solely for the interfering channel thanks to the independence between the precoding vectors and the interfering channels. $\qquad\square$

Since we have obtained a lower bound of the ergodic rates, this approximation ensures that the ergodic rate constraint for the PU will be fulfilled. Hence, this approximation comes at the cost of a possible suboptimality, but preserves the feasibility of the constraint at the PU. Our second approximation consists in forcing the transmitters to use a power allocation strategy that is independent of the channel realizations. The study of the optimization problem without this restriction is also out of the scope of this chapter. To emphasize that the power is independent of channel realizations, we will denote it by $\bar{P}_i$, for $i \in \{p, s\}$. This yields the following optimization problem:

$$
(\bar{P}_p^\star, \mathbf{u}_p^\star, \bar{P}_s^\star, \mathbf{u}_s^\star) = \mathrm{argmax}\, \mathbb{E}\{\tilde{R}_s(\bar{P}_p, \mathbf{u}_p(\mathbf{h}_{pp}), \bar{P}_s, \mathbf{u}_s(\mathbf{h}_{ss}))\}
$$

$$
\text{subject to}\ \ \mathbb{E}\{\tilde{R}_p(\bar{P}_p, \mathbf{u}_p(\mathbf{h}_{pp}), \bar{P}_s, \mathbf{u}_s(\mathbf{h}_{ss}))\} \geq \tau, \tag{P1'}
$$

$$
0 \leq \bar{P}_p \leq P_p^{\max}, 0 \leq \bar{P}_s \leq P_s^{\max}.
$$

5.4 Preliminary Results

We start by providing some preliminary results which shed light on the optimization problem and will be used to design the novel precoding scheme.

Proposition 6. The constraint over the rate of the PU is fulfilled with equality by any optimal solution, i.e.,

$$
\mathbb{E}\{\tilde{R}_p(\bar{P}_p^\star, \mathbf{u}_p^\star, \bar{P}_s^\star, \mathbf{u}_s^\star)\} = \tau. \tag{5.4}
$$

Proof. The objective $\mathbb{E}\{\tilde{R}_s(\bar{P}_p^\star, \mathbf{u}_p^\star, \bar{P}_s^\star, \mathbf{u}_s^\star)\}$, is monotonically decreasing with respect to power level P_p, while $\mathbb{E}\{\tilde{R}_p(\bar{P}_p^\star, \mathbf{u}_p^\star, \bar{P}_s^\star, \mathbf{u}_s^\star)\}$, is monotonically increasing and continuous in $\bar{P}_p$. Hence, if the primary constraint is not fulfilled with equality, one can increase the objective by reducing power $\bar{P}_p$. This is always feasible because $\tau > 0$ implies that $\bar{P}_p^\star > 0$. $\qquad\square$

Proposition 7. The optimal solution of (P1') is obtained when one of the two transmitters emits with full power, i.e., when $\bar{P}_p^\star = P_p^{\max}$ or $\bar{P}_s^\star = P_s^{\max}$.

Proof. Let us consider an optimal solution and write $\bar{P}_i^\star = \alpha_i^\star \bar{P}^\star$ for some $\alpha_i^\star \geq 0$. One can observe that both the rate of the PU and the rate of the SU are increasing functions of $\bar{P}^\star$. If none of the two transmitters transmits with full power, this means that it is possible to transmit with $\bar{P}' > \bar{P}^\star$. The transmission using $(\alpha_p^\star \bar{P}', \mathbf{u}_p^\star, \alpha_s^\star \bar{P}', \mathbf{u}_s^\star)$ is feasible and achieves a larger objective, which contradicts the optimality of $(\bar{P}_p^\star, \mathbf{u}_p^\star, \bar{P}_s^\star, \mathbf{u}_s^\star)$. As a result the proposition is proved by contradiction. $\qquad\square$

5.5   Precoding Schemes

Solving the functional optimization problem, (P1'), is difficult, even in the centralized case with perfect CSI. Hence, we tackle this problem by first restricting the space of possible precoding decisions to a codebook of precoding strategies. We design this "codebook" by building upon the results obtained in Section 5.4. Specifically, we use the fact that at least one of the transmitters emits with full power and that the primary constraint is fulfilled with equality. Restricting the space of possible precoding decisions to a limited strategy set is a key component of our approach to ensure the *coordination* of the transmitters. It is noteworthy that in this chapter, we present the results in the case of two precoding strategies but the approach can be extended to a larger codebook of precoding strategies [73].

Remark 3. We will present in the following two "precoding strategies". This refers in fact to a couple $(\bar{P}_p, \mathbf{u}_p, \bar{P}_s, \mathbf{u}_s)$, and it remains then to verify that the precoding strategies are feasible in the sense that they fulfill the ergodic primary constraint. □

5.5.1   Precoding Strategy p

In this precoding strategy, BS p transmits with its full power, $\bar{P}_p = P_p^{max}$ and using the MRC precoder $\mathbf{u}_p^{MRC}$, defined as

$$\mathbf{u}_p^{MRC} \triangleq \frac{\mathbf{h}_{pp}}{\|\mathbf{h}_{pp}\|}. \tag{5.5}$$

The secondary transmitter then transmits using the statistical ZF precoder $\mathbf{u}_s^{SZF}$, defined as

$$\mathbf{u}_s^{SZF} \triangleq \underset{\mathbf{u}}{\text{argmin}}\ \mathbf{u}^H \mathbf{R}_{sp} \mathbf{u}. \tag{5.6}$$

It remains to choose $\bar{P}_s$ so as to fulfill the rate constraint at the PU. By substituting the precoder expressions of (5.5) and (5.6) and the power of the primary transmitter, one obtains the following inequality that needs to be satisfied

$$\mathbb{E}\left\{ \log_2\left(1 + \frac{\bar{P}_p^{max}\|\mathbf{h}_{pp}\|^2}{N_0 + \bar{P}_s \lambda_{min}(\mathbf{R}_{sp})} \right) \right\} \geq \tau, \tag{5.7}$$

where $\lambda_{min}(\mathbf{R}_{sp})$ denotes the minimum eigenvalue of matrix $\mathbf{R}_{sp}$. Let us introduce the random variable

$$X \triangleq \frac{\bar{P}_p^{max}\|\mathbf{h}_{pp}\|^2}{N_0 + \bar{P}_s \lambda_{min}(\mathbf{R}_{sp})}. \tag{5.8}$$

Random variable X is Gamma distributed with PDF

$$f_X(x) = \frac{x^{M-1}e^{-\frac{x}{\lambda}}}{\Gamma(M)\lambda^M} \tag{5.9}$$

where

$$\lambda \triangleq \frac{\bar{P}_p^{max}\frac{\text{tr}(\mathbf{R}_{pp})}{M}}{N_0 + \bar{P}_s \lambda_{min}(\mathbf{R}_{sp})}. \tag{5.10}$$

It follows that a closed form expression for the rate in (5.7) can be found in [33, 4.337.5] and is given in (5.11).

$$\mathbb{E}\left\{\log_2\left(1+\frac{P_p^{max}}{N_0+P_s\lambda_{min}(\mathbf{R}_{sp})}\|\mathbf{h}_{pp}\|^2\right)\right\}=\frac{1}{\ln(2)}\sum_{j=0}^{M-1}\frac{1}{(M-j-1)!}\left(\frac{(-1)^{M-j-3}}{\lambda^{M-j-1}}e^{\frac{1}{s\lambda}}E_1\left(\frac{1}{\lambda}\right)\right.$$
$$\left.+\sum_{k=1}^{M-j-1}(k-1)!\left(\frac{-1}{\lambda}\right)^{M-j-k-1}\right). \tag{5.11}$$

It remains then to determine $\bar{P}_s$ so as to fulfill the ergodic rate constraint with equality. Using closed form expression (5.11), this can be easily done by bisection. Indeed, the ergodic rate of the PU is non-increasing in power $\bar{P}_s$. In addition, the rate constraint is fulfilled by assumption for $\bar{P}_s = 0$. If the constraint is also fulfilled for $\bar{P}_s = P_s^{\max}$, the secondary transmitter transmits with its full power. Otherwise, a simple bisection algorithm over $\bar{P}_s$ converges to a power level $\bar{P}_s$ fulfilling the ergodic constraint (5.7) with equality.

5.5.2 Precoding Strategy s

In this precoding strategy, BS s transmits with its full power $\bar{P}_s = P_s^{\max}$ and using the MRC precoder $\mathbf{u}_s^{MRC}$ defined as

$$\mathbf{u}_s^{MRC} \triangleq \frac{\mathbf{h}_{ss}}{\|\mathbf{h}_{ss}\|}. \tag{5.12}$$

The primary transmitter then transmits with the SZF precoder

$$\mathbf{u}_p^{SZF} \triangleq \underset{\mathbf{u}}{\operatorname{argmin}}\ \mathbf{u}^H\mathbf{R}_{ps}\mathbf{u}. \tag{5.13}$$

It remains to choose $\bar{P}_p$ in order to fulfill the ergodic rate constraint at the PU. Replacing the precoder expressions of (5.12) and (5.13) and the power of the secondary transmitter, one obtains

$$\mathbb{E}\left\{\log_2\left(1+\frac{\bar{P}_p|\mathbf{h}_{pp}^H\mathbf{u}_p^{SZF}|^2}{N_0+\bar{P}_s^{max}(\mathbf{u}_s^{MRC})^H\mathbf{R}_{sp}\mathbf{u}_s^{MRC}}\right)\right\}\geq\tau. \tag{5.14}$$

We can once more use Jensen's inequality for convex functions over the expectation of $\mathbf{h}_{ss}$ to obtain the following lower bound

$$\mathbb{E}\left\{\log_2\left(1+\frac{\bar{P}_p|\mathbf{h}_{pp}^H\mathbf{u}_p^{SZF}|^2}{N_0+\bar{P}_s^{max}(\mathbf{u}_s^{MRC})^H\mathbf{R}_{sp}\mathbf{u}_s^{MRC}}\right)\right\}$$
$$\geq\mathbb{E}\left\{\log_2\left(1+\frac{\bar{P}_p|\mathbf{h}_{pp}^H\mathbf{u}_p^{SZF}|^2}{N_0+\bar{P}_s^{max}\frac{1}{2}\text{tr}(\mathbf{R}_{sp})}\right)\right\}. \tag{5.15}$$

We then define the signal power divided by the channel norm $\beta \triangleq |\mathbf{h}_{pp}^H\mathbf{u}_p^{SZF}|^2/\|\mathbf{h}_{pp}\|^2$. This term is known to be distributed according to a Beta$(1, M-1)$ distribution. Using this result,

we write

$$\mathbb{E}\left\{ \log_2\left(1 + \frac{\bar{P}_p|\mathbf{h}_{pp}^H\mathbf{u}_p^{SZF}|^2}{N_0 + \bar{P}_s^{max}\frac{1}{2}\text{tr}(\mathbf{R}_{sp})} \right) \right\}$$

$$= \mathbb{E}\{\log_2(\beta)\} + \mathbb{E}\left\{ \log_2\left(\frac{1}{\beta} + \frac{\bar{P}_p\|\mathbf{h}_{pp}\|^2}{N_0 + \bar{P}_s^{max}\frac{1}{2}\text{tr}(\mathbf{R}_{sp})} \right) \right\} \qquad (5.16)$$

$$\geq \psi(1) - \psi(M) + \mathbb{E}\left\{ \log_2\left(M + \frac{\bar{P}_p\|\mathbf{h}_{pp}\|^2}{N_0 + \bar{P}_s^{max}\frac{1}{2}\text{tr}(\mathbf{R}_{sp})} \right) \right\}$$

where the last inequality is obtained by applying Jensen's inequality with respect to the expectation according to β (independent of channel norm $\|\mathbf{h}_{pp}\|$) and ψ stands for the Digamma (Psi) function.

Hence, a sufficient condition for the rate constraint at the PU is

$$\psi(1) - \psi(M) + \mathbb{E}\left\{ \log_2\left(M + \frac{\bar{P}_p\|\mathbf{h}_{pp}\|^2}{N_0 + \bar{P}_s^{max}\frac{1}{2}\text{tr}(\mathbf{R}_{sp})} \right) \right\} \geq \tau. \qquad (5.17)$$

If equation (5.17) is satisfied with $\bar{P}_p = P_p^{max}$, it is then possible to use a similar bisection scheme as in the case of precoding strategy p to obtain a power level $\bar{P}_p$ fulfilling the rate constraint at the PU.

Remark 4. Precoding strategy p does not reduce the feasibility of the cognitive scenario since it is possible to let the PU achieve the single user rate by letting the secondary transmitter transmit with zero power. In contrast, strategy s strongly reduces the feasibility region as the secondary transmitter transmits with full power. Hence, a preliminary condition before using strategy s is to verify that it is a feasible strategy. This will be done in the following using sufficient condition (5.17). $\qquad \Box$

5.6   Statistically Coordinated Precoding

We have described two precoding strategies which will form the building blocks of our algorithm. It now remains to combine in an adequate way these two schemes to obtain an efficient solution to optimization problem (P1').

Given the statistical parameters of a channel, we study whether it is possible to fulfill the primary constraint using precoding strategy s. If equation (5.17) is satisfied when using $\bar{P}_p = P_p^{max}$, this means that it is possible to fulfill the primary constraint using precoding strategy s. This equation requires only knowledge of the statistical information of the channel and not of the instantaneous channel realizations. Hence, it can be verified at the two transmitters whether (5.17) is satisfied.

If this criterion is satisfied, both transmitters transmit according to precoding strategy s *for all the channel realizations*. Otherwise, both transmitters transmit according to precoding strategy p, which always fulfills the primary rate constraint. The choice between the two precoding schemes is done by computing (5.17) and we call this step a *statistical coordination* one, as it allows the transmitters to coordinate on the basis of statistical information. This coordination step is run off-line and only once for each channel setting. For the sake of clarity, the different steps of the scheme are presented in Algorithm 5.

Remark 5. It is important to keep in mind that each strategy is implemented using only local
CSI. Hence, each transmitter knows via the statistical coordination step, which strategy is used
but does not know exactly which precoder is used at the other transmitter. □

Algorithm 5 Statistically Coordinated Precoding Scheme

- Coordination: Verify whether coordination criterion (5.17) holds with $\bar{P}_p = P_p^{max}$. If this
  is the case use precoding strategy s, otherwise use precoding strategy p.

- Precoding strategy p:

  - BS p transmits with $\mathbf{u}_p^{MRC}$ in (5.5) and $\bar{P}_p = P_p^{max}$
  - BS s transmits with $\mathbf{u}_s^{SZF}$ in (5.6) and a power level $\bar{P}_s$ fulfilling (5.7) with equality
    (obtained by bisection)

- Precoding strategy s:

  - BS s transmits with $\mathbf{u}_s^{MRC}$ in (5.12) and $\bar{P}_s = P_s^{max}$
  - BS p transmits with $\mathbf{u}_p^{SZF}$ in (5.13) and a power level $\bar{P}_p$ fulfilling (5.14) with equality
    (obtained by bisection)

5.7   Simulations

In this section, we evaluate the performance of the novel coordination-based precoding algorithm
via MC-based simulations. In particular, we compare our scheme with the conventional *inter-
ference temperature* approach. Hence, we will first adapt this approach in the case of an ergodic
rate constraint. We also provide an upper bound to evaluate the potential suboptimalities of our
algorithm.

5.7.1   Interference Temperature Approach

In this reference scheme, we assume that the primary transmitter transmits using $\mathbf{u}_p^{MRC}$ and
$\bar{P}_p^{max}$. Because of the absence of coordination between the transmitters, this is necessary to be
sure to fulfill the ergodic rate constraint at the PU. We consider then an *interference temperature*
constraint, where the secondary transmitter maximizes its signal strength, subject to a constraint
on the average interference level at the PU, which we denote by $\mathcal{I}$. We then fix the BF of the
secondary transmitter as

$$\mathbf{u}_s^{TP} = \underset{\mathbf{u}}{\arg\max} \frac{\mathbf{u}^H \mathbf{h}_{ss} \mathbf{h}_{ss}^H \mathbf{u}}{\mathbf{u}^H \mathbf{R}_{sp} \mathbf{u}} \tag{5.18}$$

and the power is then given by

$$\bar{P}_s = \frac{\mathcal{I}}{\mathbb{E}\{(\mathbf{u}_s^{TP})^H \mathbf{R}_{sp} \mathbf{u}_s^{TP}\}}. \tag{5.19}$$

It now remains to determine the maximum tolerable interference temperature, $\mathcal{I}$, i.e., such that

$$\mathbb{E}\left\{ \log_2\left(1 + \frac{P_p^{max}\|\mathbf{h}_{pp}^H\|^2}{N_0 + \mathcal{I}}\right)\right\} = \tau. \tag{5.20}$$

Such an interference level, $\mathcal{I}$, can be easily found by bisection as described in Section 5.5.

5.7.2 Upperbound

The optimal precoders, considering optimization problem (P1'), are not easily derived as they strike a generic trade-off between maximizing the signal strength and minimizing the interference. Hence, an upper bound can be easily obtained by using in each case the optimal BF. This then yields the following optimization problem

$$\begin{aligned}
\max_{\bar{P}_s, \bar{P}_p} \mathbb{E}&\left\{ \log_2\left(1 + \frac{\bar{P}_s\|\mathbf{h}_{ss}^H\|^2}{N_0 + \bar{P}_p\lambda_{min}(\mathbf{R}_{ps})}\right)\right\} \\
\text{subject to} \quad \mathbb{E}&\left\{ \log_2\left(1 + \frac{\bar{P}_p\|\mathbf{h}_{pp}^H\|^2}{N_0 + \bar{P}_s\lambda_{min}(\mathbf{R}_{sp})}\right)\right\} \geq \tau, \\
& 0 \leq \bar{P}_p \leq P_p^{max}, 0 \leq \bar{P}_s \leq P_s^{max}.
\end{aligned} \tag{5.21}$$

Similarly to Proposition 7, it is straightforward that one of the transmitters will transmit with its full power. Hence, we try whether the ergodic constraint is fulfilled using $\bar{P}_s = P_s^{\max}$ and $\bar{P}_p = P_p^{\max}$. If this is the case, the secondary transmitter transmits with full power and the primary transmitter finds by bisection a power level to fulfill the ergodic constraint with equality. Otherwise, the primary transmitter transmits with full power and it is the secondary transmitter that finds its power level by bisection to fulfill the ergodic constraint with equality.

Remark 6. This upper bound is a priori loose since the rate expression corresponds a priori to no practical BF. $\qquad\square$

5.7.3 Simulation Results

We will now compare the performance of our coordination algorithm with the interference temperature approach and the upper bound presented above. We will use MC simulations with 10000 channel realizations for a network with $M = 3$ antennas per transmitter.

The channel covariance matrices are given by

$$\mathbf{R}_{pp} = \mathbf{R}_{ss} = \mathbf{I}_3, \quad \mathbf{R}_{ps} = \mathbf{R}_{sp} = \begin{bmatrix} 1 & \rho & \rho^2 \\ \rho & 1 & \rho \\ \rho^2 & \rho & 1 \end{bmatrix} \tag{5.22}$$

for a given $\rho \in [0, 1]$.
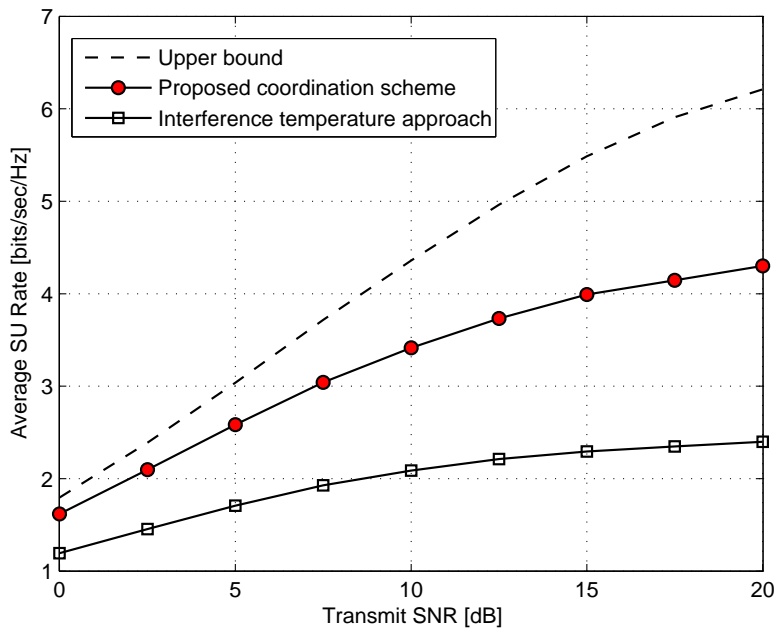
(a) Ergodic rate of the SU.
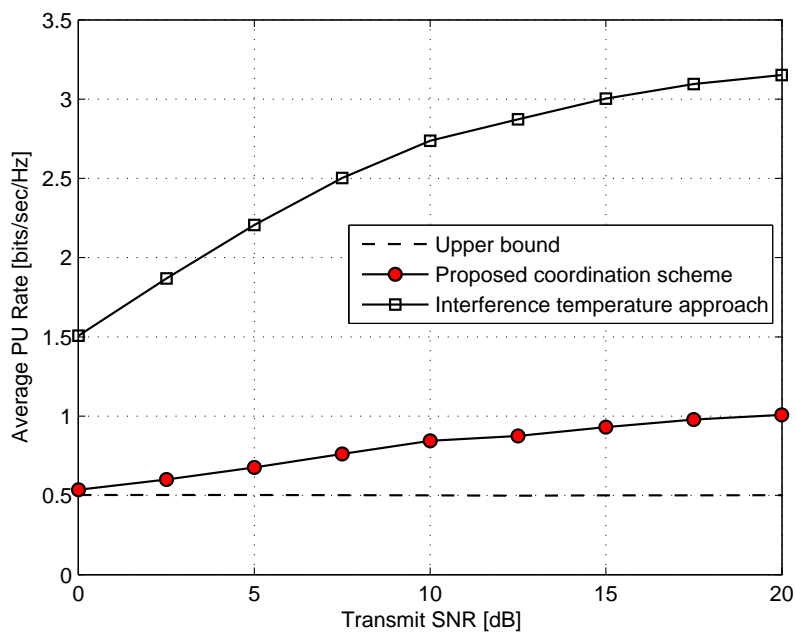
(b) Ergodic rate of the PU.

Figure 5.1: Ergodic rates of the SU and the PU, respectively, for a channel configuration with $M = 3$ and $\tau = 0.5$ bits/sec/Hz.

We show in Fig. 5.1 the rates of the SU and the PU when $\rho = 0.5$ and $\tau = 0.5$ bits/sec/Hz. As expected, all three approaches satisfy the rate constraint at the PU. The upper bound corre-

sponds to centralized processing and one observes that it satisfies the primary constraint almost with equality. The proposed coordination is outperformed by the upper bound, but provides a strong improvement compared to the interference temperature approach. This follows from a better repartition of the resources between the transmitters in the proposed coordination scheme.

5.8   Conclusions

In this chapter, we have developed a coordination scheme for a MISO underlay cognitive scenario with a rate constraint for the primary transmitter. Considering a realistic CSI configuration, where each transmitter has only access to its own channel, we propose a scheme where the secondary transmitter and the primary transmitter coordinate on the basis of the statistical information of the channel. The proposed scheme outperforms conventional approaches from the literature at the price of only low requirements, as it is not necessary for the transmitters to share any instantaneous CSI and the precoding algorithm can be run off-line. The approach developed is a novel method to deal with team decisional problems and has the potential to be generalized to many other network configurations. It can be seen however that the coordination scheme does not exploit the (locally available) instantaneous channel knowledge. Designing an *online* algorithm exploiting the locally available information is a challenging task which will be tackled in the future.

As in the previous chapters, the mixed CSIT scenario considers knowledge of the direct links between a transmitter and its assigned user, in the following chapter, a novel pilot assignment scheme will be proposed for prioritized CRNs, the transmitters of which are equipped with a large number of antennas. The goal of this channel estimation scheme is the optimization of channel estimation quality at SUs, while minimizing the impact of (synchronous) channel estimation at the primary system, due to secondary pilot sequence transmissions.

Part IV

Coordinated Channel Estimation for CRNs

Chapter 6

Channel Estimation for Large Antenna CRNs: a Pilot Decontamination Approach

6.1 Introduction

The use of multiple antennas at the secondary (and possibly primary) devices has proved to be very useful in order to allow interference rejection or avoidance mechanisms, and hence fulfilling the condition of limiting the impact caused by the secondary-generated interference to the primary system [3], [70], [2]. However, it should be noted, that MIMO based approaches (often based on ZF principles or its regularized variants), are efficient in dealing with interference, *provided* the channel vectors corresponding to intended users as well as interfering users can be estimated accurately enough. Interestingly, it was recently shown that the condition of knowing the interfering channel can be alleviated by sticking to simple spatial matched filter based receivers or transmitters. Although highly suboptimal in many interference scenarios, matched filters' gains approach optimality when the antenna numbers at the transmitter side are allowed to grow large, giving rise to the so-called *Massive MIMO* concept [74]. This phenomenon simply exploits the fact that as the number of antenna elements increases to infinity, the independent desired and interference channel vectors grow more orthogonal to each other, allowing the MRC to maximize the SNR at the desired user, while rejecting (or avoiding on the downlink) interference to others "for free". Large numbers of antennas do not have to be installed on the same base tower. Instead, they can be spread around on a larger area, such as a large building's face or roof area, making Massive MIMO more realistic than initially thought.

Although the concept of large scale antenna systems was initially investigated for cellular networks, there is a clear potential in the area of CRNs as well, where interference is even more problematic. However, this had not been addressed to the best of our knowledge. In particular, we put emphasis on the fact that even MRC filters assume that the channel vectors can be accurately estimated in Massive MIMO systems, as even a slight mismatch in the channel estimation will reduce system performance substantially when one is in the large antenna number regime. As primary and secondary systems cannot be fully coordinated, it is likely that the pilot sequences used in both systems do not satisfy orthogonality. This gives rise to the well known effect of *pilot contamination* [75–79]. Pilot contamination causes the fast saturation of the interference

rejection performance, as the number of antennas, M, increases.

Recently, a novel approach has been presented for decontaminating pilots in the context of Massive MIMO cellular networks [18]. The key idea lies in the exploitation of second order statistics (covariance matrices) for both the desired channel to be estimated as well as for the interference channels. We assume that such information can be collected and exchanged between transmitters beforehand since this is slow-varying data. A robust Bayesian channel estimator is then developed. The surprising result in [18] is that when the number of antennas grows large, such an estimator will exhibit performance identical to that obtained in a zero-interference setting, given a condition on the distribution of multipath for both desired and interfering users.

In this chapter, we take on this idea and adapt it to the context of prioritized CRNs. The main difference between cellular systems and prioritized CRNs is the notion of priority for the latter scenario. To deal with this problem, we propose a new pilot assignment scheme which is implemented at the secondary operator. This scheme aims at maximizing the channel estimation quality for SUs, while minimizing the impact created by SUs onto the primary channel estimation performance. It is shown analytically and by simulation that as the number of antennas grows large, one can have interference-free channel estimation at the primary operator while letting the SUs communicate.

6.2 Signal and Channel Models

Our model consists of a network of two service providers (SPs), a primary one, SP p and a secondary one, SP s, with full spectrum reuse (Fig. 6.1). Estimation of (block-fading) channels in the uplink is considered, and the two BSs, BS p and BS s are equipped with M antennas, each. We also assume that, both the PU as well as the SU, are equipped with a single antenna, each, and that K users belong to each SP's CA. Moreover, the pilots, of length τ, used by users belonging to the same operator are mutually orthogonal. As a result, we assume that intra-operator interference is negligible. However, non-orthogonal (possibly aligned) pilots are reused among the operators, resulting in pilot contamination from users assigned by other operators. The pilot sequence used within the CA of the k-th operator ($k \in \{p, s\}$), is denoted by

$$\mathbf{s}_k = [\begin{array}{cccc} s_{k1} & s_{k2} & \cdots & s_{k\tau} \end{array}]^T, \tag{6.1}$$

where $s_{kj} \in \mathbb{C}$, $j = \{1, \cdots, \tau\}$. The pilot symbols are normalized such that $|s_{k1}|^2 = \cdots = |s_{k\tau}|^2 = 1$ for every operator index $k \in \{p, s\}$.

We denote the receive covariance matrix $\mathbf{R}_{kl}^{(i)} \in \mathbb{C}^{M \times M}$ as $\mathbf{R}_{kl}^{(i)} = \mathbb{E}\left\{ \mathbf{h}_{kl}^{(i)} (\mathbf{h}_{kl}^{(i)})^H \right\}$, where user i is assigned to SP k and $\mathbf{h}_{kl}^{(i)}$ is the channel vector between this user and the l-th BS, $k, l \in \{p, s\}$. It is assumed that only one user per SP is active at each resource allocation block, thus, we momentarily omit the user index subscript, which will be useful later for the pilot assignment algorithm description. Channel vectors are assumed to be $M \times 1$ complex Gaussian, undergoing correlation due to the finite multipath angle spread at the BS side as in [80]:

$$\mathbf{h}_{kl} = \mathbf{R}_{kl}^{\frac{1}{2}} \mathbf{h}_{kl}^{(w)}, \quad k, l \in \{p, s\}, \tag{6.2}$$

where $\mathbf{h}_{kl}^{(w)}$ is the spatially white $M \times 1$ SIMO channel with $\mathbf{h}_{kl}^{(w)} \sim \mathcal{CN}(\mathbf{0}, \mathbf{I}_M)$.
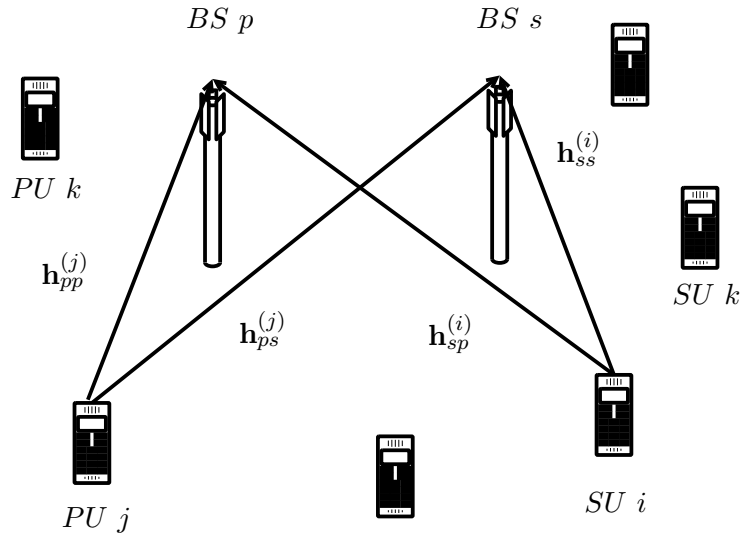
Figure 6.1: Topology of a CRN comprising of two SPs - pilot transmission phase.

During the pilot phase, the $M \times \tau$ signal received at each BS from the user assigned to $SP \ k$ is

$$\mathbf{Y}_k = \mathbf{h}_{pk}\mathbf{s}_p^T + \mathbf{h}_{sk}\mathbf{s}_s^T + \mathbf{N}_k, \tag{6.3}$$

where $\mathbf{N}_k \in \mathbb{C}^{M \times \tau}$ is the spatially and temporally additive white Gaussian noise (AWGN) with element-wise variance σ_n^2 [81].

6.3   Covariance-Aided Channel Estimation

In this section we recall some key results obtained in [18] for the conventional cellular scenario. Then, in 6.4 these results are generalized to adapt to the CR scenario.

6.3.1   Covariance-based Bayesian estimator

By taking advantage of the known long-term covariance information of the channels, and assuming that L time-synchronized cells share the spectrum, a Bayesian estimator, which is equivalent to a Minimum Mean Square Error (MMSE) estimator, is given by [18], [82]

$$\hat{\mathbf{h}}_{kk} = \mathbf{R}_{kk}\bar{\mathbf{S}}^H \left(\bar{\mathbf{S}}(\mathbf{R}_{kk} + \mathbf{R}_{lk})\bar{\mathbf{S}}^H + \sigma_n^2\mathbf{I}_{\tau M}\right)^{-1}\mathbf{y}_k, \tag{6.4}$$

where $l \neq k$, $\bar{\mathbf{S}}$ is a matrix containing the pilot vectors, defined as $\bar{\mathbf{S}} \triangleq [\mathbf{s}_1 \otimes \mathbf{I}_M, \cdots, \mathbf{s}_L \otimes \mathbf{I}_M]$, the user is assigned to $SP \ k$, and $\mathbf{y}_k$ is the vectorized received training signal, that is: $\mathbf{y}_k = \text{vec}(\mathbf{Y}_k)$ [18]. It is noted that expression (6.4) is similar to the traditional Bayesian estimator as shown in [82], [83]. The difference is that here identical pilot sequences are sent by users, and covariance information is assumed to be known at the BS side.

Applying the matrix inversion identity $\mathbf{A}(\mathbf{I} + \mathbf{BA})^{-1} = (\mathbf{I} + \mathbf{AB})^{-1}\mathbf{A}$, we can obtain a more convenient form. This form is the following

$$\hat{\mathbf{h}}_{kk} = \mathbf{R}_{kk} \left(\sigma_n^2 \mathbf{I}_M + \tau \left(\mathbf{R}_{kk} + \mathbf{R}_{lk} \right) \right)^{-1} \bar{\mathbf{S}}^H \mathbf{y}_k. \tag{6.5}$$

6.3.2 MSE Performance Analysis

We are interested in the mean squared error (MSE) of the proposed Bayesian estimator developed in [18], which in the cognitive network case can be defined as:

$$\mathcal{M}_k \triangleq \mathbb{E} \left\{ \left\| \hat{\mathbf{h}}_{kk} - \mathbf{h}_{kk} \right\|_F^2 \right\}, \tag{6.6}$$

where the user is assigned to *SP* k and $k \in \{p, s\}$ (we will be assuming that $L=2$ in the rest of the chapter). The MSE of the Bayesian estimator (6.5) with completely aligned pilots is recalled from [18] for convenience.

Proposition 8. The estimation MSE of (6.5) is given by

$$\mathcal{M}_k = \text{tr} \left(\mathbf{R}_{kk} - \mathbf{R}_{kk}^2 \left(\frac{\sigma_n^2}{\tau} \mathbf{I}_M + \mathbf{R}_{kk} + \mathbf{R}_{lk} \right)^{-1} \right), \tag{6.7}$$

where $k \neq l$.

Proof. The proof can be found in [18]. $\qquad\qquad\square$

We can easily derive the MSE of (6.5) obtained in an interference free scenario, by setting interference covariance matrices to zero in (6.5)

$$\mathcal{M}_{k,\text{no int}} = \text{tr} \left(\mathbf{R}_{kk} \left(\mathbf{I}_M + \frac{\tau}{\sigma_n^2} \mathbf{R}_{kk} \right)^{-1} \right), \tag{6.8}$$

where superscript *no int* refers to the "no interference case". The corresponding channel estimate in this case is

$$\hat{\mathbf{h}}_{kk,\text{no int}} = \mathbf{R}_{kk} (\sigma_n^2 \mathbf{I}_M + \tau \mathbf{R}_{kk})^{-1} \bar{\mathbf{S}}^H (\bar{\mathbf{S}} \mathbf{h}_{kk} + \mathbf{n}). \tag{6.9}$$

6.3.3 Large antenna number regime

Our objective is to analyze the performance of the above estimator in the large antenna number regime, M. For tractability, our analysis is based on the assumption of a Uniform Linear Array (ULA) with supercritical antenna spacing (i.e., less than or equal to half wavelength). Here, we make use of the following multipath model

$$\mathbf{h}_{kk} = \frac{1}{\sqrt{P}} \sum_{p=1}^{P} \mathbf{a}(\theta_{kk}^{(p)}) \alpha_{kk}^{(p)}, \tag{6.10}$$

where P is the arbitrary number of independent spatially separated paths, $\alpha_{kk}^{(p)} \sim \mathcal{CN}(0, \delta_k^2)$ is independent over the path index p, δ_k is the average attenuation of the channel vector and $\mathbf{a}(\theta)$

is the steering vector,as shown in [84]

$$\mathbf{a}(\theta) \triangleq \begin{bmatrix} 1 \\ e^{-j2\pi \frac{D}{\lambda} \cos(\theta)} \\ \vdots \\ e^{-j2\pi \frac{(M-1)D}{\lambda} \cos(\theta)}, \end{bmatrix} \tag{6.11}$$

where D is the antenna spacing at the BS and λ is the signal wavelength, such that $D \leq \lambda/2$. $\theta^{(p)} \in [0, \pi]$ is a random AOA. It should be noted that we can limit angles to $[0, \pi]$ because any $\theta \in [-\pi, 0]$ can be replaced by $-\theta$ giving the same steering vector.

A principal result of [18] is stated below, where the notations are adapted to our CRN model.

Theorem 2. Assume the multipath AOA, θ, yielding channel $\mathbf{h}_{kk}$ given in (6.10) for a user assigned to SP k, is distributed according to an arbitrary density $p_{kk}(\theta)$ with bounded support, i.e., $p_{kk}(\theta) = 0$ for $\theta \notin [\theta_{kk}^{min}, \theta_{kk}^{max}]$, for some fixed $\theta_{kk}^{min} \leqslant \theta_{kk}^{max} \in [0, \pi]$. If the AOA interval $[\theta_{lk}^{min}, \theta_{lk}^{max}]$, $k \neq l \in \{p, s\}$ of the interfering channel is strictly non-overlapping with the AOA interval of the desired channel, $[\theta_{kk}^{min}, \theta_{kk}^{max}]$, we have

$$\lim_{M \to \infty} \hat{\mathbf{h}}_{kk} = \hat{\mathbf{h}}_{kk,\text{no int}}. \tag{6.12}$$

Proof. The proof can be found in [18]. $\square$

From the above analysis and especially from Theorem 2, lemmas (1)-(3) and the rest of results given in [18], we conclude to the fact that the MSE performance of the covariance-aided channel estimation, in case this regards a PU, strongly depends on the degree with which the signal subspaces of covariance matrices $\mathbf{R}_{pp}$ and $\mathbf{R}_{sp}$ overlap with each other. As a result, this will lead to an interference avoidance criterion for a PU, because in case the signal subspace of one of the two aforementioned covariance matrices will be achieved to be the orthogonal complement of the signal subspace of the other covariance matrix (or at least close to orthogonal), then, the pilot contamination effect will tend to vanish in the large antenna number, M, regime.

6.4 Coordinated CR Pilot Assignment Algorithm

6.4.1 Introduction

In this section, we design a suitable coordination protocol for SUs to the above described two-operator CRN. We assume that BS p, unconstrainedly selects a user $i_\star$, where $i_\star \in \{1, \cdots, K\}$ is assigned to SP p and BS s initially visits in an exhaustive manner all the SUs, in order to acquire a subset, $\mathcal{L} \subset \{1 \cdots K\}$, the elements of which will be the indices of the SUs which are ϵ-orthogonal to user $i_\star$. We suppose that a SU within subset $\mathcal{L}$ is indexed by $j \in \mathcal{L}$. Then, BS s will schedule user terminal $j_\star \in \mathcal{L}$, which will have the best channel estimation MSE performance.

6.4.2 SU scheduling algorithm

The scheduling (optimization) problem with respect to the secondary network is the following

$$j_\star = \arg\min_{j \in \mathcal{L}} \frac{\mathcal{M}_s}{\mathrm{tr}(\mathbf{R}_{ss}^{(j)})}, \tag{6.13}$$

subject to

$$\frac{\left\|\mathbf{R}_{sp}^{(j)}\mathbf{R}_{pp}^{(i_\star)}\right\|_2}{\mathrm{tr}(\mathbf{R}_{sp}^{(j)})\mathrm{tr}(\mathbf{R}_{pp}^{(i_\star)})} < \epsilon, \tag{6.14}$$

where $j \in \mathcal{L} \subset \{1, \cdots, K\}$ belongs to SP s and ϵ is a positive system design parameter which illustrates the degree of orthogonality between the signal spaces spanned by covariance matrices $\mathbf{R}_{sp}^{(j)}$ and $\mathbf{R}_{pp}^{(i_\star)}$. In case ϵ is such that BS s cannot find such a subset $\mathcal{L}$ of users ($|\mathcal{L}| = 0$), it selects no user for the present resource block, in other words, the secondary system becomes silent.

In summary, the above explained coordinated user scheduling algorithm can be described in terms of each scheduling interval by the following steps

---

Algorithm 6 Coordinated pilot assignment for a CRN

Step 1: BS p selects a user $i_\star$ for transmission, $i_\star \in \{1, \cdots, K\}$.

Step 2: Having this information, BS s finds a user subset, $\mathcal{L}$ with $|\mathcal{L}| < K$ such that $j \in \mathcal{L}$ when

$$\frac{\|\mathbf{R}_{sp}^{(j)}\mathbf{R}_{pp}^{(i_\star)}\|_2}{\mathrm{tr}(\mathbf{R}_{sp}^{(j)})\mathrm{tr}(\mathbf{R}_{pp}^{(i_\star)})} < \epsilon. \tag{6.15}$$

In case no SU fulfills the above orthogonality criterion, BS s schedules no user (the PU functions under interference-free conditions), otherwise move to Step 3.

Step 3: BS s schedules user $j_\star \in \mathcal{L}$ where

$$j_\star = \arg\min_{j \in \mathcal{L}} \frac{\mathcal{M}_s(\mathbf{R}_{ss}^{(j)}, \mathbf{R}_{ps}^{(i_\star)})}{\mathrm{tr}(\mathbf{R}_{ss}^{(j)})}. \tag{6.16}$$

6.5   Numerical Results

In order to evaluate the performance of the proposed pilot assignment scheme, simulations of a two-SP prioritized CRN have been performed. Some basic simulation parameters are given in Table 6.1. These parameters are being kept in the following simulations unless otherwise stated.

It should be noted that in our example the AOAs follow an unbounded (Gaussian) distribution. Moreover, all user terminals have the same distance from their serving BS (800m) and the angles of their positions are uniformly distributed along this circle. The performance metric used to evaluate the proposed coordinated scheduling scheme is the normalized channel estimation MSE. Numerical results which depict the performance of the proposed coordinated scheduling

Table 6.1: Basic simulation parameters

SP CA radius	1 km
SP CA edge SNR	20 dB
Number of users per SP	10
Distance from a user terminal to its BS	800 m
Path loss exponent	3
Carrier frequency	2 GHz
Antenna spacing	$\lambda/2$
Number of paths	50
Pilot length	10

scheme with an averaging over 100 independent system topologies (user positions) are shown both for a PU and for a SU, for an angle spread of 10 degrees and for two different values of the threshold ϵ, 0.03 and 0.08, respectively. In the figures, "CBC" stands for the proposed Covariance-Based (Bayesian) Coordinated estimation algorithm, "CBU" denotes the Covariance-Based Uncoordinated estimation case, "CBIF" denotes the Covariance-Based Interference-Free case , while "LSU" stands for the conventional Least Squares Uncoordinated case and, finally, "LSIF" corresponds to the Least Squares Interference-Free case.
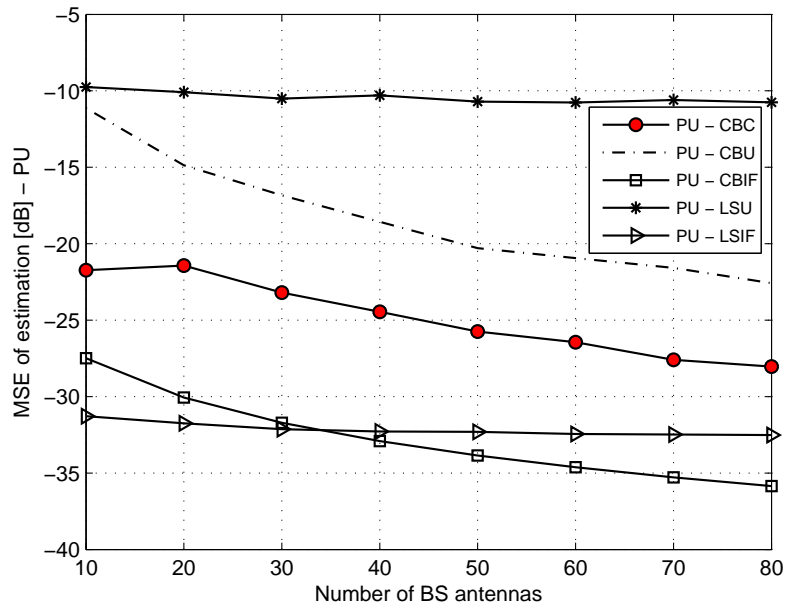

Figure 6.2: PU estimation MSE vs. BS antenna number, M, with $\epsilon = 0.03$.

From Fig. 6.2 and Fig. 6.3, we observe that the covariance-based (Bayesian) channel estimation methods -both CBU and CBC- outperform the conventional least squares (LS) estimation method for the whole range of M under examination, both concerning the PU and the SU. Also importantly, the proposed CBC scheduling algorithm shows a better performance behavior compared to the uncoordinated CBU algorithm. More specifically, as Fig. 6.2 shows, the performance
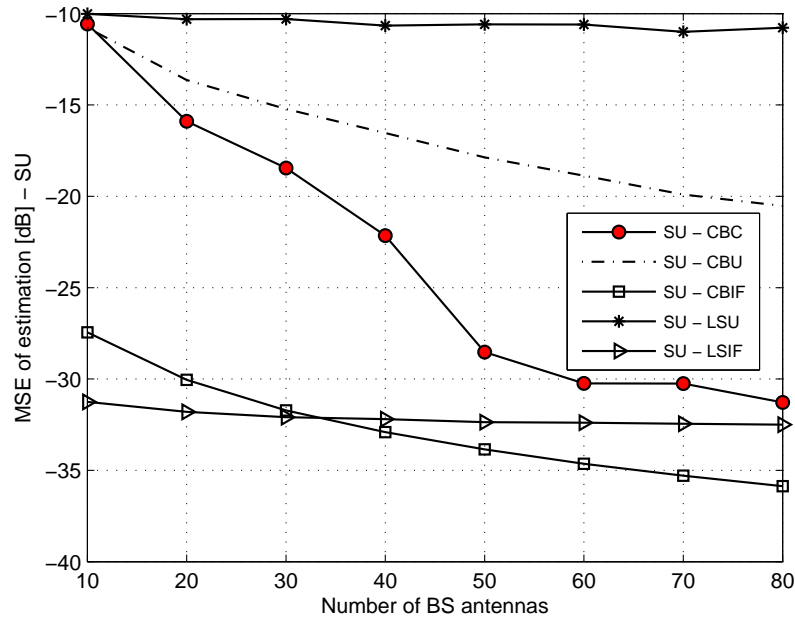
75

Figure 6.3: SU estimation MSE vs. BS antenna number, M, with $\epsilon = 0.03$.

gain of the CBC over the CBU algorithm can reach or even overcome (for smaller values of M) the value of 6dB plus the fact that the estimation performance of the PU approaches the interference-free case for large values of M, which verifies Theorem 2.
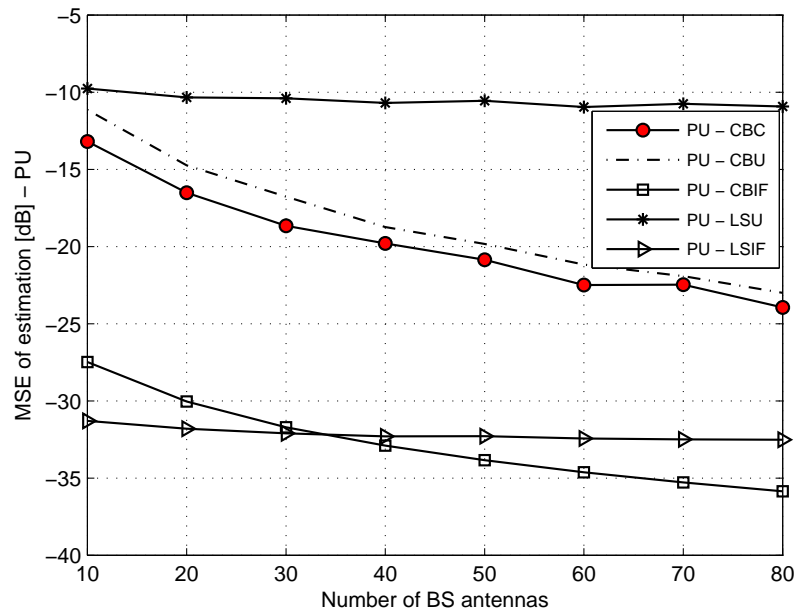

Figure 6.4: PU estimation MSE vs. BS antenna number, M, with $\epsilon = 0.08$.

The above conclusions also hold for the SU case, with the difference being in the slope of the CBC curve. Here, the SU-CBC curve fastly approaches the interference-free performance curve as the number of BS antennas becomes large. This can be explained by the fact that the orthogonality threshold value ϵ remains unchanged for the whole M range, so consequently, as M grows really large and ϵ remains the same, the SU will tend to suffer from very few or even zero outages, thus causing interference to the PU and this is the reason why the slope of the PU-CBC curve is much smaller. Due to this way of implementation, looking at the smaller M regime, the PU behaves satisfactorily and the gap between the PU-CBC and the SU-CBC is significant for small values of M (MSE of about -22dB for the PU and -10dB for the SU when $M = 10$).
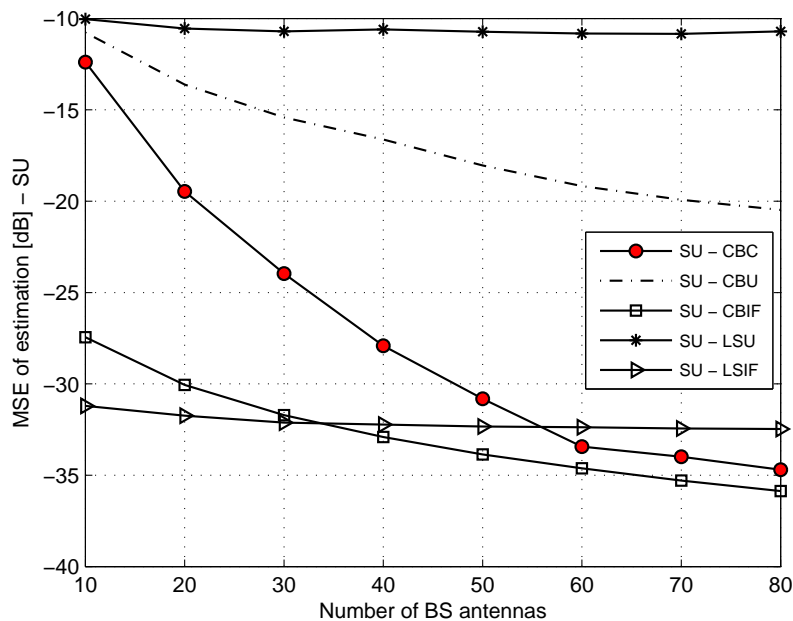

Figure 6.5: SU estimation MSE vs. BS antenna number, M, with $\epsilon = 0.08$.

In Fig. 6.4 and Fig. 6.5 the MSE performance curves of the same algorithms are derived for a larger threshold parameter, $\epsilon = 0.08$. Here, we can make similar conclusions as the above with a big difference: the PU-CBC performance has now deteriorated (-13dB for $M = 10$ antennas) and it is just marginally better than the PU-CBU one. On the contrary, the SU-CBC curve is fastly approaching the interference-free regime and it behaves almost likewise over a value of M ($M = 60$). The explanation of this phenomenon is the same as the one described above: as the threshold value is decreased for an unchanged value of M and the angle spread, the coordinated CB scheduling method works more efficiently for the PU. Hence, an important part of the pilot assignment algorithm's design is deciding on an appropriate orthogonality threshold, which will compromise between guaranteeing the interference avoidance for the PU and simultaneously limiting the outage rate of the secondary system.

6.6   Conclusions

In this chapter, we proposed a covariance-based pilot assignment algorithm within the channel estimation process itself regarding a CRN, which consists of two SPs and their corresponding users. The pilot assignment method is based upon the long-term knowledge of the second order statistics (channel covariance matrices) of the user channels within both operators. In the large BS antenna number, M, regime, it is shown that the channel estimation performance approaches an interference-free scenario and significant performance gains are presented.

Chapter 7

Conclusions and Future Research

In this thesis, we have conducted a throughput-based performance analysis of two of the most popular CR schemes, namely the interweaved and the underlay CRN approaches. Also, another focus of this dissertation, was the design and evaluation of novel, multi-antenna signal processing algorithms for CRNs, within a combined instantaneous and statistical CSI scenario. Considering such a framework, we focused on new transmission techniques with respect to both primary and secondary communication and we proposed coordination criteria, leading to a coherent selection of rate-optimal precoding schemes. Our contributions are summarized in the following:

- We initially investigated the throughput potential of interweaved and underlay CR systems, by applying a popular and low complexity spectrum sensing algorithm for the prior and standard precoding and power allocation schemes for the latter approach. More comprehensively, the achievable ergodic throughput of the two examined CRN approaches was computed and interesting comparisons were made under a common figure of merit. In this direction, we derived closed form expressions for the outage probability of primary communication, along with expressions describing the ergodic rate of the SU. It was numerically illustrated that the behavior of each of the examined CRN approaches is highly dependent on basic system parameters, such as the number of transmit antennas, the activity profile of the primary network, the quality of spectrum sensing for the interweaved approach, as well as the applied BF scheme for the underlay approach.

- Furthermore, we have studied the problem of rate-optimal receive BF and user selection, considering the uplink of a multi-user, unprioritized CRN. As the assumption of a CSI setting, whereby the involved channels would be merely instantaneously (resp. statistically) known is, to a great extent, optimistic (resp. pessimistic), we have considered a *mixed* CSI scenario. According to this scenario, the direct channel link between a serving BS and its assigned user can be estimated in its instantaneous form, whereas a cross-link can be only statistically known in the form of a covariance matrix. Focusing on this scenario, we derived a closed-form expression of the ergodic user rates, conditioned on the knowledge of the direct link between an operator and its served user. Based on an approximation of this expression, applicable to an interference-limited system, we also derived a closed form expression of the rate-optimal receive BF vector. In addition, we proposed new, low complexity user selection schemes with minimal CSI exchange between the operators, with the aim of maximizing the system's ergodic sum rate.

- The problem of rate-optimal transmit BF for a MISO underlay CRN, assuming the existence of the -previously described- *mixed* CSI, was thereafter formulated. Concentrating on downlink communication, we proposed a more practical revision regarding the classical underlay CRN approach. According to this revision, the goal of the system's design is the maximization of the secondary system's achievable ergodic rate, subject to an average rate constraint imposed on primary communication. The latter constraint forms an alternative to the classical maximum tolerable interference temperature constraint at the PU, because it also takes into consideration the strength of the direct primary link. Then, emphasizing on such a problem formulation, we posed the problem of SU rate-optimal transmit BF with mixed, distributed CSIT. This problem was examined by highlighting connections with the theory of team decisions and it was shown that the derived iterative solution outperformed the throughput potential of classical distributed precoding solutions.

- Continuing the investigation of the latter precoding problem with mixed, distributed channel knowledge, we developed a coordination scheme, according to which, the primary and the secondary transmitter coordinate on the basis of statistical (covariance) information of the global channel. The proposed precoding strategy was shown to outperform conventional approaches taken from the literature, such as the interference temperature constrained underlay scenario, merely at a price of low requirements. We concluded to such requirements with the aim of protecting the PU in any case, as it was not allowed for the transmitters to exchange any instantaneous CSI. A basic advantage of this formulation is the fact that the proposed, statistically coordinated precoding algorithm can be run off-line. It should be noted that the developed approach was also designed by utilizing a team decisional approach.

- Finally, within a prioritized CRN framework, we proposed a pilot assignment algorithm, based on channels' second order statistics and we examined the designed algorithm's potential in the context of large-scale antenna systems. Being inspired by our recent works, such as [18], which focus on solving the problem of pilot contamination, we proposed a coordinated pilot assignment algorithm. This algorithm enhances the quality of channel estimation at the primary transmitter, while removing interference caused by secondary transmissions. Importantly, we showed, both by analysis and by simulation that the performance of the designed algorithm, approaches the zero-interference regime, when the (bounded) supports of multipath AOAs of the desired and the interfering channel are non-overlapping. Our pilot assignment algorithm exactly exploits this behavior and, interestingly, significant gains are observed, in comparison with standard pilot-aided channel estimation techniques.

Future Research

The analytical performance-based comparison between the interweaved and the underlay CRN approaches, which was presented in Chapter 2, has revealed regimes in which one of the two examined paradigms outperforms the other. Also, different throughput levels are achieved for the SU, when different precoding schemes are applied with reference to the underlay approach. Therefore, different aspects of "cognition" could be investigated, apart from the classical one, which concerns the potential existence of spectrum holes. Elaborating on such cognition aspects, an unlicensed secondary network could dynamically adapt its transmission scheme according to the

circumstances, i.e., whether the primary network shows a high or a low activity rate, the quality of spectrum sensing, when it comes to the interweaved approach, as well as the targeted outage probability level at the PU.

Furthermore, in Chapter 3, we derived a closed form expression for the achievable ergodic rate of a user in terms of an unprioritized SIMO network in the uplink, as well as an approximation of this expression, applicable to interference-limited networks, i.e., networks in which interference is the major source of signal degradation, as compared to noise. Additionally, a rate-optimal BF was derived, by exploiting the latter expression, and low complexity user selection schemes were proposed, capitalizing on the derived precoding policy with *mixed* CSI. An interesting as well challenging extension could focus on the case of multi-operator CRNs, both unprioritized and prioritized ones (with different levels of priority). Proposing a rate-optimal user selection scheme for such a system is a challenging problem from a complexity point of view, especially if the notion of prioritization is added to it.

In this dissertation, we have also presented results, considering the design of transmission schemes for multi-antenna underlay CRNs, with mixed, albeit *distributed* CSIT. In Chapters 4 and 5, we studied such CR settings, which gave rise to distributed multi-agent decision making, or equivalently to a *team decisional* problem. The followed approach, either leading to an iterative distributed precoding algorithm (Chapter 4), or to a low complexity, off-line solution, obtained via statistical coordination (Chapter 5), is a novel method to deal with precoding in the existence of distributed as well as locally available channel information. Such an approach has, therefore, the potential to be generalized to many other network configurations, as the local availability of channel estimates is both realistic and practical. Moreover, the design of an *online* algorithm, also exploiting the instantaneously available channel information is a challenging task, which needs to be efficiently tackled.

Finally, we also proposed a covariance-based, pilot assignment algorithm for a CRN, as part of the channel estimation process itself. Examining a *massive MIMO* approach of the investigated cognitive system, it was shown that the performance of channel estimation, approaches the interference-free case, as the number of BS antennas becomes large. Also, significant performance (MSE) gains were reported in comparison with standard pilot-aided channel estimation techniques, making the large-antenna notion for a prioritized CRN quite promising. However, in the examined scenario, we assumed that the channels' second order statistics could be estimated in a separate manner. In practice, this could be feasible by exploiting resource blocks, where the desired and the interfering users are known to be assigned at different times. Thus, a challenging task could be the one of a specific training design for learning covariance information of a channel. One can state that, since covariance information slowly varies with time, such learning process may not consume a substantial resource overhead. Such overhead would depend on the degree of user mobility.

Chapter 8

Résumé [Français]

8.1 Contexte de la technologie CR

Le spectre *radio électromagnétique* est une ressource naturelle nécessaire pour les communications sans fil. L'utilisation du spectre est mondialement réglementée par les gouvernements dans le but de fournir des services essentiels ainsi que protéger ces services contre les brouillages préjudiciables. Toutefois, la diffusion massive des services sans fil actuels et l'évolution de la communication sans fil ont donné lieu à un grand besoin de bande, dans le but d'offrir plusieurs services et applications avec des débits de données élevés. Cette conclusion peut être faite par un regard au tableau d'allocation des fréquences de l'administration des télécommunications et de l'information nationale[1]. Selon ce tableau, il est rapporté que l'entité de presque toutes les bandes de fréquences a été attribué, ce qui conduit à un manque de bande pour les services sans fil émergents [7].

Néanmoins, selon un rapport publié par la Commission Fédérale des Communications (FCC), en 2002, il est indiqué que le spectre radio accessible devient considérablement sous-utilisé [8]. Plus concrètement, la deuxième conclusion à la page 3 de ce rapport, révèle exactement le phénomène de la sous-utilisation du spectre:

"Dans beaucoup de bandes, l'accès au spectre est un problème plus important que la rareté matérielle du spectre, en grande partie grâce à la réglementation de commandement et de contrôle héritage que limite la capacité des utilisateurs potentiels du spectre pour obtenir cet accès."

Par conséquent, la sous-utilisation du spectre radioélectrique décrit ci-dessus a donné lieu à la notion des *trous de spectre* (aussi souvent appelé comme des *espaces blancs* dans la littérature), une définition de qui est fourni ci-dessous [9]:

"Un trou de spectre est une bande de fréquences assignées à un utilisateur primaire (PU), mais, à un moment donné et d'un emplacement géographique particulier, la bande n'est pas utilisé par cet utilisateur."

L'existence de la pénurie de spectre en raison d'une exclusivité statique et de longue durée de l'utilisation du spectre réglementé dans les grandes zones géographiques [10], ainsi que la

---

[1]www.ntia.doc.gov/osmhome/allochrt.pdf.

sous-utilisation du spectre décrit, ont donné lieu à l'idée de CR [11]. Une définition d'un tel système est donnée dans [12]:

"CR est un système de communication sans fil intelligent qui est conscient de son environnement (le monde extérieur), et utilise la méthodologie de compréhension par construction-afin-de-apprendre de l'environnement et d'adapter ses états internes des variations statistiques de la fréquence radio entrant (RF) stimuli par des changements correspondants dans certains paramètres de fonctionnement (par exemple, la transmettre puissance, la fréquence porteuse, et la stratégie de modulation) en temps réel, avec deux objectifs principaux à l'esprit:

- *communications extrêmement fiables chaque fois et partout où nécessaires;*

- *utilisation efficace du spectre radioélectrique."*

8.2 État de l'art pour les systèmes CR

8.2.1 Systèmes CR: une technologie émergente et stimulant

Le concept de CR constitue à la fois une technologie émergente et prometteuse. Un des éléments les plus cruciaux de ce concept est la capacité de mesurer, sentir et apprendre un canal. En outre, c'est la capacité d'avoir la connaissance des paramètres liés aux caractéristiques de canal radio, la disponibilité du spectre et la puissance, les exigences des utilisateurs, les applications ainsi que d'autres restrictions d'exploitation [13].

En raison de leur coexistence avec les systèmes autorisés, ainsi que à cause des exigences de QoS diverses, noeuds d'accès opportunistes apportent un certain nombre de défis intéressants. Un de ces défis consiste à éviter les brouillages tant qu'utilisateurs opportunistes devraient éviter d'interférer avec les titulaires. En outre, les systèmes CR devraient soutenir une communication conscient de QoS, compte tenu de l'environnement du spectre, qui est à la fois hétérogène et dynamique. De plus, les systèmes opportunistes devraient fournir une communication transparente, indépendamment de l'existence de transmissions par les systèmes titulaires [14].

8.2.2 Paradigmes de systèmes CR

Les systèmes CR peuvent être classés en deux principaux paradigmes en ce qui concerne l'existence ou l'absence d'hiérarchie des utilisateurs. Ces deux paradigmes principaux sont systèmes prioritaires et systèmes sans ordre de priorité. Le premier groupe est constitué par l'existence d'une hiérarchie d'accès entre les utilisateurs, et aura plus de l'effort de cette thèse, tandis que la seconde est basée sur la notion de partage du spectre (absence de priorisation).

8.2.2.1 Systèmes CR prioritaires

Selon ce scénario, les utilisateurs entrent visant à utiliser le spectre de manière opportuniste, sont généralement appelés comme utilisateurs secondaires (SUs). D'autre part, les utilisateurs titulaires d'occupation sans contrainte des ressources spectrales sont désignés comme utilisateurs principaux (PUs). Un exemple illustratif d'une telle hiérarchie, consiste en l'opération de SU dans les bandes de télévision (TV). Un SU pourrait effectuer détection du spectre et utiliser des fréquences appartenant à une bande de TV si le spectre est inutilisé [10].

Dans ce qui suit, nous allons élaborer sur le fonctionnement des principales approches de conception des systèmes CR prioritaires. Plus précisément, nous allons nous concentrer sur les systèmes comprenant d'un émetteur primaire multi-antenne (TX), $TX\ p$, avec son (mono-antenne) équipement d'utilisateur assigné (UE), $UE\ p$ ainsi que d'un émetteur multi-antenne secondaire, $TX\ s$, avec son équipement d'utilisateur assigné, $UE\ s$. Les vecteurs de canal entre $TX\ i$ et $UE\ j$ sont appelés $\mathbf{h}_{ij}$.

Jusqu'à présent, trois grandes approches de conception CR prioritaires ont émergé:

8.2.2.1.1 Approche CRN entrelacée L'approche CRN entrelacée (Fig. 8.1) est basée sur l'idée de partage du spectre opportuniste. Puisque les études, comme [8] a révélé la sous-utilisation du spectre radioélectrique, ou, en d'autres termes l'existence des trous du spectre dans l'espace, le temps ou la fréquence, il est raisonnable de développer et d'enquêter des algorithmes et des techniques de détection du spectre, dont le but serait de révéler ces vides temporaires d'espace-temps-fréquence. En conséquence, après la localisation de tels vides, les systèmes secondaires peuvent fonctionner dans des dimensions orthogonales de l'espace, de temps ou de fréquence, en relation avec des signaux de communication primaire. Ainsi, de cette façon, l'utilisation du spectre est améliorée par la réutilisation opportuniste sur les trous du spectre [10].
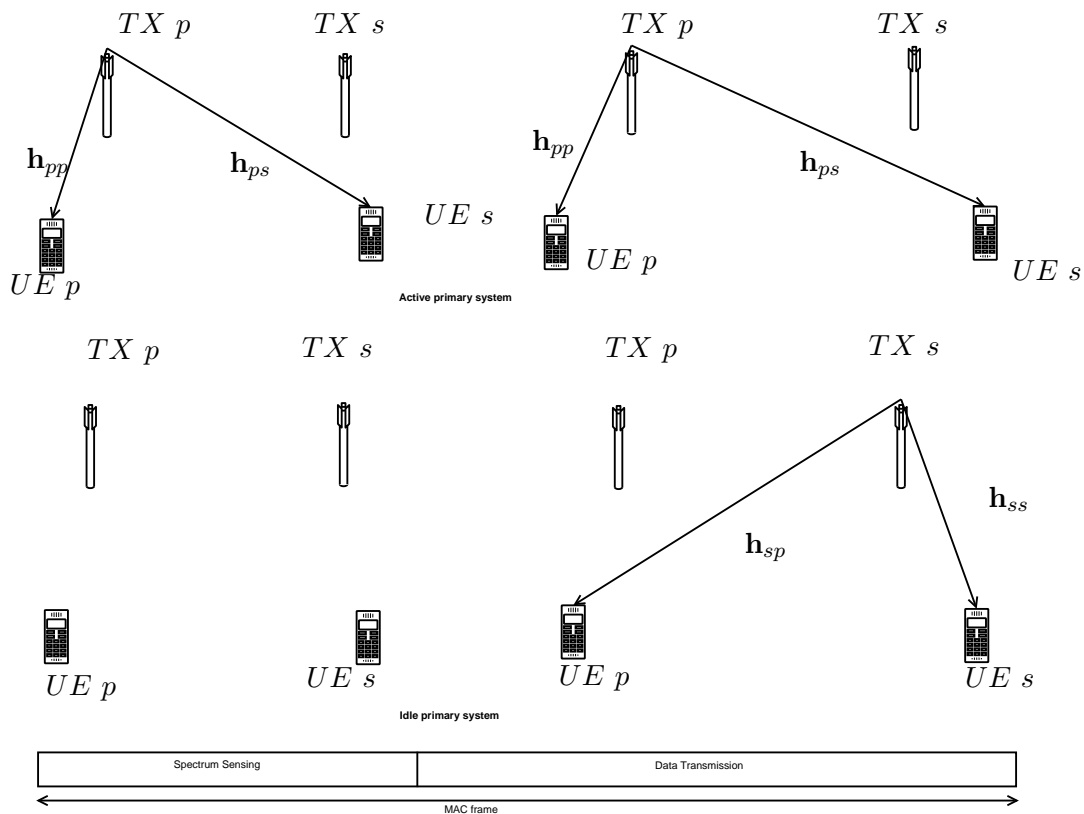

Figure 8.1: Fonctionnement d'un CRN entrelacé lors d'un contrôle d'accès au support (MAC) trame. Lorsque le système secondaire détecte l'existence de communication primaire (partie haute), il reste silencieux pendant la sous-trame de transmission de données. A l'inverse, lorsque le circuit primaire est trouvé inactif (partie basse), le secondaire décide de transmettre.

Cependant, phénomènes tels que évanouissement de canal, shadowing, bruit ainsi que l'existence de détection du spectre désuet, peuvent donner lieu à la détection imparfaite, dénommé *miss-détection* événements, qui peuvent potentiellement violer les exigences de qualité de service de PUs. Au contraire, une dépense énorme de ressources disponibles vers détection serait certainement améliorer la qualité de détection du spectre, mais au prix d'une dégradation du débit traversier du système secondaire. Ainsi, on observe que un compromis intéressant ainsi que difficile entre la qualité de la détection du spectre et la maximisation du débit d'un réseau secondaire, existe.

8.2.2.1.2 Approche CRN sous-couche Selon la sous-couche approche CRN (Fig. 8.2), un système primaire permet la réutilisation simultanée de ses ressources spectrales par un système secondaire (sans permis), à condition que l'interférence générée par des émetteurs secondaires aux récepteurs primaires est inférieure à un seuil prédéfini. En 2003, la FCC a publié un mémorandum demandant commentaire sur le modèle de température d'interférence décrite ci-dessus, dans le but de contrôler l'utilisation du spectre [8], [15]. Décider de l'interférence maximale tolérée due à une transmission secondaire vers un récepteur primaire, est une tâche difficile dans les scénarios CR sous-couche. L'interférence à un récepteur primaire donnée peut être déterminée par un SU par espionnant une transmission du système primaire, si le lien entre eux est réciproque.
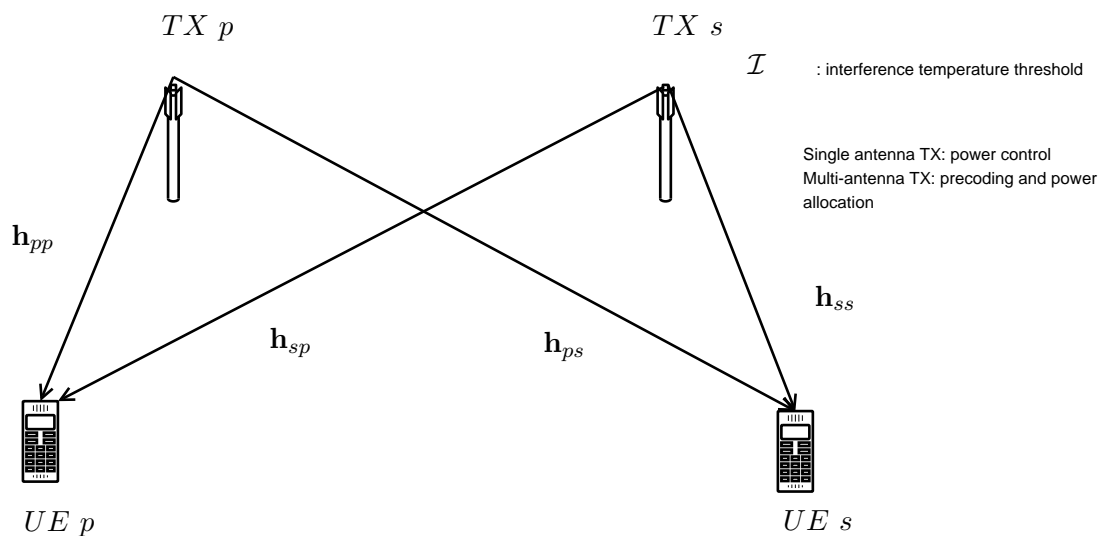

Figure 8.2: Fonctionnement d'un CRN de sous-couche. Le système secondaire coexiste avec le primaire, à condition que la puissance d'interférence vers le PU sera inférieure à un niveau prédéfini, $\mathcal{I}$.

Le principe de fonctionnement du CRN de sous-couche, c'est à dire, la limitation de la puissance de l'émetteur secondaire, imposée par une contrainte sur l'interférence causée à PU, exige une conception soignée, puisque l'émetteur secondaire peut être trop prudente dans sa puissance de sortie, afin de se conformer à la restrictions sur la base de la température interférence [10].

Fait intéressant, en dehors de la largement étudiée température d'interférence maximale tolérée au PU, autres mesures de perturbation maximale tolérable peuvent être introduits, qui sera étudiée dans les chapitres 2-5 de cette thèse. Une de ces mesures est la probabilité de

panne de communication primaire (qui sera étudiée dans le chapitre 2), en d'autres termes, la probabilité avec laquelle le taux de communication de données primaire est inférieur à un seuil prédéfini.

Une autre mesure de perturbation dans le sens de la protection de communication primaire est un débit moyen minimum, qui doit être réalisé sur le côté PU. Une telle mesure a l'avantage d'être plus réaliste et pratique, en comparaison avec celui basé sur la température d'interférence. La raison à cela est le fait que de cette façon, aussi la qualité du lien directe primaire est pris en considération, en d'autres termes, si le premier lien est forte, un plus haut niveau de interférence peut être tolérée au PU, ce qui conduit à une gestion des ressources qui améliore le débit de la communication secondaire.

L'approche CRN de sous-couche est généralement suivie dans le spectre autorisé, alors qu'il peut être également appliquée dans le cadre de bandes sans licence, dans le but de fournir des classes de service différentes à différents utilisateurs [10].

8.2.2.1.3 Approche CRN de recouvrement La prémisse de CRNs de recouvrement est que l'émetteur secondaire a connaissance de données transmis la séquence (ou un message) de PU, ainsi que de la façon dont cette séquence est codée (également appelé son livre de codes) [10]. Par suite, cette connaissance peut être exploitée par l'émetteur secondaire de différentes manières dans le but d'améliorer la performance des deux systèmes.

Cette approche ne sera pas étudié dans cette thèse. La raison en est que, selon l'approche de recouvrement, une grande quantité d'informations de côté réseau doit être disponible au niveau des nuds secondaires. Cette information de côté consiste en la connaissance des gains de canal, des techniques de codage, et éventuellement les séquences de données transmises des PUs. En conséquence, une telle demande conduit à des niveaux de complexité de codage et de décodage, qui sont supérieurs à ceux des autres méthodes CRN [10].

8.2.2.2 Systèmes CR sans priorité

Dans les systèmes de communication sans fil actuels, le spectre RF est généralement divisé en bandes de fréquence qui sont exclusivement attribuées (sous licence). Contrairement à cette approche, CRNs sans ordre de priorité partagent le spectre disponible simultanément, sans aucune restriction de priorité imposée par un (ou plusieurs) des opérateurs.

Dans ce contexte, un nombre d'avantages potentiellement se pose. Certains de ces avantages consistent à: l'amélioration de l'efficience spectrale, l'amélioration de la couverture, une augmentation de la satisfaction d'utilisateur, ainsi que l'augmentation des revenus pour les opérateurs de services et une diminution des dépenses de fonctionnement [Consultez [16] et références citées].

Cependant, l'interférence causée par des transmissions voisins doit être gérée efficacement. En supposant l'existence de plusieurs antennes à des émetteurs, les opérateurs doivent choisir entre la coopération avec d'autres opérateurs et de rivaliser avec eux [17]. Ce choix est quantifiée par un bien conçu politique de transmission (précodage).

Par conséquent, problèmes intéressants se présentent, par rapport à la politique de précodage suivie. Un objectif populaire dans de tels systèmes est la maximisation de la (moyenne) débit de données agrégées du système. Dans le Chapitre 3, un tel système est examiné, en se concentrant la communication de uplink, à l'existence d' information de canal imparfaite.
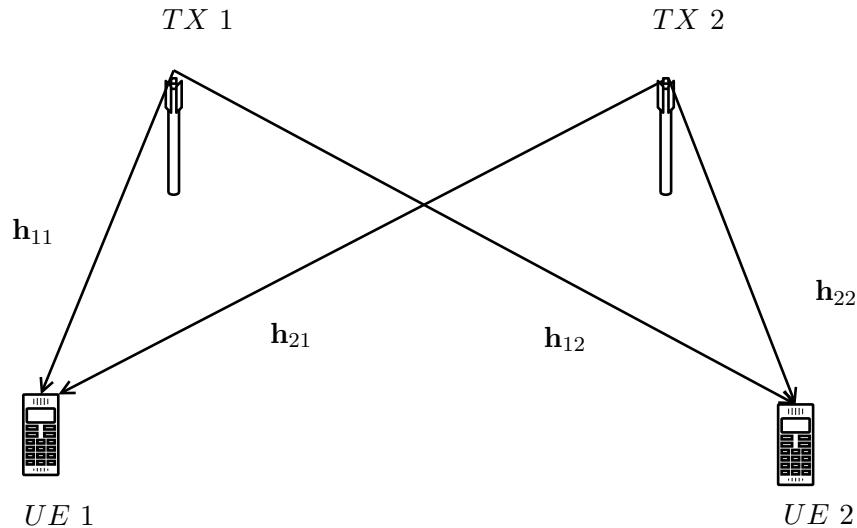
Figure 8.3: Fonctionnement d'un CRN sans ordre de priorité (communication de downlink). Les deux systèmes transmettent simultanément, et aucune règle de restriction est posée par aucun des deux systèmes.

8.2.3 Utilisation des Antennes multiples dans les systèmes CR

Une grande partie des recherches antérieures ont porté sur l'étude du problème de satisfaire une contrainte basée sur la qualité de service, pour le bien d'un système primaire, tout en maximisant le débit de communication secondaire. Vers ce sens, la recherche sur l'allocation des ressources radio pour CRN a principalement axé soit sur ??le domaine de la fréquence ou le domaine du temps, en supposant l'existence d'antennes simples à émetteurs CRN. Transmissions exploitant plusieurs antennes ont capté l'attention considérable au cours des dernières années. Antennes multiples peuvent être utilisés dans le but de réaliser suppression efficiente des interférences co-canaux pour les transmissions multi-utilisateurs avec une amélioration de la fiabilité par transformation espace-temps [Consultez [3] et références citées].

Néanmoins, le potentiel de l'utilisation de plusieurs antennes dans le cadre du partage du spectre opportuniste n'a pas encore été suffisamment compris et exploré. Antennes multiples peuvent être utilisés afin d'allouer l'espace des directions d'émission. Un tel allocation résulte à fournir CRN émetteurs secondaires avec plus degrés de liberté dans l'espace, en plus de temps et de fréquence. D'une telle manière, les systèmes secondaires peuvent intéressant équilibre entre maximiser leur débit et satisfaisant à une contrainte de qualité de service en ce qui concerne la communication primaire.

8.3 Contributions et Plan de la Thèse

L'objectif principal de cette thèse est l'analyse des performances de certains des architectures de CRN de base, en particulier l'approche entrelacée et l'approche sous-couche, ainsi que la conception et l'évaluation d'algorithmes de traitement du signal pour les CRNs de sous-couche, en présence de l'échange de CSI limitée entre émetteurs primaires et secondaires. Les algorithmes mentionnés visent à maximiser le débit de SU, tout en évitant la violation des garanties de qualité

de service à un réseau primaire établie. En outre, aussi des algorithmes de traitement du signal et de la sélection d'utilisateur sont proposées pour le cas de CRN sans priorité.

L'étude de comparaison de débit, ainsi que les systèmes de traitement de signaux conçus cherchent à apporter des réponses à un certain nombre de questions, telles que:

- Quelle approche d'un CRN avec priorité (entre la entrelacée et la sous-couche), surpasse l'autre pour différents scénarios de système, sous une contrainte de QoS communs la communication primaire? Différents scénarios de systèmes correspondent à différentes circonstances liées à: le profil d'activité de communication primaire, l'existence de antennes multiples, la qualité de la détection de spectre et autres.

- Quelle est la forme d'un (taux) optimal vecteur de réception BF, par rapport à un SIMO CRN sans priorité?

- Se concentrer sur la communication de downlink d'un MISO CRN de sous-couche, est-il possible de concevoir une politique de transmission, selon laquelle, le débit moyen de communication secondaire est maximisée, soumis à une contrainte de taux moyen au PU? Comment peut-on formuler cette problème, quand imparfaite ainsi que locale CSIT existe?

- Est-il possible de concevoir une politique de transmission de faible complexité pour le problème présenté précédemment?

- Puisque liens directs de canal doivent être estimés, dans le cadre CRN priorité, est-il possible de concevoir un système d'affectation des pilotes, qui permettra d'améliorer la qualité de l'estimation de canal? Quelle serait la performance d'un tel régime, en présence d'un grand nombre d'antennes aux émetteurs?

Un aperçu de la thèse est fourni ci-dessous et les contributions réalisées dans chaque chapitre sont résumés.

Chapitre 2 - Une étude comparative fondée sur les performances des CRNs entrelacées et CRNs sous-couche multi-antennes

Dans ce chapitre, deux des méthodes les plus populaires de conception de CRN, plus particulièrement, l'approche entrelacée et l'approche sous-couche, sont évalués, étant donné un cadre multiantenne, et comparées en termes de débit du système secondaire, sous réserve d'une contrainte de QoS communes au système primaire. Afin de procéder à une telle comparaison, nous dérivons des expressions de forme fermée pour la probabilité de panne aux PU, avec des expressions décrivant le taux moyen réalisable de la SU. Ensuite, les principaux paramètres de conception de chaque approche sont optimisés en termes de maximisation de la capacité ergodique secondaire pour une probabilité d'interruption donnée aux PU et une comparaison basée sur le débit s'effectue en référence aux différents paramètres du système tels que la probabilité d'interruption ciblée au PU, le nombre d'antennes d'émission, ainsi que la profil d'activité du réseau primaire et la qualité du processus de détection de spectre pour l'approche entrelacée. De cette façon, les avantages et les inconvénients de chacune des deux approches étudiées CRN sont révélés.

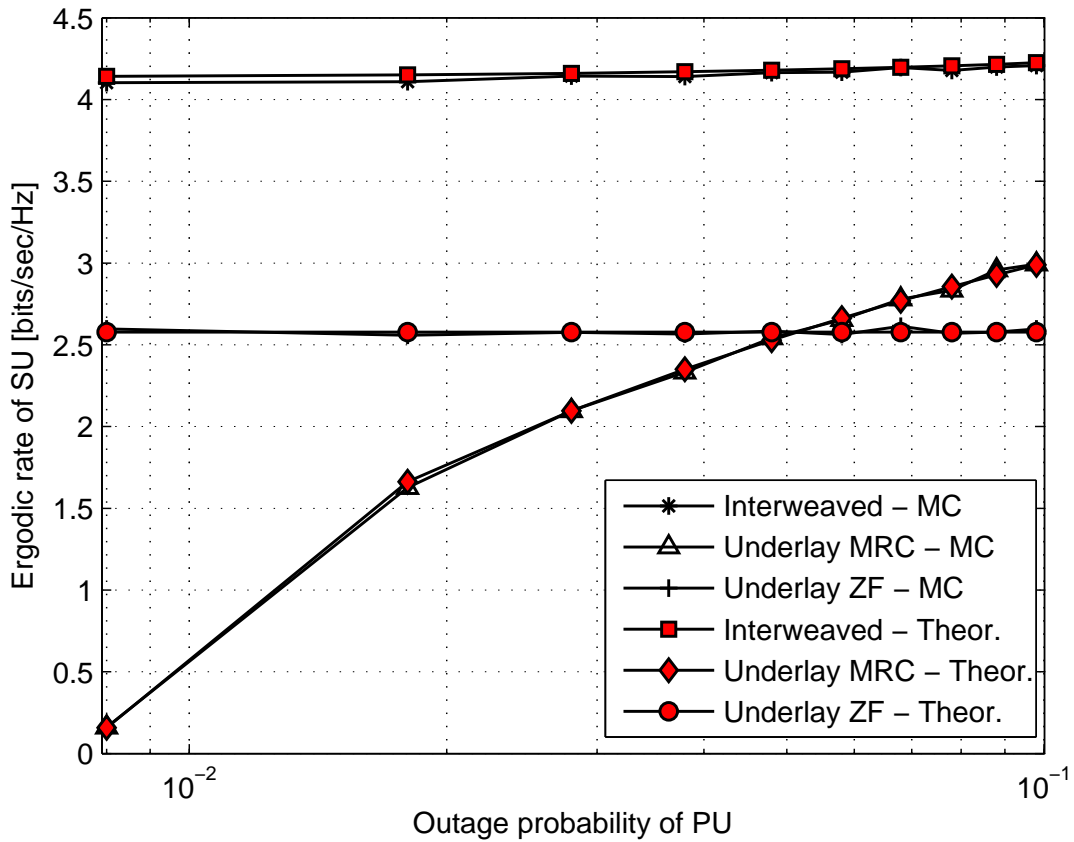Le travail dans ce chapitre a donné lieu aux publications suivantes:

Figure 8.4: Débit ergodique du SU contre probabilité d'interruption de communication primaire, M=4 antennes, $\mathcal{P}(\mathcal{H}_1) = 0.2$.

- *M.C. Filippou, D. Gesbert, and G.A. Ropokis, "Underlay versus Interweaved Cognitive Radio Networks: a Performance Comparison Study", in proc. of the 9th International Conference on Cognitive Radio Oriented Wireless Networks (CROWNCOM 2014), Oulu, Finland, 2014*

- *M.C. Filippou, D. Gesbert, and G.A. Ropokis, "A Comparative Performance Analysis of Interweaved and Underlay Multi-Antenna Cognitive Radio Networks", submitted to IEEE Transactions on Wireless Communications, Apr. 2014*
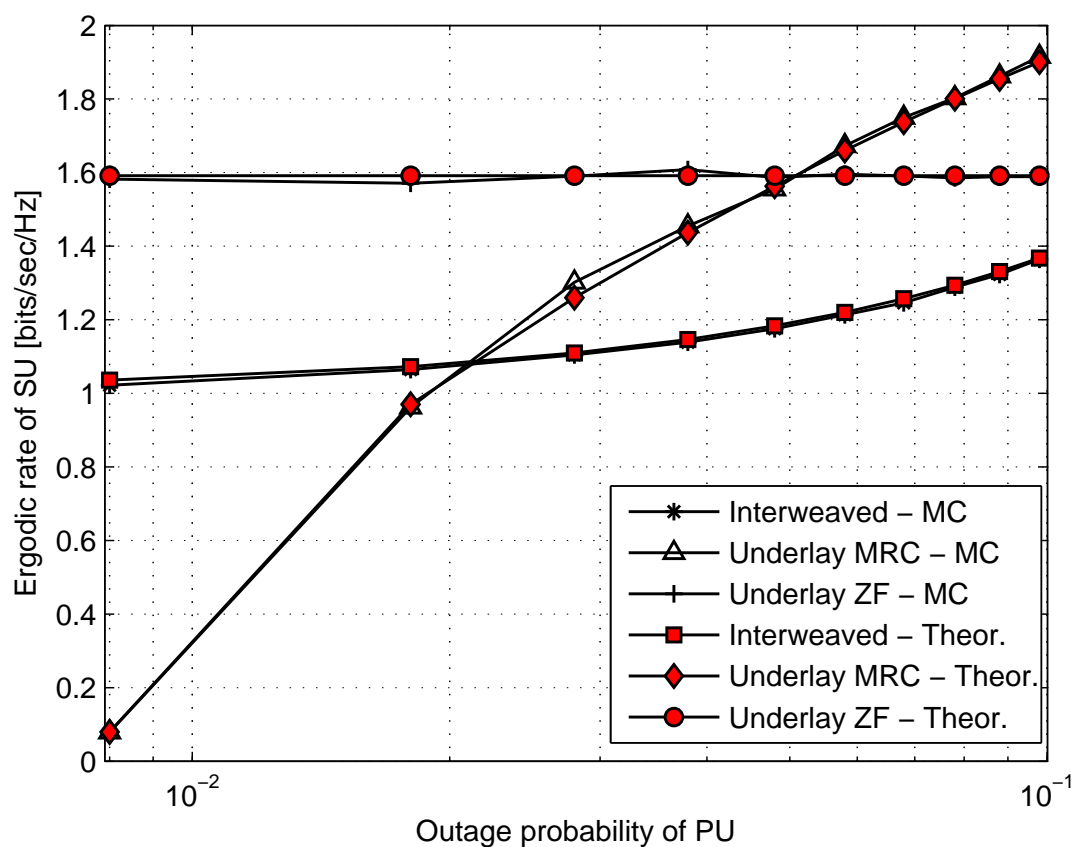
Figure 8.5: Débit ergodique du SU contre probabilité d'interruption de communication primaire, M=4 antennes, $\mathcal{P}(\mathcal{H}_1) = 0.8$.
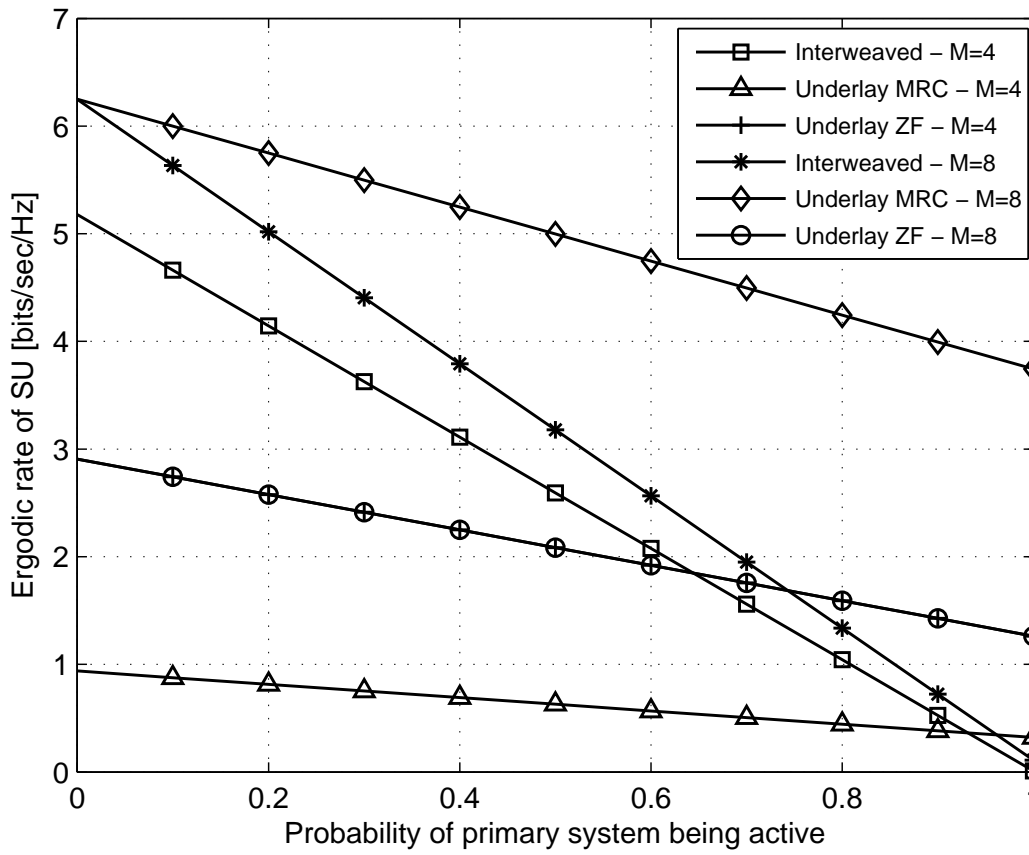
Figure 8.6: Débit ergodique du SU contre le profil d'activité du système primaire, probabilité d'interruption de PU (cible) $\mathcal{P}_o = 0.01$.
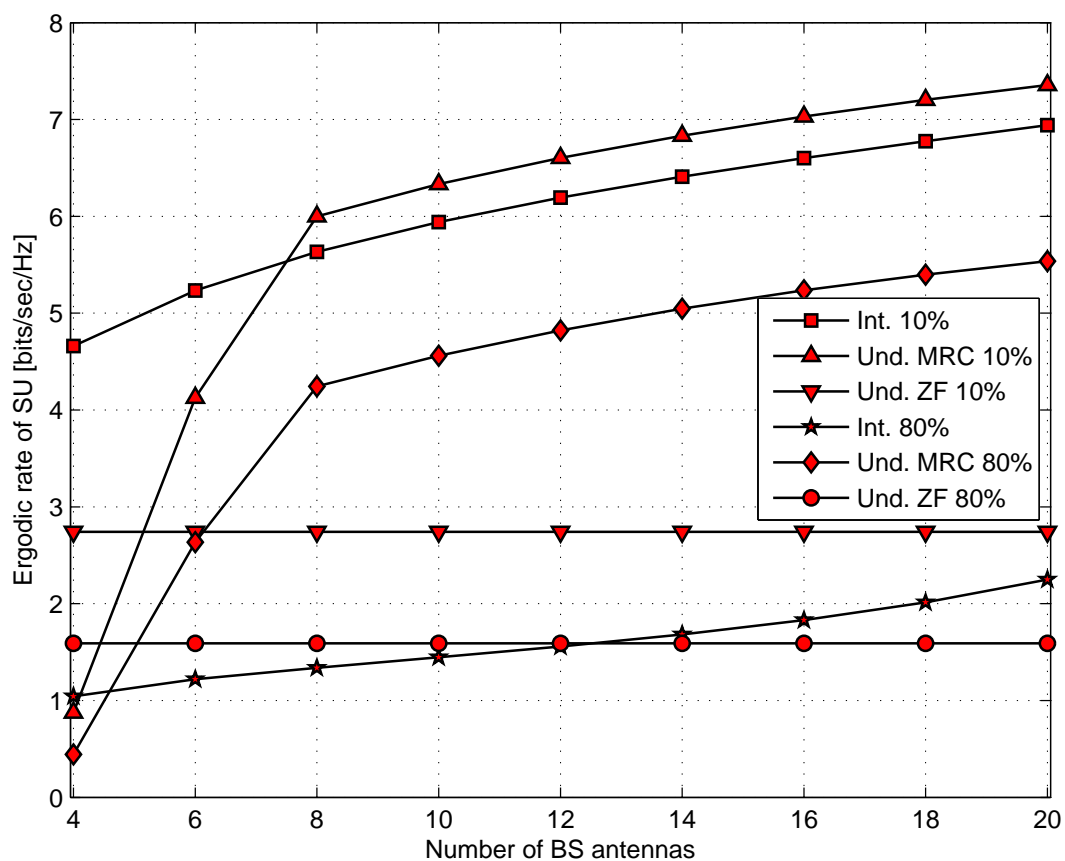
Figure 8.7: Débit ergodique du SU contre nombre d'antennes d'émission, M, probabilité d'interruption de PU (cible) $\mathcal{P}_o = 0.01$.
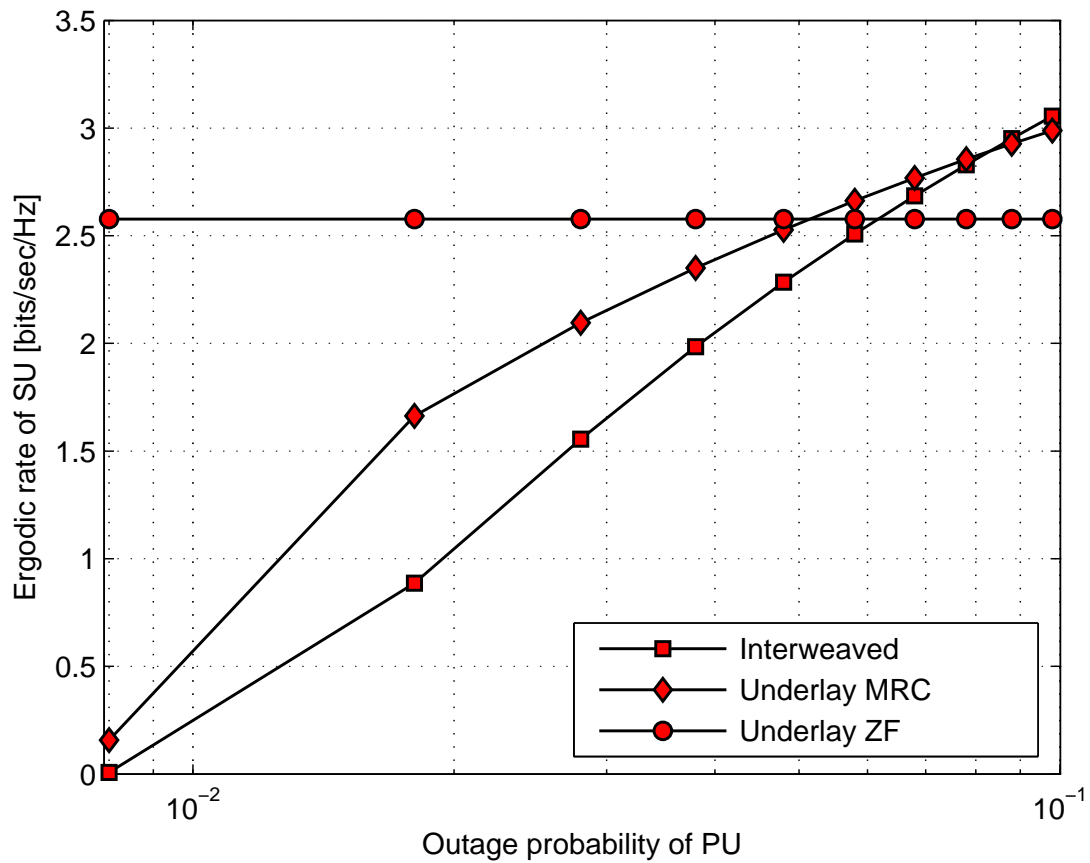
Figure 8.8: Débit ergodique du SU contre probabilité d'interruption de communication primaire, $\mathcal{P}(\mathcal{H}_1) = 0.2$, faible $BS\ p - BS\ s$ lien de force $\sigma_{00}^2 = -17$ dB.

Chapitre 3 - Taux-optimal BF et sélection d'utilisateur pour SIMO CRN sans priorité

Dans ce chapitre, l'uplink d'un SIMO CRN avec la même priorité pour les deux systèmes est considéré et le problème de taux-optimal recevoir BF est formulé et résolu. Nous considérons en particulier unn CSI scénario *mixte*, dans lequel le multi-antenne récepteurs (BSs), sont autorisés à estimer les chaînes de leurs utilisateurs assignés, alors qu'ils sont juste capables d'acquérir statistique (covariance) information des utilisateurs interférents. Ayant examiné un tel scénario CSI, nous dérivons une nouvelle, simple approximation du ergodique taux des utilisateurs (conditionnés sur la connaissance de leur lien direct), en mettant l'accent sur ??un système limité par les interférences. Ensuite, pour le régime mentionné, nous dérivons la BF vecteur taux-optimal et, enfin, nous proposons nouveaux (de faible complexité), algorithmes de sélection d'utilisateur, visant à maximiser le taux moyen global du système.

Le travail dans ce chapitre a été publié dans:

- *M.C. Filippou, D. Gesbert, and G.A. Ropokis, "Optimal Combining of Instantaneous and Statistical CSI in the SIMO Interference Channel", in proc. of Vehicular Technology Conference (VTC-Spring), Dresden, Germany, 2013*
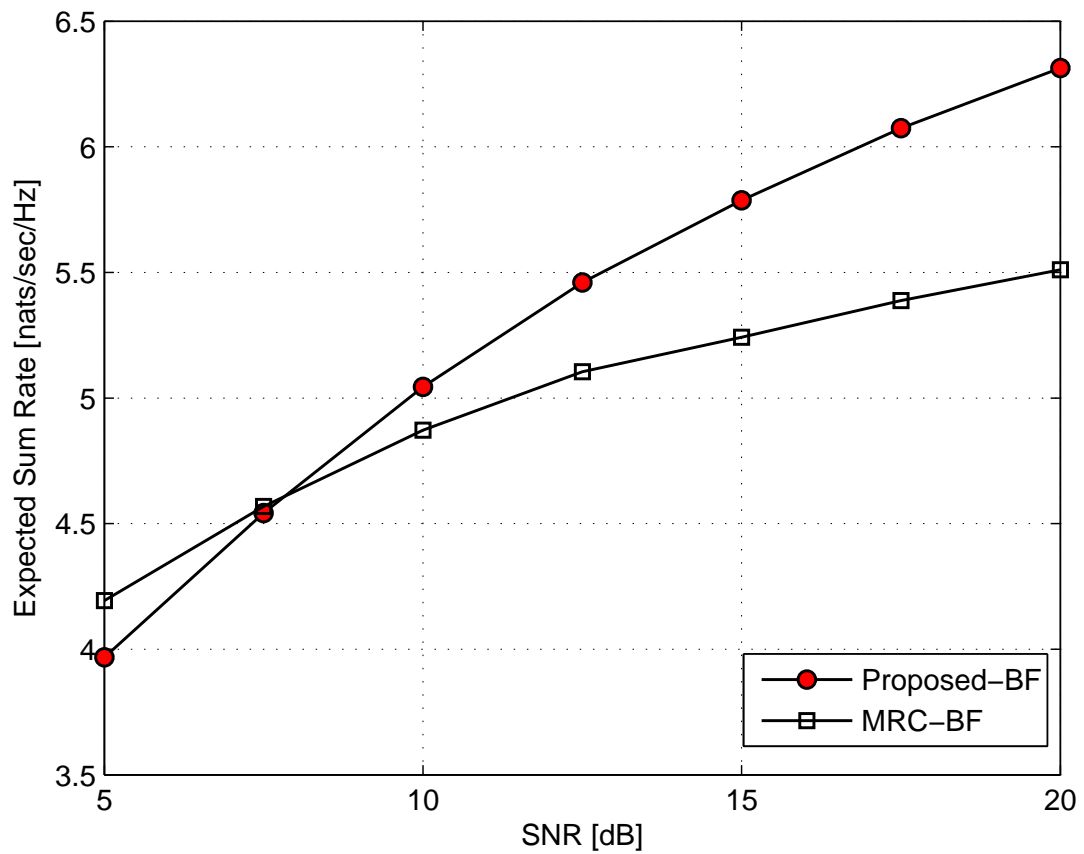
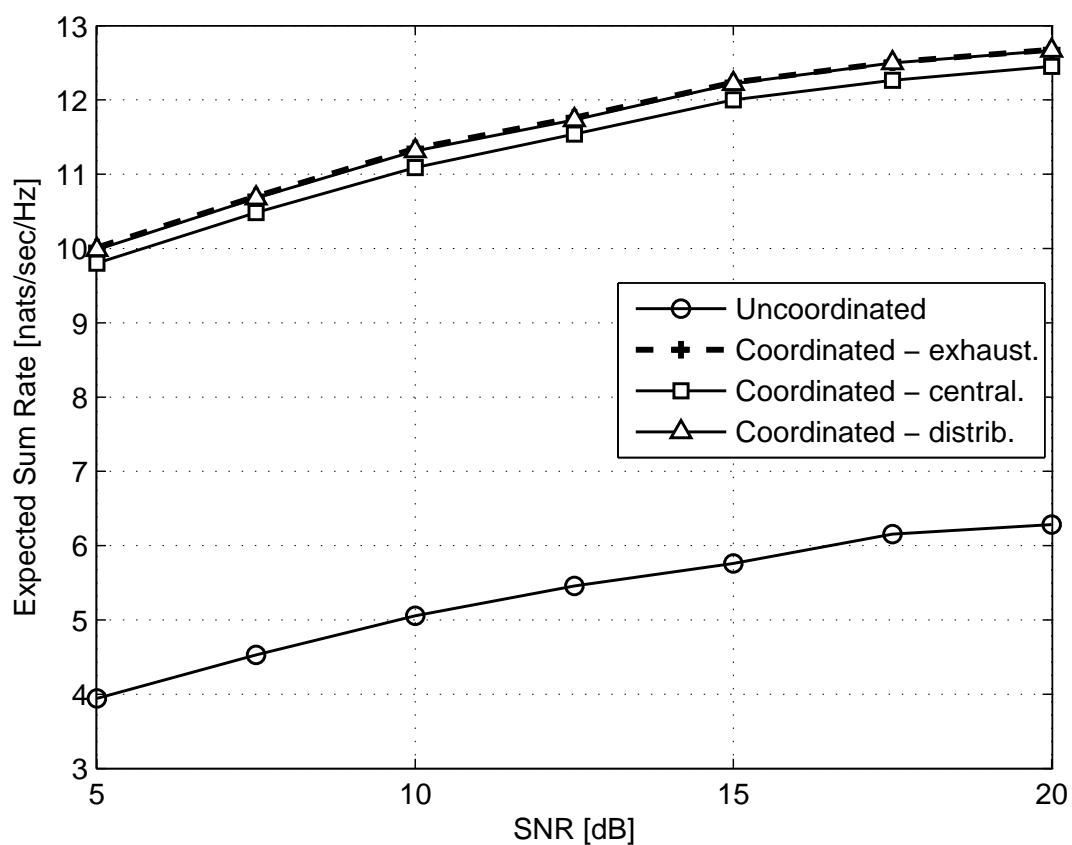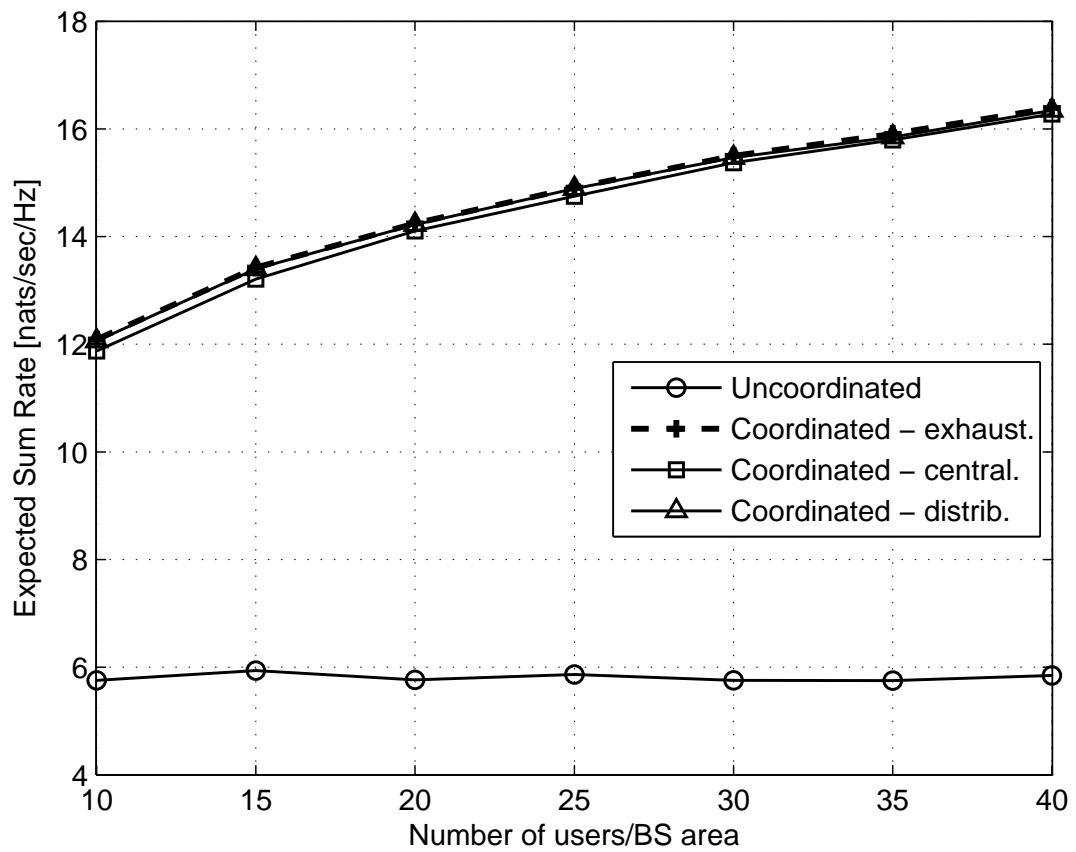Figure 8.9: Taux global moyen contre SNR pour les deux BFs examiné, 1 utilisateur/ zone de couverture.

Figure 8.10: Taux global moyen contre SNR, 10 utilisateurs/ zone de couverture.

Figure 8.11: Taux global moyen contre N, SNR=15dB.

Chapitre 4 - BF pour MISO CRN de sous-couche en utilisant la théorie de la décision de l'équipe

Le problème de la coexistence de deux liens sans fil d'antennes multiples dans un scénario de CR sous-couche, en se concentrant sur ??la communication de downlink, est examiné dans ce chapitre. La nouveauté apportée par notre configuration est triple. Tout d'abord, une contrainte cible plus réaliste pour le récepteur primaire, est considérée, par opposition à la température maximale de l'interférence tolérable. En second lieu, une structure de CSI mixte est considéré comme similaire à celui décrit dans le chapitre 3. En troisième lieu, un scénario *distribué* de prise de décision est formulée, par lequel l'information de canal instantanée n'est pas partagée entre les émetteurs primaires et secondaires. Au lieu de cela, un émetteur doit former sa stratégie de précodage basé uniquement sur CSI locale. Se cette façon, le problème est remanié comme un problème théorique de la décision de l'équipe et les précodeurs optimaux sont obtenus en résolvant les programmes semi-définies (SDPs). En conséquence, un algorithme de précodage distribué est dérivé, qui est ensuite comparé à des solutions de BF classiques. Il est numériquement montré que des gains significatifs en faveur de l'algorithme conçu, sont illustrés sur une gamme de scénarios.

Le travail dans ce chapitre a été publié dans:

- *M.C. Filippou, G.A. Ropokis, and D. Gesbert, "A Team Decisional Beamforming Approach for Underlay Cognitive Radio Networks", in proc. of the 24th Annual IEEE International Symposium on Personal, Indoor and Mobile Radio Communications (PIMRC 2013), London, United Kingdom, 2013*
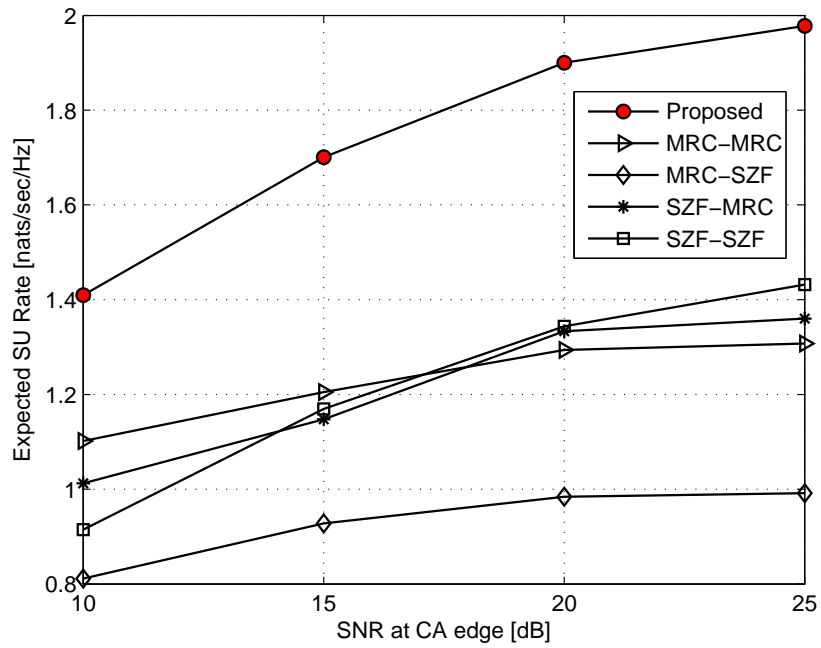
Figure 8.12: Débit ergodique du SU contre SNR moyen au niveau du bord de la zone de couverture, T=1nat/sec/Hz.
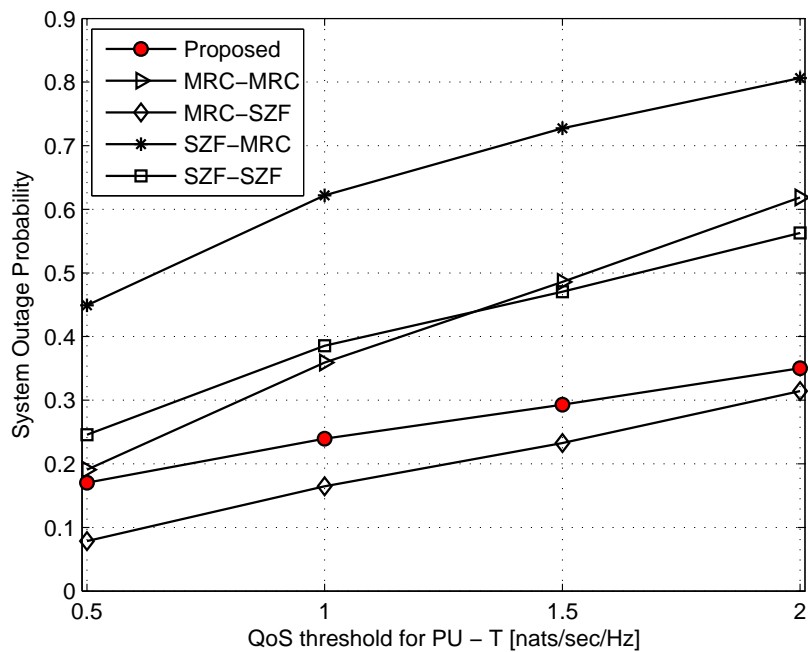

Figure 8.13: Probabilité d'interruption du système contre le seuil QoS, T au PU, SNR=20 dB.

Chapitre 5 - Précodage pour un MISO CRN de sous-couche avec de coordination statistique

Dans ce chapitre, un scénario MISO CR de sous-couche, est étudiée. Selon ce scénario, un émetteur primaire, équipé de multiples antennes, communique avec un PU qui utilise une antenne et un émetteur multi-antenne secondaire sert un SU utilisant une antenne. L'objectif des deux émetteurs est de coordonner efficacement afin de maximiser le taux ergodique du SU, soumis à une contrainte imposée sur le taux ergodique réalisable du PU. Fait important, un scénario de CSI mixte, comme décrit dans la précédente deux chapitres, est considéré, par conséquent, l'émetteur primaire doit exploiter sa connaissance statistique du canal multi-utilisateur afin de coordonner avec l'émetteur secondaire. Cette cadre, donne lieu à un problème de décision de l'équipe, qui rappelle celle formulée dans le chapitre 4. Un nouveau schéma de *coordination statistique* est développé, où les deux émetteurs coordonnent dans le manque d'échange d'CSI instantanée, afin de s'assurer que la contrainte de QoS est satisfaite, alors que le taux moyen du SU est maximisé. On montre que le schéma proposé surpasse régimes classiques issus de la littérature et a une faible complexité.

Le travail dans ce chapitre a entraîné à la publication suivante:

- *P. de Kerret, M.C. Filippou, and D. Gesbert, "Statistically Coordinated Precoding for the MISO Cognitive Radio Channel", in proc. of the Asilomar Conference on Signals, Systems, and Computers (Asilomar 2014), Pacific Grove, U.S.A., 2014*
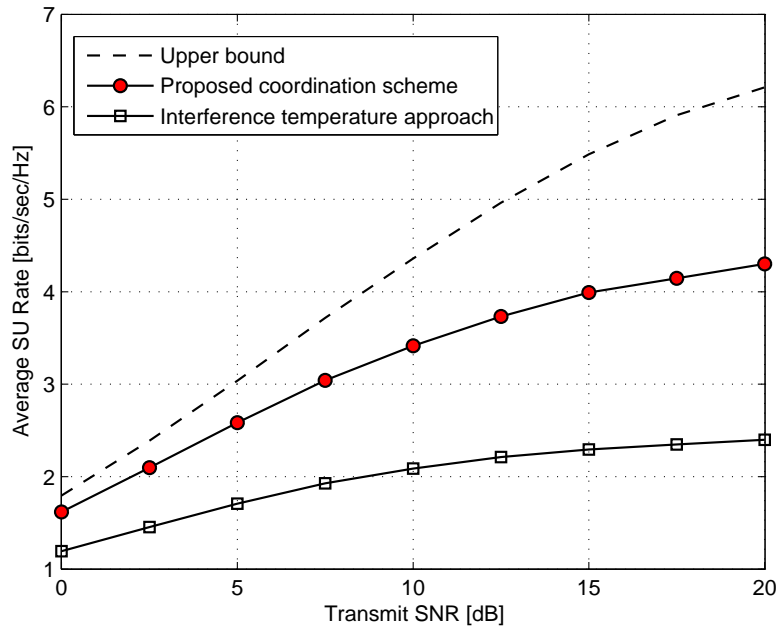
(a) Débit ergodique du SU.
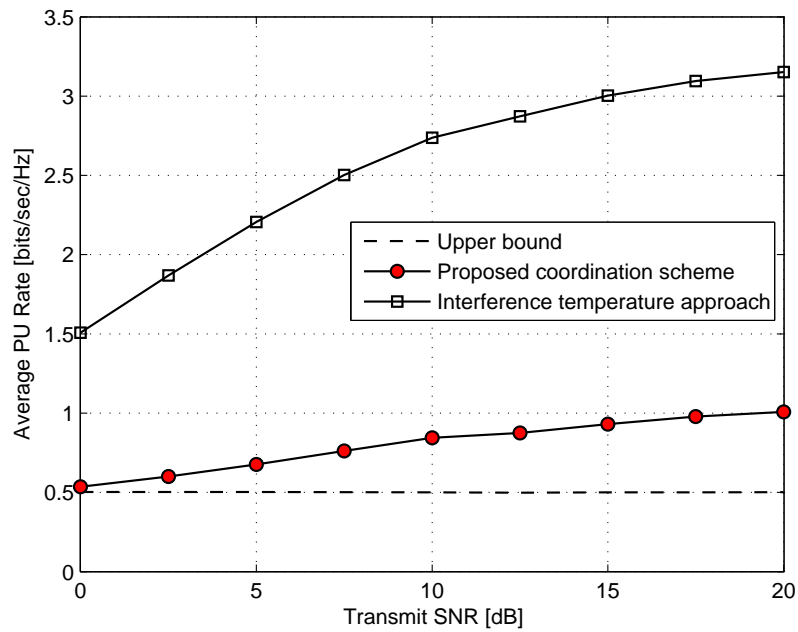
(b) Débit ergodique du PU.

Figure 8.14: Taux ergodiques du SU et du PU, respectivement, pour une configuration de canal avec $M = 3$ et $\tau = 0.5$ bits/sec/Hz.

Chapitre 6 - Estimation de canal pour CRNs avec un grand nombre d'antennes: une approche de décontamination des pilotes

En exploitant les résultats présentés dans [18], dans ce chapitre, nous formulons le problème de l'estimation de canal dans une configuration CRN avec priorité, composé d'un opérateur primaire et un opérateur secondaire. La principale différence entre les systèmes cellulaires et les CRNs de sous-couche est le notion de priorité pour le scénario cognitif. Pour faire face à cette exigence de conception, nous proposons un nouveau schéma d'affectation des pilotes qui est mis en uvre à l'égard de l'opérateur secondaire. Ce régime vise à maximiser le qualité de l'estimation de canal pour le SU, tout en minimisant l'impact créé par celui-ci sur la performance primaire d'estimation de canal. On montre analytiquement et par simulation que lorsque le nombre d'antennes devient grand, on peut réaliser l'estimation de canal sans interférence à l'opérateur principal tout en laissant les SUs communiquer. Plus précisément, nous concluons sur le fait que l'erreur quadratique moyenne (MSE) des performances de l'(covariance basé) estimation de canal, dans le cas où ce qui concerne un PU, fortement dépend du degré avec lequel les sous-espaces de signal des matrices de covariance du direct et du interférant canal chevauchement avec l'autre. Dans le but de quantifier ce résultat, nous créons un protocole de coordination appropriée pour l'affecter séquences de pilotes utilisés par les SUs du système ci-dessus.

Le travail dans ce chapitre a été publié dans:

- *M.C. Filippou, D. Gesbert, and H. Yin, "Decontaminating Pilots in Cognitive Massive MIMO Networks", in proc. of the 9th International Symposium on Wireless Communication Systems (ISWCS 2012), Paris, France, 2012 (invited paper)*

- *H. Yin, D. Gesbert, and M.C. Filippou, "Decontaminating Pilots in Massive MIMO Systems", in proc. of the IEEE International Conference on Communications, (ICC 2013), Budapest, Hungary, 2013*

- *H. Yin, D. Gesbert, M.C. Filippou, and Y. Liu, "A Coordinated Approach to Channel Estimation in Large-Scale Multiple-Antenna Systems", in IEEE Journal on Selected Areas in Communications, vol.31, no.2, pp.264-273, Feb. 2013*
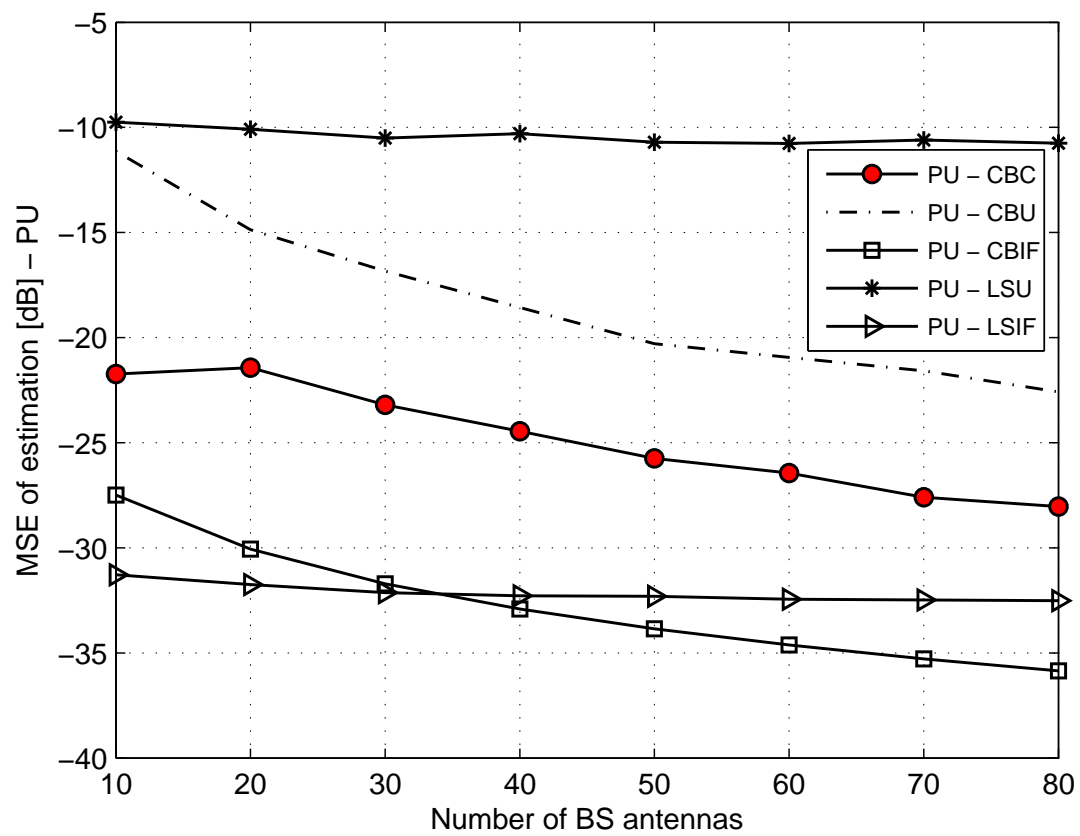
Figure 8.15: PU - MSE de l'estimation contre le nombre d'antennes (BS), M, avec $\epsilon = 0.03$.
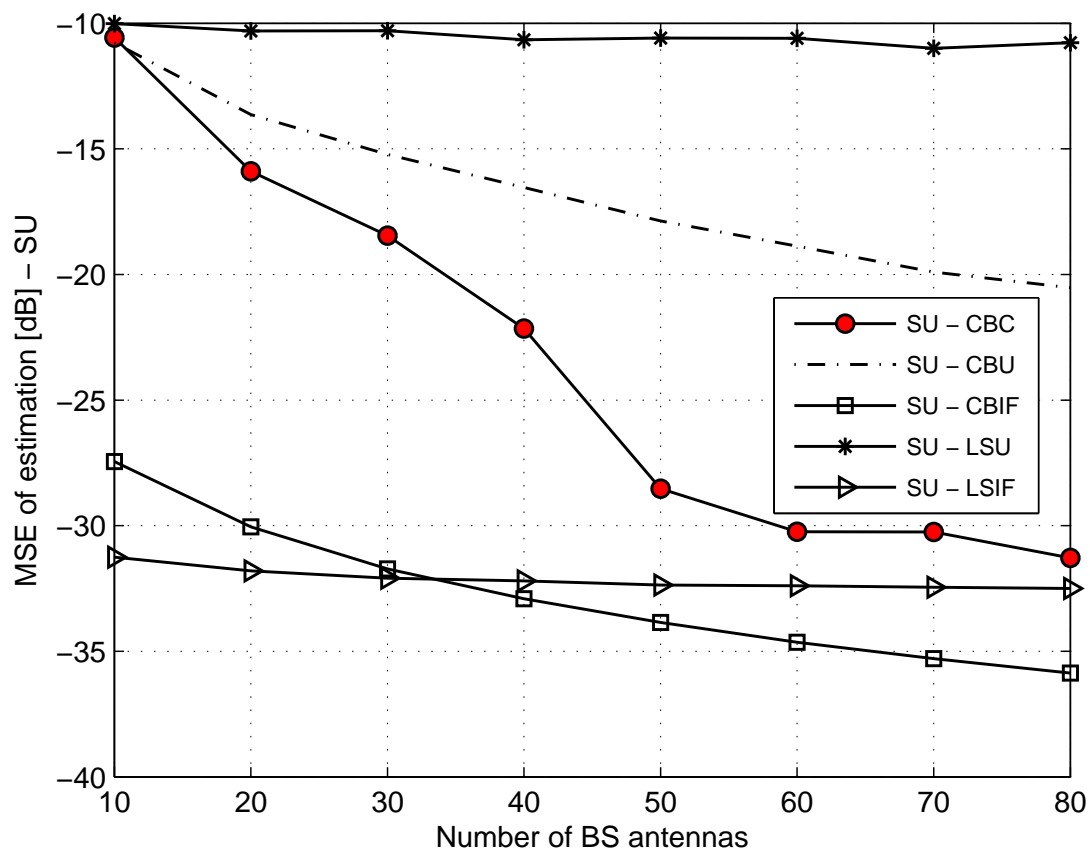
Figure 8.16: SU - MSE de l'estimation contre le nombre d'antennes (BS), M, avec $\epsilon = 0.03$.

106

Appendices

.1 Proof of Proposition 1

The outage probability of PU, considering an interweaved CRN, is described by the following expression

$$\mathcal{P}_{out}^{int} = \mathcal{P}_{out,1} + \mathcal{P}_{out,2}, \tag{1}$$

where for probability $\mathcal{P}_{out,1}$ we have

$$
\begin{aligned}
\mathcal{P}_{out,1} &= (1 - \mathcal{P}_d)\mathcal{P}\left\{ \frac{|\mathbf{h}_{pp}\mathbf{w}_p|^2}{N_0 B + |\mathbf{h}_{sp}\mathbf{w}_s^{int}|^2} < \gamma_0 \right\} \\
&= (1 - \mathcal{P}_d)\mathcal{P}\left\{ P_p\|\mathbf{h}_{pp}\|^2 - \gamma_0 P_s |\mathbf{h}_{sp}\tilde{\mathbf{h}}_{ss}^H|^2 < \gamma_0 N_0 B \right\} \\
&= (1 - \mathcal{P}_d)\mathcal{P}\left\{ X_1 - X_2 < \gamma_0 N_0 B \right\}.
\end{aligned}
\tag{2}
$$

Random variable $X_1 = P_p\|\mathbf{h}_{pp}\|^2$ is gamma distributed with probability density function (PDF): $f_{X_1}(x_1) = \frac{x_1^{M-1} e^{-\frac{x_1}{\lambda_{X_1}}}}{\Gamma(M)\lambda_{X_1}^M}$, where $\lambda_{X_1} = P_p \sigma_{pp}^2$. Also, random variable $X_2 = \gamma_0 P_s |\mathbf{h}_{sp}\tilde{\mathbf{h}}_{ss}^H|^2$ is exponentially distributed with PDF $f_{X_2}(x_2) = \frac{1}{\lambda_{X_2}} e^{-\frac{x_2}{\lambda_{X_2}}}$, where $\lambda_{X_2} = \gamma_0 P_s \sigma_{sp}^2$. As X_1 and X_2 are independent, their joint PDF $f_{X_1,X_2}(x_1,x_2)$ will be the product of the two marginal PDFs. Consequently, the computation of probability $\mathcal{P}_{out,1}$ gives

$$\mathcal{P}_{out,1} = (1 - \mathcal{P}_d)\int_0^\infty \int_0^{x_2 + \gamma_0 N_0 B} f_{X_1,X_2}(x_1,x_2)\,dx_1 dx_2. \tag{3}$$

The double integral appearing in (3) can be computed by applying [33, 3.351.1] and [33, 3.351.2] for the inner and the resulting integral, respectively. As a result, we obtain

$$\mathcal{P}_{out,1} = (1 - \mathcal{P}_d)\mathcal{P}_1, \tag{4}$$

where probability $\mathcal{P}_1$ is given by (2.9a).

Probability $\mathcal{P}_{out,2}$ is given by the following expression

$$
\begin{aligned}
\mathcal{P}_{out,2} &= \mathcal{P}_d \mathcal{P}\left\{ \frac{P_p\|\mathbf{h}_{pp}\|^2}{N_0 B} < \gamma_0 \right\} \\
&= \mathcal{P}_d \mathcal{P}\left\{ X_1 < \gamma_0 N_0 B \right\} \\
&= \mathcal{P}_d \mathcal{P}_2,
\end{aligned}
\tag{5}
$$

where $\mathcal{P}_2$ is given by (2.9b) and [33, 3.351.1] was used for the derivation. Substituting (4) and (5) to (1) we yield (2.8), thus Proposition 1 is proved.

.2 Proof of Proposition 2

Taking into consideration the followed BF and truncated power allocation policy, one will obtain the following expression for the outage probability of primary communication

$$\mathcal{P}^{und}_{out,MRC} = \mathcal{P}\left\{\frac{\mathcal{I}}{|\mathbf{h}_{sp}\tilde{\mathbf{h}}_{ss}^H|^2} < P_s\right\}\mathcal{P}\left\{\frac{P_p\|\mathbf{h}_{pp}\|^2}{N_0 B + \mathcal{I}} < \gamma_0\right\}$$
$$+ \mathcal{P}\left\{\frac{\mathcal{I}}{|\mathbf{h}_{sp}\tilde{\mathbf{h}}_{ss}^H|^2} \geq P_s, \quad \frac{P_p\|\mathbf{h}_{pp}\|^2}{N_0 B + P_s|\mathbf{h}_{sp}\tilde{\mathbf{h}}_{ss}^H|^2} < \gamma_0\right\}. \tag{6}$$

Capitalizing on the known distribution of random variables $\|\mathbf{h}_{pp}\|^2$ and $|\mathbf{h}_{sp}\tilde{\mathbf{h}}_{ss}^H|^2$, the probabilities appearing in the first term of (6) can be found in closed form, giving

$$\mathcal{P}\left\{\frac{\mathcal{I}}{|\mathbf{h}_{sp}\tilde{\mathbf{h}}_{ss}^H|^2} < P_s\right\} = e^{-\frac{\mathcal{I}}{P_s\sigma_{sp}^2}}, \tag{7}$$

which is obtained by applying integration by parts and

$$\mathcal{P}\left\{\frac{P_p\|\mathbf{h}_{pp}\|^2}{N_0 B + \mathcal{I}} < \gamma_0\right\} = \frac{\gamma\left(M, \frac{\gamma_0(N_0 B + \mathcal{I})}{P_p\sigma_{pp}^2}\right)}{\Gamma(M)}, \tag{8}$$

which is derived by applying [33, 3.351.1]. Focusing on the joint probability appearing in the second term of (6), we obtain

$$\mathcal{P}\left\{\frac{\mathcal{I}}{|\mathbf{h}_{sp}\tilde{\mathbf{h}}_{ss}^H|^2} \geq P_s, \quad \frac{P_p\|\mathbf{h}_{pp}\|^2}{N_0 B + P_s|\mathbf{h}_{sp}\tilde{\mathbf{h}}_{ss}^H|^2} < \gamma_0\right\} = \mathcal{P}\left\{|\mathbf{h}_{sp}\tilde{\mathbf{h}}_{ss}^H|^2 \leq \frac{\mathcal{I}}{P_s}, P_p\|\mathbf{h}_{pp}\|^2 - \gamma_0 P_s|\mathbf{h}_{sp}\tilde{\mathbf{h}}_{ss}^H|^2 < \gamma_0 N_0 B\right\}. \tag{9}$$

By applying a bivariate transformation, it is easy to show that the joint PDF of random variables $W_1 = |\mathbf{h}_{sp}\tilde{\mathbf{h}}_{ss}^H|^2$ and $W_2 = P_p\|\mathbf{h}_{pp}\|^2 - \gamma_0 P_s|\mathbf{h}_{sp}\tilde{\mathbf{h}}_{ss}^H|^2$ is

$$f_{W_1,W_2}(w_1, w_2) = \frac{e^{-w_1\left(\frac{1}{\sigma_{sp}^2} + \frac{P_s\gamma_0}{P_p\sigma_{pp}^2}\right)}}{P_p\Gamma(M)\sigma_{sp}^2(\sigma_{pp}^2)^M}\left(\frac{\gamma_0 P_s}{P_p}w_1 + \frac{1}{P_p}w_2\right)^{M-1} e^{\frac{-w_2}{P_p\sigma_{pp}^2}}. \tag{10}$$

As a result, the probability to be derived is the following

$$\mathcal{P}\left\{W_1 \leq \frac{\mathcal{I}}{P_s}, W_2 < \gamma_0 N_0 B\right\} = \int_0^{\frac{\mathcal{I}}{P_s}}\int_{-P_s\gamma_0 w_1}^{\gamma_0 N_0 B} f_{W_1,W_2}(w_1, w_2)\,dw_2\,dw_1, \tag{11}$$

from which a closed form expression can be obtained. After some mathematical manipulations and by applying [33, 3.351.1] and [33, 3.351.2], one can conclude to the following expression

$$\mathcal{P}\left\{W_1 \leq \frac{\mathcal{I}}{P_s}, W_2 < \gamma_0 N_0 B\right\} = \frac{\gamma\left(M, \frac{\gamma_0 N_0 B}{P_p\sigma_{pp}^2}\right)}{\Gamma(M)} - e^{\frac{-\mathcal{I}}{P_s\sigma_{sp}^2}}\frac{\gamma\left(M, \frac{\gamma_0(N_0 B + \mathcal{I})}{P_p\sigma_{pp}^2}\right)}{\Gamma(M)}$$
$$+ \frac{e^{\frac{N_0 B}{P_s\sigma_{sp}^2}}}{\Gamma(M)}\left(\frac{P_p\sigma_{pp}^2}{\gamma_0 P_s\sigma_{sp}^2} + 1\right)^{-M}\left(\Gamma\left(M, \frac{N_0 B}{P_s\sigma_{sp}^2} + \frac{\gamma_0 N_0 B}{P_p\sigma_{pp}^2}\right) - \Gamma\left(M, \frac{N_0 B + \mathcal{I}}{P_s\sigma_{sp}^2} + \frac{\gamma_0(N_0 B + \mathcal{I})}{P_p\sigma_{pp}^2}\right)\right). \tag{12}$$

After substituting (7), (8) and (12) to (6), expression (2.18) will be obtained. As a result, Proposition 2 is proved.

.3 Proof of Proposition 3

The objective function of (2.47) can be expressed as

$$U(\tau, \epsilon) = \mathbb{E}\{R_s^{int}(\tau, \epsilon)\} = \frac{(T - \tau)}{T} \left\{ \underbrace{\mathcal{P}(\mathcal{H}_0) B \mathbb{E}\{\mathcal{A}_1\}}_{\alpha}(1 - \mathcal{P}_{fa}) + \underbrace{\mathcal{P}(\mathcal{H}_1) B \mathbb{E}\{\mathcal{A}_2\}}_{\beta}(1 - \mathcal{P}_{d,B}) \right\}$$

$$\stackrel{(2.4),(2.6)}{=} \frac{(T - \tau)}{T} \left\{ \alpha \left(1 - \mathcal{Q}\left(\sqrt{\tau f_s} \left(\frac{\epsilon - N_0}{N_0} \right) \right) \right) + \beta \left(1 - \mathcal{Q}\left(\sqrt{\tau f_s} \left(\frac{\epsilon - m_1}{m_1} \right) \right) \right) \right\}. \tag{13}$$

By substituting the equality constraint of (2.47) to (13), the following one variable objective function can be obtained

$$U(\tau) = \frac{(T - \tau)}{T} \left(\alpha \left(1 - \mathcal{Q}(t_1 \sqrt{\tau f_s} + t_2) \right) + \beta (1 - \mathcal{Q}(\delta)) \right), \tag{14}$$

where $t_1 = \frac{P_p \sigma_{00}^2}{N_0}$ and $t_2 = \frac{\delta m_1}{N_0}$. Taking the first derivative of (14) with respect to τ, we obtain

$$\frac{\partial U(\tau)}{\partial \tau} = -\frac{1}{T} \alpha \left(1 - \mathcal{Q}(t_1 \sqrt{\tau f_s} + t_2) \right) + \frac{(T - \tau) \alpha t_1 f_s}{2T \sqrt{2\pi} \sqrt{\tau f_s}} e^{-\frac{(t_1 \sqrt{\tau f_s} + t_2)^2}{2}} - \frac{1}{T} \beta \left(1 - \mathcal{Q}(\delta) \right). \tag{15}$$

Taking the derivative of (15) we obtain

$$\frac{\partial^2 U(\tau)}{\partial \tau^2} = -e^{-\frac{(t_1 \sqrt{\tau f_s} + t_2)^2}{2}} \left(\frac{\alpha t_1 f_s}{T \sqrt{2\pi} \sqrt{\tau f_s}} + \frac{(T - \tau) \alpha t_1 f_s^2}{4T \sqrt{2\pi} (\tau f_s)^{\frac{3}{2}}} + \frac{(T - \tau) \alpha t_1^2 f_s^2 (t_1 \sqrt{\tau f_s} + t_2)}{4T \sqrt{2\pi} (\tau f_s)} \right) \leq 0, \tag{16}$$

thus, according to the second derivative criterion, function $U(\tau, \epsilon(\tau))$ is concave for every $\tau \in [0, T]$, which completes the proof.

Bibliography

[1] K. Hamdi, W. Zhang, and K. Letaief, "Uplink scheduling with QoS provisioning for cognitive radio systems," in *IEEE Wireless Communications and Networking Conference, 2007.WCNC 2007.*, Mar. 2007, pp. 2592 –2596.

[2] K. Hamdi, W. Zhang, and K. Ben Letaief, "Joint beamforming and scheduling in cognitive radio networks," in *IEEE Global Telecommunications Conference, 2007. GLOBECOM '07.*, Nov. 2007, pp. 2977 –2981.

[3] R. Zhang and Y.-C. Liang, "Exploiting multi-antennas for opportunistic spectrum sharing in cognitive radio networks," *IEEE Journal of Selected Topics in Signal Processing*, vol. 2, no. 1, pp. 88 –102, Feb. 2008.

[4] D. Gesbert, S. Hanly, H. Huang, S. Shamai Shitz, O. Simeone, and W. Yu, "Multi-cell MIMO cooperative networks: A new look at interference," *IEEE Journal on Selected Areas in Communications*, vol. 28, no. 9, pp. 1380 –1408, Dec. 2010.

[5] M. K. Simon and M.-S. Alouini, *Digital communication over fading channels.* John Wiley & Sons, 2005, vol. 95.

[6] M. Abramowitz and I. A. Stegun, *Handbook of mathematical functions.* Dover publications, 1965.

[7] A. Goldsmith, S. Jafar, I. Maric, and S. Srinivasa, "Breaking spectrum gridlock with cognitive radios: An information theoretic perspective," *Proceedings of the IEEE*, vol. 97, no. 5, pp. 894–914, May 2009.

[8] Federal Communications Commission, "Spectrum policy task force report, FCC 02-155," 2002.

[9] P. Kolodzy *et al.*, "Next generation communications: Kickoff meeting," in *Proc. DARPA*, vol. 10, 2001.

[10] E. Biglieri, A. J. Goldsmith, L. J. Greenstein, N. Mandayam, and H. V. Poor, *Principles of Cognitive Radio.* Cambridge University Press, 2012.

[11] J. Mitola and G. Q. Maguire Jr, "Cognitive radio: making software radios more personal," *IEEE, Personal Communications*, vol. 6, no. 4, pp. 13–18, Aug. 1999.

[12] S. Haykin, "Cognitive radio: brain-empowered wireless communications," *IEEE Journal on Selected Areas in Communications*, vol. 23, no. 2, pp. 201–220, Feb. 2005.

[13] T. Yucek and H. Arslan, "A survey of spectrum sensing algorithms for cognitive radio applications," *IEEE Communications Surveys Tutorials*, vol. 11, no. 1, pp. 116–130, First 2009.

[14] I. Akyildiz, W.-Y. Lee, M. Vuran, and S. Mohanty, "A survey on spectrum management in cognitive radio networks," *IEEE Communications Magazine*, vol. 46, no. 4, pp. 40 –48, Apr. 2008.

[15] T. C. Clancy, "Formalizing the interference temperature model," *Wireless Communications and Mobile Computing*, vol. 7, no. 9, pp. 1077–1086, 2007.

[16] E. Karipidis, D. Gesbert, M. Haardt, K.-M. Ho, E. Jorswieck, E. G. Larsson, J. Li, J. Lindblom, C. Scheunert, M. Schubert *et al.*, "Transmit beamforming for inter-operator spectrum sharing," in *2011 Future Network & Mobile Summit (FutureNetw)*. IEEE, 2011, pp. 1–8.

[17] Z. Ka, M. Ho, and D. Gesbert, "Spectrum sharing in multiple-antenna channels: A distributed cooperative game theoretic approach," in *IEEE 19th International Symposium on Personal, Indoor and Mobile Radio Communications. PIMRC 2008*. IEEE, 2008, pp. 1–5.

[18] H. Yin, D. Gesbert, M. Filippou, and Y. Liu, "A coordinated approach to channel estimation in large-scale multiple-antenna systems," *IEEE Journal on Selected Areas in Communications*, vol. 31, no. 2, pp. 264 –273, Feb. 2013.

[19] S. Srinivasa and S. Jafar, "The throughput potential of cognitive radio: A theoretical perspective," in *Fortieth Asilomar Conference on Signals, Systems and Computers, 2006. ACSSC '06*, Oct. 2006, pp. 221–225.

[20] A. Giorgetti, M. Varrella, and M. Chiani, "Analysis and performance comparison of different cognitive radio algorithms," in *Second International Workshop on Cognitive Radio and Advanced Spectrum Management, 2009. CogART 2009.*, May 2009, pp. 127–131.

[21] M. Khoshkholgh, K. Navaie, and H. Yanikomeroglu, "Access strategies for spectrum sharing in fading environment: Overlay, underlay, and mixed," *IEEE Transactions on Mobile Computing*, vol. 9, no. 12, pp. 1780–1793, Dec. 2010.

[22] X. Kang, Y.-C. Liang, H. Garg, and L. Zhang, "Sensing-based spectrum sharing in cognitive radio networks," *IEEE Transactions on Vehicular Technology*, vol. 58, no. 8, pp. 4649–4654, Oct. 2009.

[23] Y. Wang, P. Ren, F. Gao, and Z. Su, "A hybrid underlay/overlay transmission mode for cognitive radio networks with statistical quality-of-service provisioning," *IEEE Transactions on Wireless Communications*, vol. PP, no. 99, pp. 1–17, Mar. 2014.

[24] A. Ghasemi and E. Sousa, "Fundamental limits of spectrum-sharing in fading environments," *IEEE Transactions on Wireless Communications*, vol. 6, no. 2, pp. 649–658, Feb. 2007.

[25] C.-X. Wang, X. Hong, H.-H. Chen, and J. Thompson, "On capacity of cognitive radio networks with average interference power constraints," *IEEE Transactions on Wireless Communications*, vol. 8, no. 4, pp. 1620–1625, Apr. 2009.

[26] L. Musavian and S. Aissa, "Ergodic and outage capacities of spectrum-sharing systems in fading channels," in *IEEE Global Telecommunications Conference, 2007. GLOBECOM '07*, Nov. 2007, pp. 3327–3331.

[27] L. Sboui, Z. Rezki, and M.-S. Alouini, "A unified framework for the ergodic capacity of spectrum sharing cognitive radio systems," *IEEE Transactions on Wireless Communications*, vol. 12, no. 2, pp. 877–887, Feb. 2013.

[28] H. Suraweera, P. Smith, and M. Shafi, "Capacity limits and performance analysis of cognitive radio with imperfect channel knowledge," *IEEE Transactions on Vehicular Technology*, vol. 59, no. 4, pp. 1811–1822, May 2010.

[29] S. Stotas and A. Nallanathan, "On the outage capacity of sensing-enhanced spectrum sharing cognitive radio systems in fading channels," *IEEE Transactions on Communications*, vol. 59, no. 10, pp. 2871–2882, Oct. 2011.

[30] B. Makki and T. Eriksson, "On the ergodic achievable rates of spectrum sharing networks with finite backlogged primary users and an interference indicator signal," *IEEE Transactions on Wireless Communications*, vol. 11, no. 9, pp. 3079–3089, Sep. 2012.

[31] I. F. Akyildiz, W.-Y. Lee, M. C. Vuran, and S. Mohanty, "Next generation/dynamic spectrum access/cognitive radio wireless networks: a survey," *Computer Networks*, vol. 50, no. 13, pp. 2127–2159, Sep. 2006.

[32] Y.-C. Liang, Y. Zeng, E. Peh, and A. T. Hoang, "Sensing-throughput tradeoff for cognitive radio networks," *IEEE Transactions on Wireless Communications*, vol. 7, no. 4, pp. 1326–1337, Apr. 2008.

[33] I. S. Gradshteyn and I. M. Ryzhik, *Table of integrals, series, and products*, 7th ed. Elsevier/Academic Press, Amsterdam, 2007.

[34] D. Tse, *Fundamentals of wireless communication.* Cambridge university press, 2005.

[35] E. Jorswieck, E. Larsson, and D. Danev, "Complete characterization of the Pareto boundary for the MISO interference channel," *IEEE Transactions on Signal Processing*, vol. 56, no. 10, pp. 5292 –5296, Oct. 2008.

[36] D. Love, R. Heath, V. Lau, D. Gesbert, B. Rao, and M. Andrews, "An overview of limited feedback in wireless communication systems," *IEEE Journal on Selected Areas in Communications*, vol. 26, no. 8, pp. 1341 –1365, Oct. 2008.

[37] E. Bjornson, R. Zakhour, D. Gesbert, and B. Ottersten, "Cooperative multicell precoding: Rate region characterization and distributed strategies with instantaneous and statistical CSI," *IEEE Transactions on Signal Processing*, vol. 58, no. 8, pp. 4298 –4310, Aug. 2010.

[38] J. Lindblom, E. Larsson, and E. Jorswieck, "Parameterization of the MISO interference channel with transmit beamforming and partial channel state information," in *42nd Asilomar Conference on Signals, Systems and Computers, 2008*, Oct. 2008, pp. 1103 –1107.

115

[39] I. Wajid, Y. Eldar, and A. Gershman, "Robust downlink beamforming using covariance channel state information," in *IEEE International Conference on Acoustics, Speech and Signal Processing, 2009. ICASSP 2009.*, Apr. 2009, pp. 2285 –2288.

[40] S. Jafar, S. Vishwanath, and A. Goldsmith, "Channel capacity and beamforming for multiple transmit and receive antennas with covariance feedback," in *IEEE International Conference on Communications, 2001. ICC 2001.*, vol. 7, 2001, pp. 2266 –2270.

[41] Y. Gu and A. Leshem, "Robust adaptive beamforming based on interference covariance matrix reconstruction and steering vector estimation," *IEEE Transactions on Signal Processing*, vol. 60, no. 7, pp. 3881 –3885, Jul. 2012.

[42] J. Yang, E. Bjornson, and M. Bengtsson, "Receive beamforming design based on a multiple-state interference model," in *2011 IEEE International Conference on Communications (ICC)*, Jun. 2011, pp. 1 –6.

[43] H.-C. Lee, D.-C. Oh, and Y.-H. Lee, "Coordinated user scheduling with transmit beamforming in the presence of inter-femtocell interference," in *2011 IEEE International Conference on Communications (ICC)*, Jun. 2011, pp. 1 –5.

[44] E. Vagenas, G. Paschos, and S. Kotsopoulos, "Beamforming capacity optimization for MISO systems with both mean and covariance feedback," *IEEE Transactions on Wireless Communications*, vol. 10, no. 9, pp. 2994 –3001, Sep. 2011.

[45] H. Boche and M. Schubert, "A new approach to power adjustment for spatial covariance based downlink beamforming," in *2001 IEEE International Conference on Acoustics, Speech, and Signal Processing, 2001. Proceedings. (ICASSP '01).*, vol. 5, 2001, pp. 2957 –2960 vol.5.

[46] M. Rubsamen and A. Gershman, "Robust adaptive beamforming based on multidimensional covariance fitting," in *2010 IEEE International Conference on Acoustics Speech and Signal Processing (ICASSP)*, Mar. 2010, pp. 2538 –2541.

[47] M. Kountouris, R. de Francisco, D. Gesbert, D. Slock, and T. Salzer, "Low complexity scheduling and beamforming for multiuser MIMO systems," in *IEEE 7th Workshop on Signal Processing Advances in Wireless Communications, 2006. SPAWC '06.*, Jul. 2006, pp. 1 –5.

[48] V. Raghavan and S. Hanly, "Statistical beamformer design for the two-antenna interference channel," in *2010 IEEE International Symposium on Information Theory Proceedings (ISIT)*, Jun. 2010, pp. 2278 –2282.

[49] T. Cover and A. Thomas, *Elements of information theory.* Wiley-Interscience, Jul. 2006.

[50] M. Kobayashi and G. Caire, "Joint beamforming and scheduling for a multi-antenna downlink with imperfect transmitter channel knowledge," *IEEE Journal on Selected Areas in Communications*, vol. 25, no. 7, pp. 1468 –1477, Sep. 2007.

[51] T. Yoo and A. Goldsmith, "On the optimality of multiantenna broadcast scheduling using zero-forcing beamforming," *IEEE Journal on Selected Areas in Communications*, vol. 24, no. 3, pp. 528 – 541, Mar. 2006.

[52] P. Svedman, S. K. Wilson, L. J. Cimini, and B. Ottersten, "Opportunistic beamforming and scheduling for OFDMA systems," *IEEE Transactions on Communications*, vol. 55, no. 5, pp. 941 –952, May 2007.

[53] Y. Ma and D. I. Kim, "Rate-maximization scheduling schemes for uplink OFDMA," *IEEE Transactions on Wireless Communications*, vol. 8, no. 6, pp. 3193 –3205, Jun. 2009.

[54] J. Zhang and J. Andrews, "Adaptive spatial intercell interference cancellation in multicell wireless networks," *IEEE Journal on Selected Areas in Communications*, vol. 28, no. 9, pp. 1455 –1468, Dec. 2010.

[55] G. Dimic and N. Sidiropoulos, "On downlink beamforming with greedy user selection: performance analysis and a simple new algorithm," *IEEE Transactions on Signal Processing*, vol. 53, no. 10, pp. 3857 – 3868, Oct. 2005.

[56] Y. Zhang and A.-C. So, "Optimal spectrum sharing in MIMO cognitive radio networks via semidefinite programming," *IEEE Journal on Selected Areas in Communications*, vol. 29, no. 2, pp. 362–373, 2011.

[57] R. Zhang and S. Cui, "Cooperative interference management with MISO beamforming," *IEEE Transactions on Signal Processing*, vol. 58, no. 10, pp. 5450–5458, 2010.

[58] H. Du and T. Ratnarajah, "Transmit beamforming in MIMO cognitive radio network via semidefinite programming," in *2011 IEEE 73rd Vehicular Technology Conference (VTC Spring)*, May 2011, pp. 1 –5.

[59] L. Zhang, Y.-C. Liang, Y. Xin, and H. Poor, "Robust cognitive beamforming with partial channel state information," *IEEE Transactions on Wireless Communications*, vol. 8, no. 8, pp. 4143–4153, 2009.

[60] K. Wang, N. Jacklin, Z. Ding, and C. Chi, "Robust MISO Transmit optimization under outage-based QoS constraints in two-tier heterogeneous networks," *IEEE Transactions on Wireless Communications*, vol. PP, no. 99, pp. 1–15, 2013.

[61] Y.-C. Ho, "Team decision theory and information structures," *Proceedings of the IEEE*, vol. 68, no. 6, pp. 644–654, 1980.

[62] R. Zakhour and D. Gesbert, "Team decision for the cooperative MIMO channel with imperfect CSIT sharing," in *2010 Information Theory and Applications Workshop (ITA)*, Feb. 2010, pp. 1–6.

[63] S. Han and C. Yang, "Downlink multicell cooperative transmission with imperfect CSI sharing," in *2011 IEEE International Conference on Acoustics Speech and Signal Processing (ICASSP)*, 2011, pp. 3024–3027.

[64] Z.-Q. Luo, W.-K. Ma, A.-C. So, Y. Ye, and S. Zhang, "Semidefinite relaxation of quadratic optimization problems," *IEEE Signal Processing Magazine*, vol. 27, no. 3, pp. 20 –34, May 2010.

[65] M. Grant and S. Boyd, "CVX: Matlab software for disciplined convex programming, version 2.0 beta," http://cvxr.com/cvx, Sep. 2012.

[66] R. Zhang, "Optimal power control over fading cognitive radio channel by exploiting primary user CSI," in *Proc. IEEE Global Communications Conference (GLOBECOM)*, 2008.

[67] Y. Huang and D. P. Palomar, "Rank-constrained separable semidefinite programming with applications to optimal beamforming," *IEEE Trans. Signal Process.*, vol. 58, no. 2, pp. 664–678, Feb 2010.

[68] R. Fritzsche and G. P. Fettweis, "CSI distribution for joint processing in cooperative cellular networks," in *Proc. IEEE Vehicular Technology Conference (VTC Fall)*, 2011.

[69] B. Wang, Y. Wu, and K. J. R. Liu, "Game theory for cognitive radio networks: An overview," *Elsevier Computer Networks*, pp. 2537–2561, 2010.

[70] G. Scutari and D. Palomar, "MIMO cognitive radio: A game theoretical approach," *IEEE Transactions on Signal Processing*, vol. 58, no. 2, pp. 761 –780, Feb. 2010.

[71] G. Scutari, F. Facchinei, P. Song, D. P. Palomar, and J.-S. Pang, "Decomposition by partial linearization: Parallel optimization of multi-agent systems," *IEEE Trans. Signal Process.*, vol. 62, no. 3, pp. 641–656, Feb. 2014.

[72] P. de Kerret and D. Gesbert, "CSI sharing strategies for transmitter cooperation in wireless networks," *IEEE Wireless Commun. Mag.*, vol. 20, no. 1, pp. 43–49, Feb. 2013.

[73] P. de Kerret, M. C. Filippou, and D. Gesbert, "Statistically coordinated precoding for the MISO cognitive radio channel," 2014, in preparation.

[74] T. L. Marzetta, "Noncooperative cellular wireless with unlimited numbers of base station antennas," *IEEE Transactions on Wireless Communications*, vol. 9, no. 11, pp. 3590–3600, Nov. 2010.

[75] B. Gopalakrishnan and N. Jindal, "An analysis of pilot contamination on multi-user MIMO cellular systems with many antennas," in *2011 IEEE 12th International Workshop on Signal Processing Advances in Wireless Communications (SPAWC)*, Jun. 2011, pp. 381 –385.

[76] J. Hoydis, S. ten Brink, and M. Debbah, "Massive MIMO: How many antennas do we need?" in *Proc. 2011 49th Annual Allerton Conference on Communication, Control, and Computing (Allerton)*, Sep. 2011, pp. 545 –550.

[77] J. Jose, A. Ashikhmin, T. L. Marzetta, and S. Vishwanath, "Pilot contamination problem in multi-cell TDD systems," in *Proc. IEEE International Symposium on Information Theory (ISITo09)*, Seoul, Korea, Jun. 2009, pp. 2184–2188.

[78] ——, "Pilot contamination and precoding in multi-cell TDD systems," *IEEE Transactions on Wireless Communications*, vol. 10, no. 8, pp. 2640–2651, Aug. 2011.

[79] H. Q. Ngo, T. L. Marzetta, and E. G. Larsson, "Analysis of the pilot contamination effect in very large multicell multiuser mimo systems for physical channel models," in *2011 IEEE International Conference on Acoustics, Speech and Signal Processing (ICASSP)*, May 2011, pp. 3464 –3467.

[80] A. J. Paulraj, R. Nabar, and D. Gore, *Introduction to space-time wireless communications.* Cambridge University Press, 2003.

[81] A. Scherb and K. Kammeyer, "Bayesian channel estimation for doubly correlated MIMO systems," in *Proc. IEEE Workshop Smart Antennas*, 2007.

[82] E. Bjornson and B. Ottersten, "A framework for training-based estimation in arbitrarily correlated Rician MIMO channels with Rician disturbance," *IEEE Transactions on Signal Processing*, vol. 58, no. 3, pp. 1807–1820, 2010.

[83] S. M. Kay, *Fundamentals of Statistical Signal Processing: Estimation Theory.* Englewood Cliffs, NJ: Prentice Hall, 1993.

[84] J.-A. Tsai, R. Buehrer, and B. Woerner, "The impact of AOA energy distribution on the spatial fading correlation of linear antenna array," in *IEEE 55th Vehicular Technology Conference, 2002. VTC Spring 2002.*, vol. 2, 2002, pp. 933 – 937 vol.2.